Using satellite imagery and novel low altitude aerial imagery to classify coastal wetland vegetation for change detection at Whatipu Scientific Reserve, Auckland, NZ

Grant Lawrence

A thesis submitted to Auckland University of Technology in partial fulfillment of the requirements for the degree of Master of Science (MSc)

School of Health and Environmental Sciences

Auckland University of Technology (AUT)

2015

Supervisor/s: Dr. Barbara Breen & Dr. Craig Bishop

Table of Contents

List of Figures and Tables **IV**

List of Appendix Figures **V**

Acronyms **VI**

Attestation of Authorship **VII**

Acknowledgements **VIII**

Abstract **VIII**

1 Introduction and Literature Review **1**
1.1 Wetlands *1*
Wetland ecosystems 1
Coastal Wetland ecological classification 2
1.2 Remote Sensing for Wetland Mapping *4*
1.3 A review of remote sensing sensors and coastal applications *5*
Field Spectrometers 6
Low to medium spatial resolution optical sensors 8
High spatial resolution optical sensors 9
Hyperspectral sensors 10
Active Systems (RADAR) 11
Aerial Imagery 11
1.4 Remote Sensing Classification *12*
Visual Interpretation 12
Pixel-Based Classification 13
Object-based Classification 14
Hybrid Approaches 16
1.5 Remote Sensing Training and Validation Datasets *17*
1.6 Change Detection *18*
1.7 Wetland Remote Sensing in New Zealand *19*
1.8 Introduction to Whatipu wetland *20*
1.9 Research problems, aims *21*
1.10 Objectives *22*
1.11 Structure of Thesis *23*

2 Methods **24**
2.1 Study Area *24*
Case Study Area 26
2.2 Wetland Classification Scheme *27*
2.3 Datasets and data acquisition *29*
Spectral Reflectance Data 31
Low Altitude Aerial Imagery 35
Satellite data 38
Ancillary Datasets 40
Training and Validation Data 41
2.3 Software *43*
ViewSpec Pro 43
Pix4Dmapper 43
ENVI 5.2 43
ArcGIS 43
2.4 Data Pre-processing *44*
Low Altitude Aerial Imagery Pre-processing and Preparation 46
Satellite Image Pre-processing and Preparation 49
2.5 Data Processing, Post Processing and Analysis *56*
Field-based Spectral Reflectance Data Analysis 56

Training Data Analysis 57
Satellite Image Classification Processing 58
Accuracy Assessment 59
Post classification processing 59
Change Analysis 60
2.6 Case Study *61*
Visual Interpretation 61
Digitization – Manual classification 62
Comparison 63

3 Results **64**
3.1 Spectral Reflectance Data *64*
Spectral Properties of Plants 64
WorldView Simulated Signatures 64
Spectral Signatures Comparison 65
3.2 UAS Results *68*
3.3 ROI Spectral Separability *69*
Comparison of Simulated Spectra with Satellite Spectra 70
3.4 Satellite Classifications *72*
Supervised Classifications 72
3.5 Wetland Vegetation Change from 2011 and 2015 *79*
3.6 Case Study Results *83*

4 Discussion **85**
4.1 Spectra of Whatipu Vegetation *85*
4.2 Training and Validation Samples *86*
4.3 Land Cover Classification *87*
Classification Accuracy and Limitations 87
4.4 Change Detection *90*
4.5 Low Altitude Aerial Imagery *91*

5 Conclusions **92**

References **93**

Appendices **101**

List of Figures and Tables

1 Introduction and Literature Review **1**

Table 1.1 Wetland and Coastal sand dune ecosystems in the Auckland Region 3

2 Methods **24**

Figure 2.1 Whatipu Scientific Reserve 25

Figure 2.2. Case study area 26

Table 2.1 Whatipu classification scheme 27

Table 2.2 Key imagery and spectral datasets used in various stages of this project 30

Figure 2.3 Spectroradiometer field-of-view and associated calculations 32

Table 2.3 Spectral signatures of native and extoic vegetation 34

Table 2.4 Un-manned Aerial System components and characteristics 35

Figure 2.4 Flight plan 37

Table 2.5 Spectral bands of the WorldView-2 and WorldView-3 Sensors 38

Figure 2.5 WorldView Image scenes 39

Table 2.6 WorldView imagery metadata 40

Table 2.7 Ancillary dataset used in various stages of this project 41

Table 2.8 Training samples used in the classification of satellite imagery 42

Figure 2.6 Spectral response functions of WorldView-2 sensor bands 45

Figure 2.7 Georeferrenced photo points 46

Figure 2.8 Pointcloud generated in Pix4Dmapper 47

Figure 2.9 Mosaic editor 48

Figure 2.10 Geometric correction of multi-date imagery 50

Figure 2.11 WorldView-2 (2011) preprocessing images 52

Figure 2.12 WorldView-2 (2011) preprocessing spectral signatures 52

Figure 2.13 WorldView-3 (2015) preprocessing images 53

Figure 2.14 WorldView-3 (2015) preprocessing spectral signatures 53

Figure 2.15 Pampas (Cortaderia Selloana) specimen at Whatipu 61

Table 2.9 Image interpretation elements applied to Pampas 62

Figure 2.16 Pampas (Cortaderia Selloana) specimen at Whatipu, aerial perspective 62

3 Results **64**

Figure 3.1 Features of a typical vegetation curve 64

Figure 3.2 Spectral signatures: raw field signature and simulated WorldView signature 65

Figure 3.3 Mean vegetation spectral reflectance 66

Figure 3.4 Spread of spectral reflectance at WorldView NIR2 band 67

Figure 3.5 Orthomosaic of southern Whatipu 68

Figure 3.6 Red – NIR feature space scatterplots of training data 69

Table 3.1 Statistics of separability analysis 70
Figure 3.7 Comparison of simulated WorldView and satellite derived spectral signatures 71
Figure 3.8 Whatipu Scientific Reserve, showing 2011 supervised classifications 73
Table 3.2 Confusion matrix results of 2011 Supervised classifications 74
Figure 3.9 Whatipu Scientific Reserve, showing 2015 supervised classifications 75
Table 3.3 Confusion matrix results of 2015 Supervised classifications 76
Firgure 3.10 NDVI difference image 79
Figure 3.11 Final manually edited supervised classifications 80
Table 3.4 Whatipu vegetation land cover change statistics 81
Figure 3.12 Example of land cover differences seen imagery and classification (2011-2015) 82
Figure 3.13 Pampas cover in Case study area - Whatipu Scientific Reserve 84
Table 3.5 Case study statistics 84
Figure 3.14 Examples of pampas polygons 84

List of Appendix Figures

Appendix **101**
Appendix 1. Digital Surface Model of southern Whatipu 101
Appendix 2. Shadow Detection Mask 101
Appendix 3. 2011 Training and Validation polygons 102
Appendix 4. 2015 Training and Validation polygons 103
Appendix 5. Satellite derived spectral signatures 104
Appendix 6. Sample area for Change Analysis 105
Appendix 7. 2011 NDVI result (left) and 2015 NDVI result (right) 106

Acronyms

AAT	Automatic Aerial Triangulation
AHS	Airborne Hyperspectral Scanner
ANOVA	Analysis of Variance
ASD	Analytical Spectral Devices
AVHRR	Advanced Very High Resolution Radiometer
AVIRIS	Airborne Visible/Infrared Imaging Spectrometer
AUT	Auckland University of Technology
BBT	Bundle Block Adjustment
CAA	Civil Aviation Authority
CIR	Colour Infrared
DEM	Digital Elevation Model
DOC	Department of Conservation
DSM	Digital Surface Model
EO	Earth Observation
ETM+	Enhanced Thematic Mapper Plus
FOV	Field of View
FWHM	Full Width at Half Maiximum
GIS	Geographic Information System
GPS	Global Positioning Systems
GSD	Ground Sample Distance
IKONOS	Comes from the Greek term eikōn for image
ISODATA	Iterative Self-Organizing Data Analysis Technique algorithm
JERS-1	Japan Earth Resources Satellite -1
LCDB	Land Cover Database
LiDAR	Airborne Light Detection and Ranging
MD	Minimum Distance Classifier
MFE	Ministry for the Environment
MLC	Maximum Likelihood Classifier
MS	Multispectral
NNDiffuse	Nearest Neighbor Diffusion
NVS	National Vegetation Survey
OBIA	Object Based Image Analysis
NASA	National Aeronautics and Space Administration
NDVI	Normalized Differential Vegetation Index
NIR	Near Infrared
NZ	New Zealand
RADARSAT-1	Canada's lst Synthetic Aperture Radar (SAR) satellite
RIMU	Research Investigations and Monitoring Unit
RGB	Red, Green, Blue
RMA	Resource Management Act 1991
ROI	Region of Interest
RS	Remote Sensing
SAR	Synthetic Aperture Rader
SDI	Shadow Detection Index
SPOT	Satellite Pour I'Observation de la Terre
TM	Landsat Thematic Mapper
UAS	Unmanned Aerial Systems
UAV	Unmanned Aerial Vehicles
VNIR	Visual Near Infrared
WV-2	WorldView-2Satellite
WV-3	WorldView-3 Satellite

Attestation of Authorship

I hereby declare that this submission is my own work and that, to the best of my knowledge and belief, it contains no material previously published or written by another person (except where explicitly defined in the acknowledgements), nor material which to a substantial extent has been submitted for the award of any other degree or diploma of a university or other institution of higher learning.

Signed Lawrence

Date 08-05-2016

Acknowledgements

I would like to express my sincere appreciation to my principle supervisor Dr. Barbara Breen for all the advise, support and constant positive input throughout my Masters. It was through her persistence, understanding and kindness that I completed my undergraduate degree and was encouraged to undertake postgraduate education. Also, thank you to my external supervisor Dr. Craig Bishop for your constructive comments and editing of my thesis, and also for providing me with opportunities beyond my research.

I recognise that this project would not have been possible without the support of Auckland Council granting me a research permit at Whatipu Scientific Reserve and the Research Investigation and Monitoring Unit (RIMU) for the Student Partnership Scholarship. Thanks also to Holly Cox from Auckland Council's Biosecurity Team, for funding sensor equipment. And thank you to Jade Khin from RIMU for providing wetland-monitoring data. Thank you to DigitialGlobe Foundation for the satellite imagery grant.

Thank you to those who joined me at Whatipu and helped with fieldwork with such enthusiasm: Phill Wainwright, Dan Breen, Sridevi Ravi, Katrin Hoffmann and Hins Zhang. A special thank you to Megan Teh for your commitment during the trials and tribulations of preliminary flights and to Lorenzo Fiori for your discussions and assistance during flights at Whatipu. Thank you to Dr. John Robertson for all your technical support and helping me get my project off the ground. I would also like to thank all my friends and colleagues at the Institute for Applied Science Postgraduate office for all your support and much needed distractions over the past year: especially Jarrod Cussens, Steph Borelle, Chandima Fernando.

I am also extremely grateful to my family and friends for supporting me in pursuing my goals, in particular my parents; Carolyn and Mark, siblings; Rhys, Marc, Drew and Kelly, and their partners, and girlfriend Clio. Your patience and support throughout will never be forgotten.

Abstract

Wetland vegetation mapping is an important technical task for managing and maintaining essential ecosystem services that wetlands provide. Despite their importance, wetland ecosystems are highly threatened in New Zealand with less than 10% of pre-human extent remaining. Remote sensing has advantages over traditional techniques, allowing non-destructive sampling of resources and enabling users to gain critical information more quickly and cheaply. The potential for remote sensing to provide an increased understanding of coastal wetland environments has not been realized in New Zealand.

The collection and satellite simulation of spectral data for 14 species at Whatipu Scientific Reserve provides valuable information for the application of imagery classification and for future research. Despite low spectral separability between these species, a relatively accurate land cover map was established for each of the multi-date satellite imagery sets, with individual class accuracies between 75% and 99%, depending on vegetation type. This indicates that high-resolution multispectral imagery (2m spatial resolution) such as WorldView 2 and 3 satellite imagery products show good potential for the identification and classification of coastal wetland vegetation.

In addition, although satellite remote sensing platforms are useful for vegetation mapping they still require field training and validation samples. This study investigated the use of low altitude Un-manned Aerial System (UAS) imagery (6cm spatial resolution) for the collection of training and validation data crucial for the classification of multispectral satellite imagery. By using ancillary data and UAS imagery, I minimised the need for extensive field surveys that are potentially destructive, timely and expensive. The land cover changes determined from the multi-date classifications at Whatipu show minimal change in the past 4.5 years, however changes that were detected are significant, particularly with the expansion of exotic shrubland species. The high-resolution UAS imagery also provided sufficient detail to accurately identify exotic Pampas (*Cortaderia Selloana*) in comparison to high-resolution (36cm spatial resolution) satellite imagery products.

1 Introduction and Literature Review

1.1 Wetlands

Wetland ecosystems

Wetlands are ecosystems that appear along elevation and hydrological gradients between terrestrial and aquatic ecosystems. Wetlands are defined as including permanently or intermittently wet areas, shallow water, and land/water margins that support a natural communities of plants and animals that are adapted to wet conditions (Johnson & Gerbeaux, 2004). They perform many valuable functions including habitat provision for vegetation, and other species, flood mitigation, water purification and nutrient removal (Clarkson, Ausseil, & Gerbeaux, 2013).

Despite their importance less than 10 percent of New Zealand wetlands remain, making them a highly threatened ecosystem (Ausseil et al., 2008). In the past wetlands were seen as an impediment to development and access to resources. Wetlands were subjected to fire by early Maori for fishing, horticulture and defense, and drainage by European settlers for agriculture and urban development (Wardle, 1991). Many of the Wetlands in New Zealand are degraded and remain under significant threat from anthropogenic activity. These activities, summarised from Wardle (1991) include on-going loss through drainage and conversion to other land uses, the introduction of invasive species, nutrient enrichment, trampling, dewatering and desalination.

Their importance is specifically outlined in the Resource Management Act 1991 (RMA) where wetlands are identified as matters of national importance and priorities for preservation and protection of wetlands for future generations are made. This is complemented by national policies (MFE, 2008), which contains provisions intended to prevent loss and degradation of freshwater environments, including wetlands. To prevent further wetland loss and conserve existing wetlands for biodiversity and ecosystems services, it is therefore important to inventory and monitor wetlands.

Coastal Wetland Ecological Classification

There are many types of wetland ecosystems in New Zealand. Coastal wetlands in particular, are an important component of the New Zealand landscape. Coastal wetlands are transitional environments found within coastal watersheds and often influenced by both marine and freshwater hydrology. Although typically associated with saline wetlands, coastal wetlands also include freshwater wetland communities that are only occasionally influenced by salt spray. A common example in New Zealand is dune slack wetlands. These form in hollows between sand dunes and comprise complex vegetation mosaics, including restiad rushlands and sedge vegetation communities (Sykes & Wilson, 1987).

The Department of Conservation (DOC) produced a classification system for New Zealand vegetation as a tool to be used in the classification and mapping of terrestrial habitats (Singers & Rogers, 2014). The classification hierarchy is based on key environmental drivers, which included climatic variables, substrates, soils and landforms. This resulted in 152 ecosystems being recognised, 22 of which are recognised as wetland ecosystems and five that are classified as active coastal sand dunes. Wetlands are further divided into three water fertility zones based on Johnson and Gerbeaux (2004) and Dobson (1979), resulting in nine oligotrophic bog classes, eight mesotrophic systems known as fens or marshes, and five eutrophic systems known as swamps or marshes (Singers & Rogers, 2014). Auckland Council recognises 35 indigenous terrestrial and freshwater ecosystems (and their variants) that occur within the Auckland Region (Singers et al., 2013). These classes are based on the ecosystem classification system developed by the Department of Conservation and are intended to be complementary. Of the 22 wetland and five active coastal sand dune ecosystems in DOC's ecosystem classification system, Auckland Council has identified 11 that occur in the Auckland Region (Table 1.1).

These classifications are intended to provide guidance for defining terrestrial ecosystems in efforts related to monitoring and mapping and also provide useful information for remote sensing classification schemes.

Table 1.1 Eleven Wetland and Coastal sand dune ecosystems in the Auckland Region (Singers & Rogers, 2014)

Primary ecosystem driver	Secondary ecosystem driver	Tertiary ecosystem driver	Quaternary ecosystem driver	Ecosystem Unit
Wetland - High water tables permanently or seasonally wet soils	Oligotrophic—low nutrient status and high acidity [Bogs]	Warm temperate	Hillslopes and depressions with kauri podzols, e.g. Wharekohe or Te Kopuru soils	WL1: Manuka–mingimingi–Machaerina scrub/sedgeland
			Depressions or the lagg of raised bogs with organic soils	WL2: Manuka–wirerush–restiad rushland
			Raised bogs on in-filled lagoons/river oxbows with deep organic soils	WL3: Bamboo rush, wirerush restiad rushland
	Mesotrophic—moderate fertility and weak to neutral acidity [Fens and marshes]	Warm temperate to cold	Freshwater margins of estuaries, tidal rivers, coastal lagoons and some inland lakes	WL10: Oioi restiad rushland/reedland
			Depressions, and lake and lagoon margins	WL11: Machaerina sedgeland
			Lake and lagoon margins	WL15: Herbfield (lakeshore turf)
	Eutrophic—high fertility and weak acidity to weak alkalinity [Swamps and marshes]	Warm to cool temperate	Depressions and terraces with recent and organic soils	WL18: Flaxland
			Depressions, and lake and lagoon margins with recent and organic soils	WL 19: Raupo reedland
			Depressions with recent and organic soils	WL 20: Coprosma–Olearia scrub
Active coastal sand dunes	Warm to mild temperate	Semi-arid to humid	Dunes with raw sandy soils in association with atmospheric salinity (e.g. spume and salt-spray)	DN2: Spinifex–pingao grassland/sedgeland
	Warm to cool temperate	Semi-arid to humid	Dune plains (including deflation hollows, dune slacks, damp sand plains and stream terraces) and exposed coastal hill slopes with raw sandy soils	DN5: Oioi–knobby clubrush sedgeland

1.2 Remote Sensing for Wetland Mapping

For inventorying and monitoring wetlands, remote sensing has many advantages. Remote sensing is a relatively low cost means of acquiring continuous data over large areas in often remote and inaccessible locations such as natural wetland environments. It is also a convenient non-destructive tool for efficient mapping of the environment over a range of spatial scales. Remote sensing data are available in digital format and relatively easy to integrate with geographic information systems (GIS). In particular using remotely sensed data for land cover classification can be costly and less time-consuming than traditional field surveys for large geographic areas (Ozesmi & Bauer, 2002).

Many types of remote sensing have been used to study wetlands, beginning with aerial photography in the early twentieth century. Since the 1970's the range of remote sensing option available has considerably increased. The launch of NASA's Landsat satellite in 1972 was heralded as the first earth observation satellite and is considered the global standard for remote sensing satellites (Hamilton, 1977). Since this time the availability of remote sensing, data has helped scientist and land managers to study and map the earth's surface in a wide variety of applications.

The high heterogeneity of wetland vegetation has limited earlier use of satellite imagery for detailed vegetation mapping. However this has become technically feasible with the availability of high-resolution satellite imagery e.g. WorldView-2 (Hassan et al., 2014), IKONOS (Dillabaugh & King, 2008), and Quickbird (Labaa et al., 2008). There are also numerous techniques to extract information from imagery products. Pixel-based supervised classifiers are still the most common image information extraction techniques (Xie, Sha, & Yu, 2008), although other object-based techniques (Lechner et al., 2012) and hybrid techniques (Lane et al., 2014) are also emerging. There are many examples of thematically detailed vegetation mapping using pixel-based techniques with satellite imagery at medium to fine scales in natural environments.

Fine scale vegetation mapping is a complex task. Critical to the success of the classification of satellite images is the collection of training samples. Training samples are usually collected from fieldwork or from high-resolution aerial or satellite imagery. When mapping heterogeneous landscapes the collection of training samples sufficient to describe

classification scheme is often difficult (Lu & Weng, 2007). One of the appeals of remote sensing is the ability to use non-destructive methods, where-by reducing time spent in the field. Collection of training samples from very high-resolution (< 1m) aerial or satellite imagery can be complicated by the coarseness and probability of mixed-pixels that may occur. My research is intended to fill this gap by collecting low-altitude high-resolution imagery to accurately identify vegetation for the collection of training samples.

1.3 Remote Sensing Sensors and Coastal Applications

Remote sensing (RS) imagery can be acquired by sensors onboard a wide range of air-borne and space-borne platforms. Air-borne platforms include Un-manned Aerial Vehicles (UAV) and piloted aircraft, while space-borne refers to satellite platforms. These survey platforms have similar characteristics although the differences in their altitude and stability result in varied image properties (Gomez, 2001) and ultimately determine the capabilities and application of the data collected. In addition, data acquired from RS platforms is captured using a wide variety of sensors. Sensors are often designed to fit the specifications (e.g. specific payload, dimensions, power and capture conditions) of the RS platform and include Red-Green-Blue (RGB), multispectral and hyperspectral sensors with wavelengths ranging from visible to microwave, and with spatial resolutions from sub-meter to kilometers. RS typically depends upon passive energy sources such as the sun or the earth (Aggarwal, 2003) exceptions with LiDAR and radar. Imaging sensors are capable of measuring electromagnetic radiation within wavebands (multiple wavelengths) to discrete wavelengths; each region of wavelength has its own strengths in terms of the information that can contribute to image processing and information extraction. RS operates on the premise that objects (including vegetation) have unique spectral features (of reflectance and absorption) and therefore the objects can be identified from imagery according to their unique characteristics. Many of the Earth's surface materials have diagnostic spectral absorption/reflectance features in the visible through to the shortwave infrared (SWIR) regions of the electromagnetic spectrum. Theoretically these should allow unique identification and mapping of surface material using RS and GIS processes.

A wide range of instruments can be used to collect spatial and spectral information. In the last 50 years of remote sensing research, imagery has been acquired by a range of platforms from airborne to spaceborne using a range of sensors from multispectral to hyperspectral with

wavelengths ranging from visible through near-infrared to shortwave infrared, and spatial resolutions from sub-meter to kilometers with temporal frequencies of daily up to annually. In the following sections, research directed towards wetland mapping is considered under sensor types used in remote sensing of coastal wetland systems.

1. Field spectroradiometers
2. Low to medium spatial resolution optical sensors
3. High spatial resolution optical sensors
4. Imaging hyperspectral sensors
5. Active Systems (radar)
6. Aerial Imagery
7. GIS procedures using imagery

It is important to define the difference between spectral image sensor capabilities (e.g. multispectral and hyperspectral). A generally accepted definition of multispectral sensors is that containing a discontinuous and broad wavebands (e.g. WorldView-3 has 8 wavebands), whereas hyperspectral sensors are capable of viewing continuous wavebands (e.g. AVIRIS has 224 wavebands) typically collecting 200 or more (Richards & Jia, 2005). Note that is not necessarily the difference in spatial resolution between multispectral and hyperspectral data but the spectral resolution that defines a sensors capabilities for vegetation analysis. Furthermore, it is the narrowness and contiguous nature of these hyperspectral wavebands that accomplishes such detailed data sets (Shippert, 2003). Spectral resolution is generally more important for vegetation mapping/analysis especially when targets of interest are highly heterogeneous and contain mixed vegetation communities (Zomer, Trabucco, & Ustin, 2009).

Field Spectrometers

Considered a remote sensing technique in its own right, field spectroscopy is a key tool for understanding and improving image analysis (Adam, Mutanga, & Rugege, 2010). The spectral range covered by spectroradiometers usually starts at visible wavelengths (400nm) and goes up to near infrared (1000nm) or mid-infrared (2500nm). Therefore, most of the reflectance data captured includes responses beyond the wavelengths visible to the human eye.

There are many roles for spectroradiometer data in remote sensing for charactering reflectance of vegetation. Milton et al., (2009) differentiate between the following applications, (1) discrimination of vegetation using airborne and spaceborne imagery, (2) as a source of data for quantitative models and spectral libraries.

The spectral absorption/reflection features of vegetation are not fixed; in fact, the response can vary considerably. The spectral response can vary within an individual plant, species or a community (Fyfe, 2003). Due to the large amount of potential variation within vegetation, Price (1994) suggested that several species may have similar overlapping spectra and may not be unique. Identifying and attributing intra-species and interspecies variation is therefore an important task when attempting to discriminate between species (Hestir et al., 2008). Many studies have successfully discriminated and classified wetland vegetation at multiple spatial scales using field spectroscopy, to then be scaled up to airborne or spaceborne remotely sensed imagery (Cho et al., 2008; Clark, 2012; Schmidt & Skidmore, 2003).

Schmidt and Skidmore (2003) studied spectral reflectance data of 27 coastal saltmarsh wetland species, measured at canopy level using a GER 3700 spectrometer, to evaluate the potential for discriminating species and identifying optimal bands for mapping vegetation in the Dutch Waddenezee wetland. They found six bands in the visible, near-infrared and shortwave infrared were suitable for discriminating species. Cho et al., (2008) compared the spectral response of three shrub and three tree species showing that reflectance in the visible near-infrared in leaves was higher than that of canopy data for all six species measured. Using lab-based hyperpsectral data, collected with a spectroradiometer (FieldSpec Pro FR, ASD), Vaiphasa et al., (2005) were able to distinguish 16 vegetation types in mangrove wetland in Thailand. The results of one-way ANOVA and Jeffries-Matusita (JM) distance demonstrated the best discrimination was possible with four bands located with the red-edge, near-infrared and mid-infrared regions. Similar results where found by Everitt et al., and (2015) and Quyang et al., (2013) both finding that best discrimination for vegetation was found in the NIR region.

Additionally, vegetative responses to changes in the environment and differences in onset of biological queues potentially increase or decrease the likelihood of unique spectra. Many studies have investigated changes in the spectral characteristics of vegetation that correspond to various stages of the phenological cycle (Jakomulska, 2003). Forster and Kleinschmit

(2009) determined that not only was the multi-temporal spectral response of vegetation producing different trends for mixed grasslands when compared to common reed species but they were also able to recognise potential dates of highest differentiation for the vegetative groups respectively. They found that in the near infrared (804nm), which is commonly associated with high separability, that the phenological window for differentiation is greatest during June and July (summer months).

Field spectroradiometer measurements rely on the illumination of the sun as the light source of the sample target. The inability to control the uniformity of illumination makes changing light conditions in the field a common issue, even on clear days. To achieve consistent spectral measurements in the field, it is important to regularly perform instrument calibration using calibration material, often a white reference. These references, such as the Spectralon® (Labsphere Inc.) panels are assumed to have a Lambertian surface with 100% reflectance, thus acting as an ideal diffuse reflector for calibration and baseline measurements.

Low to medium spatial resolution optical sensors

Low spatial resolution is defined as image pixels of the earth surface at ground resolutions 30m or greater, and medium resolution as ground resolutions between 2.0 – 30m (Navulur, 2006). In general, low and medium spatial resolution imagery may be adopted for regional scale mapping when a high-level vegetation class is required (Xie et al., 2008).

Some of the most recognisable satellites providing low to medium spatial resolution imagery used in remote sensing Earth Observation are the Landsat satellite fleet. Since the launch of the first Landsat satellite in 1972, the TM and ETM+ imaging sensors have archived millions of images with nearly continuous records of global surface data. Landsat products have been applied to vegetation mapping and monitoring mainly at regional scales, for example Landsat ETM+ medium resolution imagery combined with ancillary data (topographic and soil) have been used to map wetland vegetation in the southwest Montana, USA (Baker et al., 2006). Multi-temporal Landsat data from 1986 to 2002 were also used to study wetland pattern changes in the Minjian River estuary in China (Zheng, Zeng, & Chen, 2006). Due to differences in Landsat fleet sensors characteristics, this study also highlights the importance of making appropriate calibrations and corrections to imagery prior to spectral comparison.

Medium resolution imagery has also been used for detecting and classifying remote wetlands and classifying saltmarsh habitats in the North Norfolk, UK (Sanchez-Hernandeza, Boyd, & Foody, 2007). Due to the limited spatial resolution Landsat imagery and similar products are usually used to map vegetation at community level (e.g. wetland vs. forest). It is often challenging for low to medium imagery to map at species level, especially in heterogeneous environments.

High spatial resolution optical sensors

High-resolution sensors are those that collect image pixels with ground resolutions of 0.5-2.0m. Most recent satellite spaceborne sensors produce imagery of high spatial resolutions (e.g. the WorldView fleet, Quickbird, IKONOS, SPOT). The technological advances in sensor resolution, traditionally achieved only by airborne sensors, has meant that spaceborne imagery can be used for finer detailed vegetation mapping. This increase in mapping scale allows satellite imagery to be used for local to regional to global vegetation classifications and to be used to validate the vegetation cover in other low-resolution satellite imagery (Xie et al., 2008).

High-resolution imagery from WorldView-2 satellite imagery (0.5m panchromatic and 2m multispectral) has provided useful spatial and spectral information for mapping wetland vegetation. Worldview-2 satellite imagery was used to map dune and marsh vegetation formations on the French Atlantic coast (Rapinel., 2014). They classified WV-2 imagery into 16 natural and semi-natural vegetation types, and five non-natural and non-vegetated classes, aided by ancillary thematic data.

High resolution Quickbird imagery (0.6m panchromatic and 2.4m multispectral) was used to identify and map submerged plants down to species level in lake Mogan, in central Anatolia, Turkey (Dogana, Akyurekb, & Beklioglua, 2009). High resolution Quickbird imagery was also used to map plant communities and monitor invasive plants in the Hudson River Research Reserve, New York (Labaa et al., 2008). Classification of high spatial resolution IKONOS satellite imagery (1m panchromatic and 4m multispectral) also indicates strong potential for mapping wetland vegetation. Twelve vegetation classes of terrestrial and aquatic

vegetation were mapped using IKONOS imagery at three riparian marshes near Ottawa, Ontario (Dillabaugh & King, 2008).

Imagery acquired from high-resolution spaceborne sensing systems can also be integrated with other high-resolution data from airborne platforms. Maxa and Bolstad (2009) combined high-resolution IKONOS imagery with LiDAR-based elevation data in north-central Wisconsin, to map wetland types. They mentioned that the addition of elevation information was particularly useful for distinguishing wetlands from other terrestrial vegetation on sloping terrain.

Hyperspectral sensors

Hyperspectral imaging data is defined as imagery data that has hundreds of narrow spectral bands between 400 and 2500nm of the electromagnetic spectrum (Govender, 2007) and is usually captured with airborne platform (with the exception being the Hyperion spaceborne sensor). This section will focus on the spectral nature of hyperspectral imagery products, not the spatial dimension as depending on the altitude of the aircraft the spatial resolution can vary considerably. Greater spectral information allows more in-depth discrimination of vegetation types and which is often considered to be lacking in multispectral optical sensors (Cochrane, 2000).

Hirano et al., (2003) used hyperspectral Airborne Visible/Infrared Spectrometer (AVIRIS) with 224 spectral bands and 30m spatial resolution imagery to map wetland vegetation in a section of the Everglades National Park, Florida, USA. Another Airborne hyperspectral sensor, HyMap, which has 126 bands, was used to map wetland vegetation communities of the Australian Great Attesian Basin Springs (White & Lewis, 2012). Both studies used hyperspectral imagery to map vegetation down to species level, exlpoiting the high dimensionality and disrciminatory power more spectral information provides.

Hyperspectral imagery has proved to be useful for wetland vegetation discrimination. However, hyperspectral imagery acquisition is often considerably more expensive and more time consuming to process. However, due to advances in smaller more affordable hyperspectral sensors and affordability of unmanned aerial vehicles (UAV's) the potential for high quality multi-temporal hyperspectral data has increased (Jay et al., 2009).

Active Systems

Satellite radar data can be collected any time of day and isn't dependent on weather. Therefore, whilst providing different information to optical sensors, it can be advantageous for remote sensing (Ozesmi & Bauer, 2002). Using ESR-1 synthetic aperture radar (SAR) data to detect the presence of water in wetlands of Big Cypress National Preserve, Florida, USA, Kasiscke and Bourgeau-Chavez (1997) were able to distinguish vegetation communities based on soil moisture and the presence or absence of flooding water, in addition to detecting canopy structure. By integrating radar with optical (multispectral and aerial colour composite) and topographic data, Corcoran et al., (2012), illustrated significant improvements on single data classification for mapping wetland vegetation in Minnesota, USA.

Aerial Imagery

Aerial imagery (photographic/film) was the first form of remote sensing employed for mapping wetland environments. Now aerial imagery comes in a variety of forms including, black and white film, colour film and digital RGB, and is commonly collected by airplanes, although satellites, un-manned aerial vehicles (UAV), balloons and kites are also used. Regarding wetland mapping, aerial imagery is primarily used to provide contextual information for field surveys or training and validation of automated land cover classification.

The long and sustained archive of aerial photography and imagery has become a useful tool for long-term change analysis studies. Lishawa et al., (2013) used multi-temporal aerial imagery to reconstruct *Typha* invasion at ten dates spanning 1955 to 2007 at Illinois Beach State Park, Illinois, and another eight dates spanning 1963 to 2009 at Cheboygan Marsh, Michigan coupled with paleobotanical analysis of pollen cores.

Although similar to other optical imagery (e.g. Multispectral), aerial imagery typically has relatively low spectral resolution and high spatial resolution. Therefore, images are most commonly analysed using manual photointerpretation techniques.

1.4 Remote Sensing Classification

Classification of remotely sensed imagery involves assigning a class attribute to an image pixel, or cluster of pixels. This can be done using manual methods such as visual interpretation and delineation or by using automated computer methods such as un-supervised or supervised classification models. Classifying remotely sensed data remains a challenge because of many factors that may affect the success of a classification including the complexity of the landscape in a study area, the variety of remotely sensed data available, and variety of image processing and classification approaches available to analysts.

Visual Interpretation

Visual interpretation (photo interpretation) of remotely sensed imagery is still a common method in wetland vegetation mapping. Visual interpretation mapping relies on the interpreter to make qualitative decisions based on image elements. The basic elements commonly used to aid visual image analysis and identification of features is: tone, size, texture, pattern, shadow, and geographic location (Ustin, 2004). These techniques aim to introduce consistency to the identification, classification and delineation process. The most common method used to delineate and map vegetation is an on-screen (heads-up) digitising method; traditionally this was done on paper. This process involves viewing digital imagery on a screen and digitising features over the imagery.

Using manual interpretation methods, Harvey and Hill (2001) mapped fourteen tropical freshwater swampland cover types in Northern Australia, using airborne aerial imagery. They also compared accuracies with automated classification of satellite imagery and found manual interpretation provided superior detail, although more time intensive.

Visual interpretation to classify wetland land cover isn't limited to aerial (airborne) imagery. High-resolution satellite imagery IKONOS was used to manually interpret wetland types in north-central Wisconsin (Maxa & Bolstad, 2009). High-resolution (2m) multispectral WorldView-2 imagery was used to map 15 species in the Paya Idah Wetlands, Indonesia (Salari et al., 2014). To enhance discrimination visual interpretation of true and false color images the interpreter used various reflectance-band combinations.

Recent advances in un-manned aerial vehicle platforms for capturing digital imagery, typically of high spatial, but low spectral resolutions, has shown that visual interpretation for fine scale mapping is a suitable method to extract meaning information (Samad et al., 2013). The ultra-high resolution of imagery provides for accurate identification of fine scale image objects.

Although visual interpretation of imagery is useful for mapping wetlands, most recent research has focused on using automated classification techniques to save time and reduce cost of mapping efforts.

Pixel-Based Classification

Remote sensing of vegetation has previously been dominated by pixel-based methods such as supervised or un-supervised classification methods. These methods employ cluster classification algorithms, e.g. K-mean and ISODATA for unsupervised and Maximum Likelihood Classification (MLC) for supervised classifications.

The unsupervised classifiers are iterative clustering algorithms that operate by relying only on pixel-based spectral statistics to establish the classification themes. No training data is required to define the class themes. These algorithms are widely available in image processing and statistical analysis software and often used as an exploratory method to indicate dissimilarity between potential themes. An advantage of this method is the time consuming training phase of supervised classification methods is avoided.

For example, an unsupervised classification procedure was applied to a wetland area in Turkey to identify vegetation to near-species level; some classes were grouped due to spectral similarity to form community level classes (Dogana et al., 2009). The authors also used a value-based mask to reduce data and remove water features.

By contrast, a supervised classification algorithm clusters pixels by user-defined training data to establish the classification themes. The training data usually consists of areas of pixels of known identity to train the algorithm to recognise pixels outside of the training areas. Supervised methods are usually preferred to un-supervised methods because the classes of interest are predefined often increasing the output accuracy is often increased.

An example of the MLC was used to produce 20-class land cover maps for four marshland habitats within a reserve (Labaa et al., 2008). Overall, classification accuracies of 73.6%, 68.4%, 67.9%, and 64.9% are encouraging results that MLC classification offers significant potential using high-resolution satellite imagery.

Pixel-based methods are still commonly used, especially for broad scale vegetation mapping; however managing land cover classifications at the spatial scale of pixel can introduce significant weaknesses. A persistent issue is that a pixel may not equal that of the land cover feature of interest, or that of mixed pixels, whereby the pixels spatial extent covers more than one type of land cover class, producing pixel misclassification (Aplin & Smith, 2008). One solution to the problem associated with pixel based classification methods may be to operate at the spatial scale of the object of interest, rather than relying on the extent of image pixels.

Object-based Classification

High resolution imagery pixels are typically much smaller than the objects being classified, object-based image analysis (OBIA) not only uses the spectral information used in pixel-based methods, but can also include textural, structural and relational information on image objects (Aplin & Smith, 2008). This is particularly important when classifying features within wetlands using remotely sensed imagery, because the fine scale of wetland floral variation and the low degree of spectral dissimilarity makes delineation of features a persistent challenge.

The development of robust object orientated classification techniques is well suited to the development of the high-resolution imagery products and capabilities and provides a valid alternative to the ‘traditional’ pixel based classification techniques. Since the emergence of high spatial resolution satellite sensor imagery (WorldView, SPOT, IKONOS etc.), object-based classification has been applied extensively to this type of data in an attempt to overcome pixel-based misclassification and within-object variation that can lead to misclassification with low spatial resolution satellite imagery.

By removing the possibility of misclassifying individual pixels, OBIA classification methods can be more accurate than pixel-based. Whiteside and Ahmad (2015) found object-based

methods generated better accuracy results than pixel-based classification methods when mapping broad scale land cover with medium spatial resolution multispectral ASTER data. Weih and Riggan (2010) also compared object-based vs. pixel-based classification for land-use/land-cover mapping applications and found that when combining colour infrared (CIR) high-spatial aerial imagery with medium resolution SPOT-5 satellite imagery, an object-based classification will outperform both supervised and unsupervised pixel-based classification methods. They also emphasised the importance of high-resolution (1m) imagery, concluding that the presence of HSR imagery improved classifiers more than multi-temporal datasets, especially with object based classifications. However, Fernandes et al., (2014) demonstrated OBIA classification was more accurate and less complex when produced from a multispectral satellite image (WorldView-2) than in airborne images (2 meter and 0.5 meter spatial resolution respectively).

Current literature regarding OBIA is dominated by high-spatial resolution satellite imagery applications. There are however a few applications using OBIA on very high spatial resolution (VHR) captured from air-borne platforms; e.g. Giljum (2014) used OBIA to classify Helicopter borne VHR (8cm) imagery (RGB), although map accuracy of 60% it is promising.

However Visser and Wallis (2010) found when mapping submerged Chalk stream macrophytes with sub-centimeter spatial resolution CIR imagery, the accuracy of the object-based method was considerably lower than the pixel-based classification (Maximum Likelihood) method tested. This is most likely due to underdevelopment of the rule set that defined the OBIA. It is likely that development of more sophisticated rule set defining the image object attributes will increase the accuracy of OBIA, although this is both time consuming and in some case requires expert botanical knowledge.

Typically, the presence of high spatial resolution imagery has greater impact on the classification success of imagery than the type of classification method used in to process the imagery. The use of OBIA in combination with very high-resolution imagery, such as that acquired from UAS is a promising direction for improved wetland classification accuracies.

Hybrid Approaches

Combining classification has also shown to increase mapping accuracies. Using a hybrid pixel-based and object-based approach with additional ancillary thematic data Rapinel et al., (2014) yielded kappa indexes varying from 0.90 0 0.88 for classifications. They also compared the hybrid approach against standalone pixel-based methods and found that difficulties spectrally separating natural vs. non-natural vegetation classes was reduced in the object-based approach by the addition of contextual information.

Pixel based hybrid classification approaches using additional metrics derived directly from the satellite imagery have also proven to improve classification accuracy. Lane et al., (2014) used additional normalised difference vegetation index (NDVI) and image texture metrics to classify 22 classes of aquatic and wetland habitats, improving overall accuracy from 82.9% using all eight WorldView-2 bands, to 86.5% with the addition of NDVI and texture metrics.

1.5 Remote Sensing Training and Validation Datasets

Critical to the success of image classification is the collection of training and validation samples. Training and Validation datasets are a set of measurements (e.g. points, pixels, and polygons) whose class is known by the analyst. These datasets must be collected based on information derived directly from the imagery (to be classified) or from aerial imagery, field surveys, or thematic maps. Collecting sufficient training and validation samples is a prerequisite for imagery classification processing. Training samples are used to train the supervised classification algorithms to identify unknown pixels, whereas validation samples are used during the accuracy assessment to test the quantity and or percentage of correctly classified image pixels.

It is recommended that training and validation samples be used independently, although the same collection strategy should be employed for each dataset so they are equally representative of class populations. Typically, the more samples the better, as increasing the sample size tends to increase characterisation of the class populations (Foody et al., 2006). Although collecting more samples often requires more time and effort, either in the field (GPS) or on-screen digitising.

There are three generally recognised strategies for collecting training and validation sample: single-pixel, block-pixel and polygon. Chen and Stow (2002) investigated the effect of these training strategies on classification accuracies. For spectrally homogenous classes, a single-pixel approach was more successful. For spectrally heterogeneous classes block-pixels or polygons was advantageous, and reduces collection time to define class populations. Another consideration must be made for the spatial resolution of the remote sensing data in light of probability of mixed pixel occurrences (where a single pixel represents multiple classes) (Lu & Weng, 2007). Therefore the spatial resolution, complexity of the landscape and availability of ground reference data must be considered when selecting training and validation data.

1.6 Change Detection

All wetlands are dynamic. They change over both short and long time scales, and at continuous or periodical rates (Johnson & Gerbeaux, 2004). As wetland conditions change, so too does the vegetation in a process known as succession. Detecting change due to external pressures is an important aspect of understanding the natural world. According to Singh (1989), "Change detection is the process of identifying differences in the state of an object or phenomenon by observing it at different times." Analysing temporal effects of change using multi-temporal datasets is the foundation of change detection. In principle the process of assessing change is quite simple; it involves the comparison of two or more images of the same areas, at different times, to detect changes in wetland area, composition or structure. However, change detection within wetlands is a difficult task to perform with remotely sensed imagery, made more difficult because of the high natural temporal variability within wetland ecosystems. Singh (1989) highlighted the need for comparable data types, acquisition dates and analysis techniques to get a better change detection outputs. Emphasis on accounting for additional factors like difference in sensor calibration, atmospheric condition, scene illumination, whilst also making considerations for the different spectral properties of land cover features.

Lu et al., (2004) reviewed various change detection techniques using remotely sensed data, like univariate image differencing, image regression, image ratioing, vegetation index differencing, principal component analysis, post-classification comparison, direct multi-date comparison.

1.7 Wetland Remote Sensing in New Zealand

Remote sensing has played an important role in assessing and monitoring wetland environments in New Zealand. The use of Remote sensing data dates back to the early twentieth century, with Crown aerial survey archives from 1936 onwards.

Cochrane and Male (1977) used Landsat TM imagery to map seasonal sediment discharges along the New Zealand coast. Satellite remote sensing is also widely applied in New Zealand. Dymond et al., (1996) used Landsat TM imagery to map vegetation distribution and patterns in Gisborne. Israel & Fyfe (1996) used SPOT XS imagery to detect estuarine intertidal and sub-littoral vegetation and to monitor the health and distribution of eelgrass communities in Otago. Gao et al., (2004) classified and mapped mangrove wetland forests within Waitemata Harbour, Auckland, using SPOT imagery. They were able to identify and determine relative mangrove health and accurately mapped 83% of stunted and 96% of lush mangrove forests using a knowledge-based approach.

Several classifications of ecosystems and communities have been produced in New Zealand, usually related to particular biomes or geographic areas. The New Zealand Land Cover Database (LCDB) classified 33 classes of land cover and land use from satellite imagery, of which four are related to wetland ecosystems. Now in the fourth version, the analysis was initially done using the *SPOT* satellite imagery from 1996/97 and *Landsat -7 ETM+* from 2001/2 and more recently from the Quickbird or IKONOS. The LCDB provides a consistent minimum mapping unit of 1 hectare across all versions. LCDB was created to classify the national extent of New Zealand by the land cover and land use for monitoring the landscape changing overtime and its management (Thompson, Grüner, & Gapar, 2003).

A review of the potential use of satellites in New Zealand for mapping freshwater environments by Ashraf et al., (2010) identified several suitable platforms. However, they concluded that using high spatial and spectral resolution images fit better in assessing freshwater environments.

1.8 Introduction to Whatipu Wetland

Whatipu Dune Wetland Complex

The Whatipu wetland is one of New Zealand's most dynamic wetland systems and as a result provides an outstanding location to apply remote sensing techniques to assess and monitor wetlands. The wetland contains a wide range of environmental gradients that provide habitat for an even wider range of vegetation communities. In this landscape dominant habitats include dunelands, duneslacks, sand rivers, sandflats and stabilised rear dune. These habitats form complex and heterogeneous vegetation composition and associations (e.g. various mixes of indigenous and exotic vegetation). The physical drivers at Whatipu include, progradation of coastline sediments (Williams, 1977), dune development and relative levels of water inundation from feeder streams and the naturally high rainfall. The landscape is also highly modified from a century and a half of agriculture and industrial pressure (ARC, n.d). Dune slack wetlands at Whatipu are primarily restiad Oioi (*Apodasimia similis*) rushland and dune lakes tend to harbor stricter wetland species such as *Schoenoplectus tabernaemontani* and *Machaerina articulate*, while dominant exotic species (e.g. *Cortaderia spp. Ulex europaeus, Lupinus arboreus, Pennisetum clandestinum*) are usually found on dune habitats (foredunes, stabilised reardunes and duneflats) (Pegman & Rapson, 2005). The southern American Pampas grasses (*Cortaderia jubata* and *C. selloana*) are environmental weeds and pose a high threat to the structure of dunes and the survival of rare native species at Whatipu (Gosling, Shaw, & Beadel, 2000). Both *Cortaderia spp.* found in New Zealand are present at Whatipu, of which is considered the highest priority site in the Auckland region due to its significant ecological values and the potential impacts of Pampas on the dune wetlands systems and coastal habitats (Craw, 2015). Pampas is widespread at Whatipu and is common beneath the cliffs, on the old fore-dunes and on the raised shrubland belt behind the old fore-dunes. Pampas is also scattered throughout the mosaics of permanent wetlands, and on the edges of ephemeral wetlands and sand river habitats.

1.9 Research problems, aims

This thesis will improve on previous mapping efforts by using satellite remote sensing techniques to investigate the spatial and temporal nature of coastal wetland vegetation of Whatipu Scientific Reserve.

This research aims to determine spectral signatures of common species at Whatipu Scientific Reserve to assess the spectral separability and determine if species-specific spectral signatures are unique. Fourteen native and exotic species were sampled and representative signatures were developed and implemented in a spectral library.

This research aims to identify land cover through the use of satellite imagery at Whatipu Scientific Reserve. This research created a classification map using field spectroradiometer data, low altitude UAS aerial imagery, and eight-band multispectral WorldView imagery. The classifications were carried out on the multispectral satellite imagery. The high resolution UAS imagery was used as a non-destructive alternative to ground surveys for the collection of training and validation.

This research also aims to assess the use of low altitude very-high resolution aerial imagery and high-resolution satellite imagery using manual visual interpretative methods for detecting invasive weed species. By applying this technique to a subsection of both imagery datasets within the Whatipu reserve, a species-specific classification map was created and classification results were compared. These results were also compared with the final classification results of the automated classification procedure.

This research was done using remote sensing software and GIS that helped with identification of vegetation and detection of change in vegetation cover.

1.10 Objectives

Objective One: Use field hyperspectral reflectance measurements to develop spectral signatures of dominant wetland and dryland vegetation at Whatipu and to assess their spectral separability.

Objective Two: Investigate the use of low altitude, high spatial resolution Unmanned Aerial System imagery for ground-truthing (training and validation sample collection) of satellite imagery classifications.

Objective Three: Compare performance of pixel-based classification methods using high-spatial multispectral satellite imagery to identify dominant wetland vegetation at Whatipu wetland dune complex.

Objective Four: Undertake change analysis to identify if and how Whatipu vegetation has changed between 2011 and 2015.

Objective Five: Case Study: Investigate the use of low altitude, high spatial resolution Unmanned Aerial System imagery for identification and delineation of invasive species at Whatipu.

1.11 Structure of Thesis

Chapter 2 of this thesis comprises a critical assessment of literature relating to New Zealand wetlands and remote sensing research and techniques. It investigates different remote sensing methodologies for extracting meaningful information and the value of remote sensing as a tool for mapping, monitoring of wetlands.

In Chapter 3, focuses on the acquisition of remote sensing datasets and the methodology to preprocess the datasets for classification. It then looks at classification scheme and classification techniques used to derive land cover classes of vegetation and non-vegetated cover at Whatipu, followed by the Change analysis techniques used to determine how land cover has changed between 2011 and 2015. This chapter is concluded by the Case Study methodology used to investigate the potential of low altitude UAS imagery for identifying invasive species in Whatipu.

Chapter 4 presents the results of field spectroradiometer data analysis, classification outputs and accuracy comparisons. The final land cover thematic maps and results are then shown, along with the change analysis results and the results of the Case study.

In Chapter 5, the results of spectral reflectance data analysis, the training datasets, classification outputs, validation datasets and the Case study are then discussed with regard to relevant literature.

Conclusions arising from this research are presented in Chapter 6.

2 Methods

2.1 Study Area

New Zealand has few remaining intact, natural areas of active duneland, and there is limited spatial information describing their vegetation. Whatipu scientific reserve remains, one of the few large areas of intact duneland systems in New Zealand (Hilton, Macauley, & Henderson, 2000). The reserve is situated on Auckland's west coast, on the northern side of the entrance to the Manukau Harbour (Figure 2.1). The area covers 820ha from Whatipu to Karekare point and is made up of extensive low-lying wetlands and coastal dunelands and sandflats.

Whatipu contains a wide range of habitats for flora and fauna, including: foredune, duneslack wetlands, dune lakes, and native and exotic scrub (Pegman & Rapson, 2005). The vegetation at Whatipu consists >100 species of native and exotic vegetation including stabilising communities, foredune communities, herb meadows, and wetland communities. Pegman and Rapson (2005) identified 12 major vegetation communities in the southern end of Whatipu including wet and sandy communities.

The major drivers of vegetation community distribution at Whatipu are identified primarily as geomorphological dynamics (fluctuating coastal dune accretion and erosion, and mobility of dunes) (Pegman & Rapson, 2005) and to a lesser extent hydrological regime. The area has a dynamic history of beachfront progradation (Williams, 1977) and has been significantly influenced by disturbances such as stock grazing up until the 1970's and commercial logging between 1850 and 1911. The substrate is fine predominantly fine sand made up of quartz, feldspar, augite originated from Awhitu peninsula to the south, and titano-magnetite from Taranaki volcanic region (Williams, 1977). The Whatipu beach, dunes and wetlands border the Waitakere Ranges reaching heights of 200m and contain historic sea caves. The Whatipu dune lands are a relatively recent addition to the north island landscape, forming over the last 150 years. Since European arrival and the subsequent forest clearance in the mid 1850's sediment discharge from the harbours rapidly increased, likely causing the accretion of sediments recorded at Whatipu (Williams, 1977).

Because of this unique environment, Whatipu is protected as a Scientific Reserve by the Department of Conservation in 2001 under the Reserves Act (1977) and managed by Auckland Council Regionals Parks administration. Declaration as a Scientific Reserve

restricts access to dogs and vehicles whilst allowing for the protection and preservation of the area for scientific study, research, education and the country's benefit. Current uses of the area include fishing, walking, camping and birdwatching.

The regional climate is sub-tropical temperate. Based on 30-year observations between 1981 and 2010, the areas annual rainfall is between 1200 and 1300 mm and median annual average temperature between 15 and 16°C (NIWA, 2013). Prevailing southwesterly winds are generally moderate to strong, especially on exposed coastal sites. Auckland airport, east of Whatipu, inside the Manukau Harbour receives an annual wind speed of 19 km/hr (9.7knots) (NIWA, 2013).

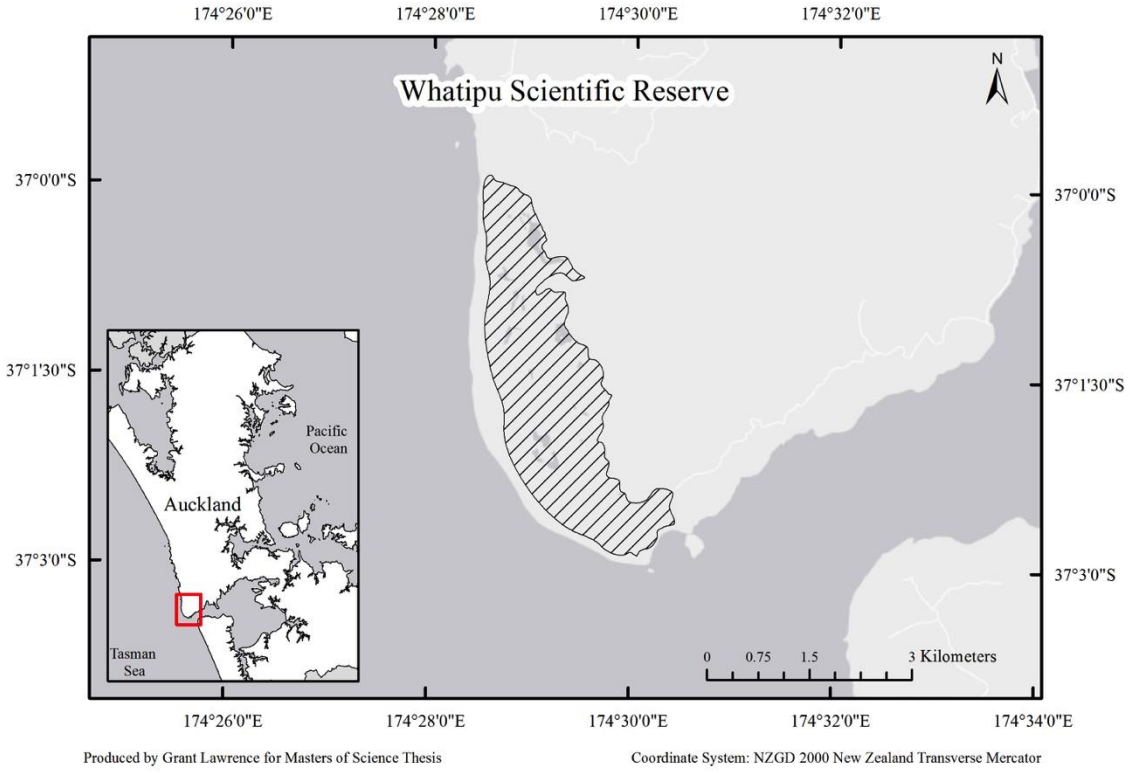

Figure 2.1 Whatipu Scientific Reserve (not the official boundary).

Case Study Area

The area chosen for the multi-sensor invasive species detection case study is in the southern section of the Whatipu Scientific Reserve (Figure 2.2). All three data sets used for the comparison have sufficient overlap in this section of the reserve. The southern area is significantly more modified than the rest of the reserve due to access from the Whatipu road and the settlement and historical grazing access from the adjacent farm, although doesn't necessarily represent the area where Pampas is most dense.

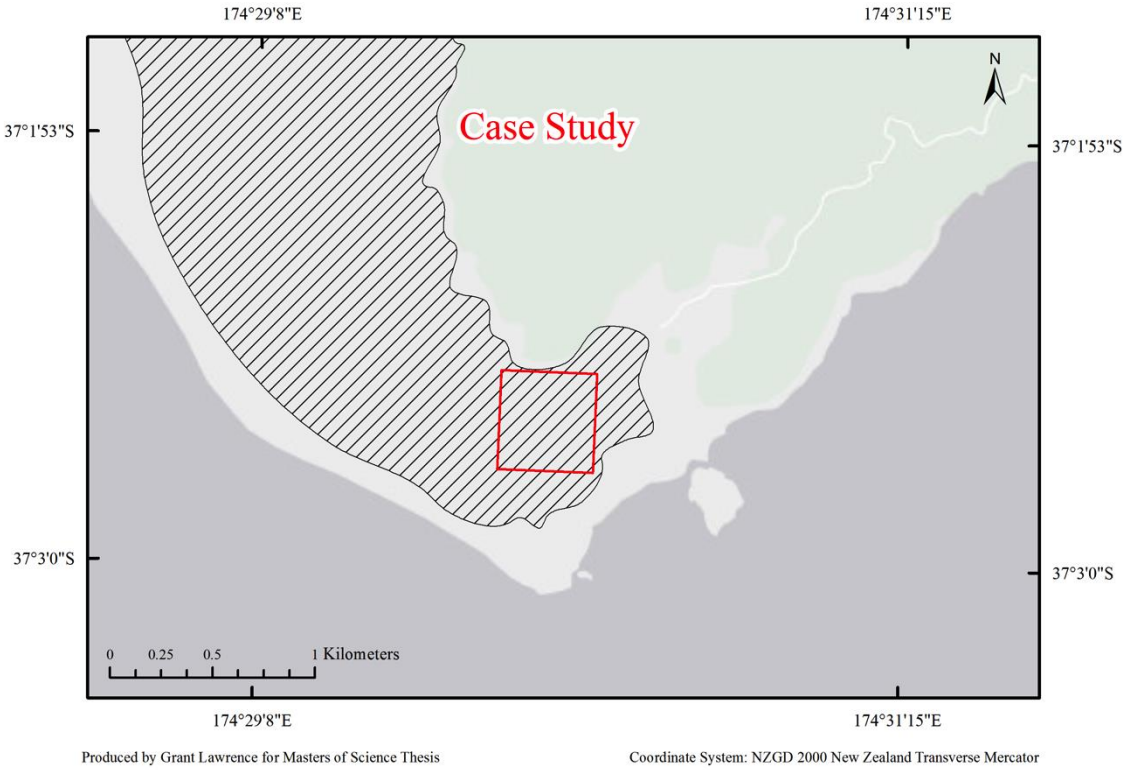

Figure 2.2. Case study area

2.2 Wetland Classification Scheme

Details of the classes to be used in this study can be found in Table 2.1. Preparation of classification scheme is a perquisite in the classification process. Many plants grow equally well in wetland conditions and upland or dryland conditions. To clarify what plants may be found the wetland site, a list of wetland species was used; "*Wetland Indicator Status Ratings for New Zealand Species"* (Clarkson et al., 2013) in the National Vegetation Survey (NVS) Database. In the listing, wetland plants are divided into five indicator categories based on the frequency of occurrence in wetland (Clarkson, 2013).

- Obligate (OBL): almost always in wetlands
- Facultative wet (FACW): usually found in wetlands
- Facultative (FAC): sometimes found in wetlands
- Facultative upland (FACU): seldom found in wetlands
- Upland (UPL): rarely found in wetlands

This list provided useful information about the species distribution that could be expected at Whatipu. The wetland indicator statuses were used as a guide to develop the wetland and non-wetland classifications along with additional literature with information specific to Whatipu vegetation distribution and the assemblages and communities commonly found there (Pegman & Rapson, 2005). Common or dominant species within the wetland were grouped aided by their wetland indicator status. Obligate and Facultative wetland status species were used to classify areas of strict wetland and Facultative and Facultative upland were used to classify areas in ephemeral and drier wetland areas, these also aligned with the community assemblages noted by Pegman and Rapson (2005) and dominant land cover types established by Thomas Civil and Environmental Consultants (Dixon, 2013).

Table 2.1 Whatipu classification scheme

Land cover Type	Class	Dominant Species Code	Rating	Origin
Wetland vegetation	*Apodasmia similis* rushland	APOsim	FACW	Endemic
	Eleocharis acuta rushland	ELEacu	OBL	Non- Endemic
	Schoenoplectus tabernaemontani reedland	SCHtab	OBL	Non- Endemic
	Typha orientalis reedland	TYPori	OBL	Non- Endemic
	Machaerina articulate reedland	MACart	OBL	Non- Endemic
	Pennisetum clandestinum grassland	PENcla	N/A	Exotic
	Native shrubland	CORaus	FACW	Endemic
		PHOten	FACW	Endemic
		LEPsco	FAC	Non- Endemic
		COProb	FACU	Endemic
		FICnod	FACU	Non- Endemic

		MELram	FACU	Non- Endemic
		MUEcom	FACU	Non- Endemic
	Exotic shrubland	CORsel	FAC	Exotic
		LUParb	UPL	Exotic
	Ulex europaeus shrubland	ULEeur	FACU	Exotic
Duneland vegetation	*Spinifex sericeus/Ficinia spiralis* duneland	N/A	N/A	
	Carex pumila sandfield	CARpum	FAC	Non- Endemic
Un-vegetated	Openwater			
	Un-vegetated sand			

Only dominant cover species were selected for the classification of the scene. Selecting dominant species was undertaken because the number of species found in the wetland (>100 native and exotic species) would require extensive field surveys to spectrally characterise each of the species and to collect spatial information for ground-truthing (training and validation). Additionally dominant species composition can often tell a lot about other species that may be there by association and is common practice in habitat remote sensing (Cho, Malahlelac, & Ramoeloa, 2015). Including too many species in the classification request can also lead to misclassification if the species are relatively uncommon in the scene.

2.3 Datasets and data acquisition

Spectral reflectance data was used in this study to assess the spectral separability of common duneland and wetland species at Whatipu and to characterise their spectral variability for future use. The low-altitude aerial imagery captured using the Un-manned aerial vehicle (UAS) was collected in place of undertaking extensive field surveys for ground-truthing (training and validation sampling) of satellite classifications. It was also used in the case study assessing the effect of image resolution for detection of invasive species using manual visual interpretive techniques. The multi-date WorldView (2 & 3) satellite imagery was used for automated classifications and change analysis of land-cover at Whatipu. Table 2.2 shows the characteristics of key image and spectral dataset used in this study.

Ancillary datasets contributed to the creation of training and validation samples. Training and validation samples creation are technically a processing step in the creation of automated classification, however due to their importance they have been treated as an independent dataset and described in this section.

The following datasets were fundamental for the development of the multi-date vegetation maps, change analysis and for the case study of this project.

- *Spectral Reflectance Data*
- *Low Altitude Aerial Imagery*
- *Satellite Imagery*
- *Ancillary Data*
- *Training and Validation Data*

Table 2.2 Key imagery and spectral datasets used in various stages of this project.

Contribution		Dataset Information					
Project stage	**Contribution**	**Data Sets**	**Platform**	**Acquisition Date**	**Spatial Resolution**	**Spectral Resolution**	**Source**
Time 1 (2011)	Automated classification	WV-2 Multispectral Imagery	Satellite	April 2011	2m	8 Band	DigitalGlobe
	ROI and validation	WV-2 pan sharpened	Satellite	April 2011	50cm (panchromatic)	3 Band (RGB)	DigitalGlobe
	ROI and validation	Colour composite Aerial Imagery	Piloted Aircraft	January 2011	1m	RGB	Land Information New Zealand (LINZ)
Time 2 (2015)	Automated classification	WV-3 Multispectral Imagery	Satellite	January 2011	1.2	8 Band	DigitalGlobe
	ROI and validation	WV-3 pan sharpened	Satellite	January 2011	36cm (panchromatic)	3 Band (RGB)	DigitalGlobe
	ROI and validation	Colour composite Aerial Imagery	UAS	February 2015	6cm	RGB	Collected in this study
	Spectral analysis	Spectral reflectance signatures	Hand-held Spectroradiometer	February 2015	n/a	Hyperspectral	Collected in this study
Case Study	Manual classification	WV-3 pan sharpened	Satellite	January 2011	36cm (panchromatic)	3 Band (RGB)	DigitalGlobe
	Manual classification	Colour composite Aerial Imagery	UAS	February 2015	6cm	RGB	Collected in this study

Spectral Reflectance Data

An ASD® FieldSpec® HandHeld 2™ Spectroradiometer (Analytical Spectral Devices Inc.) was used the capture the reflectance measurements of vegetation at Whatipu. This instrument measures in the VNIR (Visible Near-Infrared), sensitive in wavelengths from 325 to 1075nm with a sampling interval of 3nm. These data points are automatically interpolated by cubic-splines to produce 1nm interval data points. Only bare fiber with 25° field-of-view was used for the sampling in this study.

A Handheld GPS was used to capture location of each sample, a Sony point-and-shoot camera was used to document and ID filed objects and metadata were manually collected, recorded, and tabulated on field sheets. Spectral data, GPS, photos and metadata were transferred to a laboratory work station where they were read by the customised software and stored in a format to be transferred the spectral a database at a later date.

Metadata is important for the interpretation of scientific data, quality assessment and long-term feasibility of the spectral data sets (Huni et al., 2007). In order to better understand electromagnetic radiation and vegetation relationships, contributing absorption/reflectance needs to be correctly identified and attributed. This can be assisted by vigorous collection of metadata enabling outliers to be excluded to maximise a true reference spectra. The factors that affect standardised measurements for spectral information are summarised to include: environmental, viewing geometry, illumination geometry, properties of the target, and the calibration of the instrument and reference standard (Pfitzner, Bollhofer, & Carr, 2006; Zomer & Ustin, n.d.).

Spectral Sampling

All sampling was undertaken in late February 2015, during 2hrs either side of solar noon to ensure high sun angle and direct line to the sun resulting in adequate lighting thereby reducing shadowing. Weather conditions during time of collection were variable, an effort was made to limit sampling during times of high cloud cover. Sampling area was limited to the southern end of Whatipu in areas visible in imagery captured by Satellite and UAS sensors. The southern area of the Whatipu wetland was chosen due to its accessibly and proximity to the public car parking at the main public entrance Whatipu Beach. Samples were

typically taken from specimens on the fringe of the wetland, as access to the wetland was limited to tracks and near tracks.

Standards for the collection of field data were:

- Only cloudless conditions were used
- Readings were taken from nadir
- Recalibrate after eavery set or when illumination conditions change
- An average number of 10 samples were collected per species
- The samples were averaged over 10 readings internally by the spectroradiometer
- Collection of spectra took place between two hours of solar noon
- A bare fibre optic with a 25° field of view was used
- Homogenous targets were selected to provide the best endmembers possible
- The height above the targets was kept approximately 0.15 metres. The resulting FOV was 22 cm in diameter (see figure 2.3)

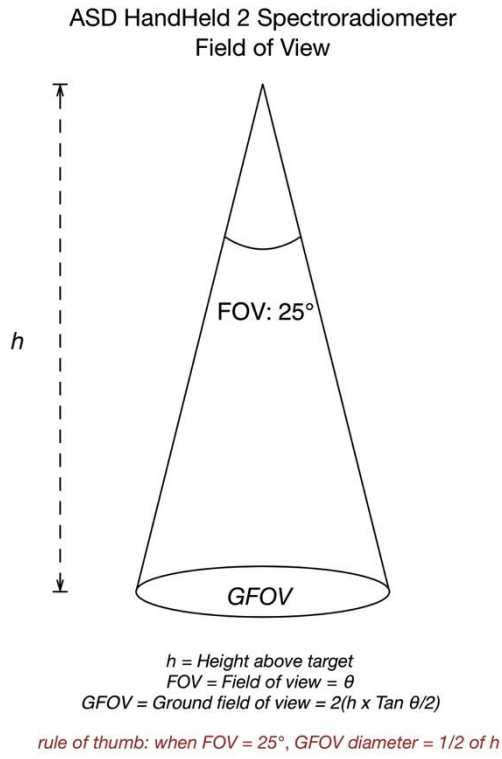

Figure 2.3 Spectroradiometer field-of-view

For calibration a Spectralon® white panel (99% reflectance) was used at the time of measurement the time of measurement and/or when there was a change in illumination conditions. Calibration comprises measuring irradiance that is used to convert incoming radiance to reflectance. At times weather conditions during time of collection were extremely

variable, an effort was made to limit sampling during times of high cloud cover. In some situations, the capture of extraneous materials such as leaf litter, soil or other vegetation could not be avoided due to the sparse foliage structure of some species. Reflectance samples of several species were collected, which included several specimens per species to account for intraspecies (in-species) variation. The number of spectra captured per species varied slightly with the size or variation exhibited by the individual specimens, and an effort was made to randomise sampling from different areas of the individual with consideration for different vegetative components.

Spectral Data

Spectra of a total of 14 species were collected (see Table 2.3). The species assembled are by no means sufficient to characterise the variety found in New Zealand or the Whatipu vegetation. However, as a first step the number and variety collected suffices for the purpose of assessing the spectral separability and classification of some New Zealand native vegetation and determinng the possibilty for classification success in imagery. Field spectra were evaulauted and visually inspected for their quality and categorised in the species classes.

Table 2.3 Spectral signatures of native and extoic vegetation collected at Whatipu

Latin name	**Common name & Maori name**	**Species code**	**Structural Class**	**Total Spectra**
Apodasmia similis	Jointed wire rush, Oioi	APOsim	Rushes	54
Coprosma robusta	Karamu	COProb	Dicotyledonous Trees & Shrubs	20
Cordyline australis	Cabbage tree, Ti kouka	CORaus	Monocotyledonous Trees and Shrubs	9
Cortaderia selloana	Pampas grass	CORsel	Grasses	17
Eleocharis acuta	Sharp spike sedge	ELEacu	Sedges	14
Ficinia nodosa	Knobby club rush, Wiwi	FICnod	Sedges	22
Leptospermum scoparium	Manuka, kahikatoa	LEPsco	Dicotyledonous Trees & Shrubs	26
Lupinus arboreus	Tree lupin	LUParb	Dicotyledonous Trees & Shrubs	33
Melicytus ramiflorus	Whitey wood, Mahoe	MELram	Dicotyledonous Trees & Shrubs	23
Muehlenbeckia complexa	Wire vine, scrub Pohuehue	MUEcom	Dicotyledonous Lianes	11
Pennisetum clandestinum	Kikuyu grass	PENcla	Grasses	7
Phormium tenax	Flax, Harakeke	PHOten	Monocotyledonous Herbs	19
Schoenoplectus tabernaemontani	Kuawa	SCHtab	Sedges	15
Ulex europaeus	Gorse	ULEeur	Dicotyledonous Trees & Shrubs	20

Low Altitude Aerial Imagery

The low altitude high resolution aerial imagery was acquired in the southern region of the Whatipu Scientific reserve covering approximately 100 ha of the wetlands and dunelands. Aerial imagery for this project was collected using an Un-manned Aerial System (UAS) made up of off the shelf products (Table 2.4). The UAS flight areas were located within the reserve and conducted with the permission of the Auckland Council. We successfully conducted 31 flights over six days in early march 2015 and collected 15,195 images.

The quadcopter is small (465 x 465 x 190 mm) and lightweight (1200 – 1300g including sensor and battery). Because the quadcopter has a small payload capacity (250g), we used a lightweight (122g) compact digital camera (Sony, Action Cam, HDR-AS100v, Tokyo, Japan) as the image sensor. It was additionally chosen for image georeferencing functionality. The camera was mounted underneath the quadcopter and captured images in interval mode (1 per second). The UAS has a continuous flight time of 8-10 minutes requiring battery replacement after each flight and has a horizontal flight range within 800m of the operator (due to radio transmitter limitations and Civil Aviation Authority line of sight restrictions). The maximum vertical height was programmed to 50 m to ensure a high-resolution product. UAS flights are highly dependent of weather and could only be conducted in fine conditions with no rain and light wind (<10knots).

Table 2.4 Un-manned Aerial System components and characteristics

UAS	Components	Weight (g)	Price(NZD)
Quadcopter	Blade® 350 **QX2** Quadcopter	1006	500_{each}$
	Blade® 350 **QX3** Quadcopter	955	
Battery	2200 mAh 11.1 30c Li-Po Battery &	188	50_{each}$
	3000 mAh11.1 30c Li-Po Battery	253	
Transmitter	Spektrum 6-Cahnnel Transmitter	n/a	$400
Sensor	Sony HDR-AS100v (with Waterproof case)	122	$600
Total		**1265g - 1330g**	**$1550**

Blade products are designed and intended for a wide variety of uses including both recreational and commercial, however they are not specifically designed for aerial mapping applications. However, the Blade products align with many of the characteristics of commercial UAV systems, such as they are lightweight and easily deployable, easy to use and very little training required. They can also be retrofitted with a variety of sensors with easily integratable products, they have safety mechanisms in place such flight vertical and horizontal limits.

Aerial Image Acquisition

Flight planning

Before any field sampling it was imporant to establish a flight plan, whereby specifying the flight scanning pattern, the number of flights, number flight lines per flight and their direction, the amount of overlap and the altitude. While keeping in mind the desired resolution of the output images. These pieces of information along with launch/landing locations and weather data are used to develop a flight plan prior to heading into the field. Using the pre-determined flight plan, we navigated to the launch/landing locations and began the flight procedures.

Flight procedure

Pre-field checks:

- Test all system batteries (sensor, quadcopter and transmitter) using voltage meter.
- Ensure sensor memory cards are cleared.

Begin start-up sequence

- Install a charged Quadcopter battery, plug it in and close the hatch.
- Install the sensor, making sure the positoin is secure and will not loosen from flight vibration.
- Turn on Transmitter.
- On a level surface, turn on Quadcopter and allow the Blade and Transmitter to initialise.
- Wait for binding and GPS lock, this is indicated by solid green light (Safe mode). May take between 30-90 seconds.
- Arm and Fly. To Arm: From throttle at trim position props start by moving the throttle stick to the inside bottom corners and then releasing them in a fluid sequence. The props will begin to spin, locking the home position. The aircarft is ready to fly.

Flight Plan Execution

The flight of the Quadcopter was directed by the Transmitter operator. Navigation of the survey area and the direction of flight is dictated by moving the directional stick inline with the desired flight path. It was especially useful to have at least one other person to help maintain straight lines of flight. This was achieved by positioning a second person at the end of the line (Figure 2.4) who assisted the directing of the craft during flight.

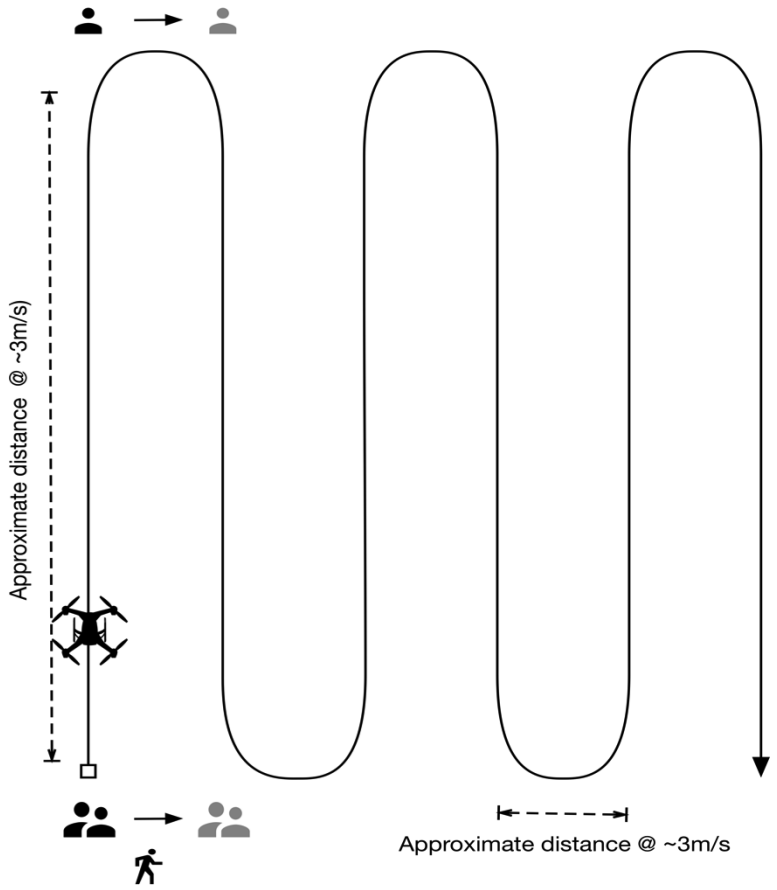

Figure 2.4 Flight plan

Landing

There are two options for landing the Blade 350:

- Guide the aricraft back manually to where you wish to land, reducing the throttle until landed then engage the cut throttle button to disarm the motors.
- Activate the Return Home function to return the aircraft to the assigned home location and land automaically.

Shut-down procedure

1. Turn off the power switch on the aircraft.
2. Turn of the power on the transmitter.
3. Unplug and remove the battery form the aircraft.

Aerial images, GPS data and any other supplementary data were transferred to the geospatial workstation at AUT. Additional field trip logs were made for general maintenance of the UAS and Safety. Other post field procedures included, the charging of all system batteries; sensor, quadcopter, transmitter, radio.

Satellite data

The primary datasets for this project consist of one multispectral (MS) WorldView-2 (WV-2) scene and one MS WorldView-3 (WV-3) scene captured four years apart, at 22:50:43 GMT, 18 April 2011 and 22:11:51 GMT, 01 January 2015 respectively. DigitalGlobe Inc. granted the Worldview datasets, providing all eight spectral bands and panchromatic image for each date. WorldView-2 (WV-2), launched in October 2009, was the first commercial high-resolution satellite to provide eight spectral sensors in the VNIR range at 1.84m spatial resolutions, also having a high-resolution panchromatic sensor at 46cm spatial resolution. WV-3, launched in august 2014, sensors match WV-2's multispectral range (8 bands) whilst increasing the spatial resolution to 1.24m and 31cm for the panchromatic band. Wavelength characteristics for each dataset from WV-2 and WV-3 are displayed in Table 2.5.

Table 2.5 Spectral bands of the WorldView-2 and WorldView-3 Sensors

Spectral band	**Wavelength center (nm)**	**Wavelength min - max (nm)**
Coastal	427, 425	400 - 450
Blue	478, 480	450 - 510
Green	546, 545	510 - 580
Yellow	608, 605	585 - 625
Red	659, 660	630 - 690
Red edge	724, 725	705 - 745
Near infrared 1 (NIR1)	831, 832	770 - 895
Near infrared 2 (NIR2)	908	860 - 1040
Panchromatic	630	450 - 800

The Standard Satellite Imagery, also referred to as 2A, is a product that is supplied preprocessed; radiometric, sensor and geometric corrections. The standard product is resampled to a cartographic projection and the metadata for this product contains information for rational functions model. Standard (2A) Imagery products are radiometrically corrected, sensor corrected, and projected in a plane using the map projection and datum of the customer's choice. Standard 2A imagery also has a coarse DEM applied to it, which is used to normalise for topographic relief with respect to the reference ellipsoid. This is an effort to minimise the effect of terrain distortions. The degree of normalisation is relatively small, so while this product has terrain corrections, it is not considered orthorectified. All standard products have uniform GSD throughout the image product.

The imagery covered the western Auckland region including the 7km^2 of the Whatipu dune and wetland area (Figure 2.5). Table 2.6 lists the scene parameters for each image. All scenes were supplied in a format suitable for land cover analysis.

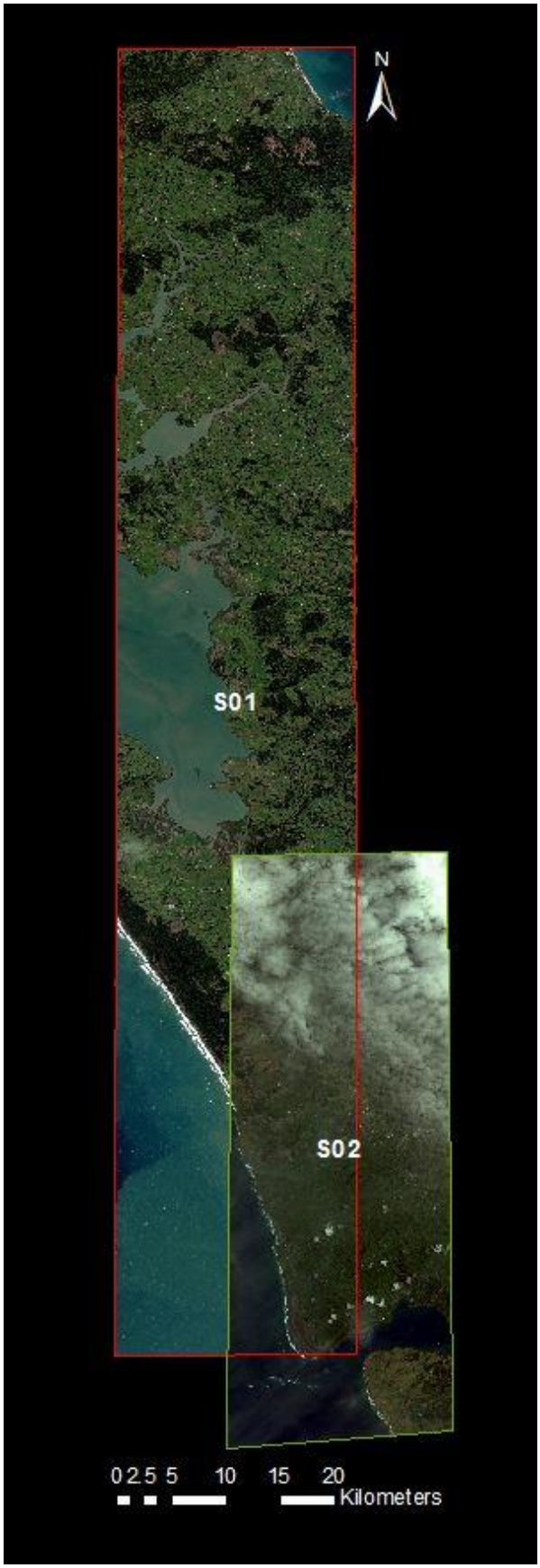

Figure 2.5 WorldView Image scenes. Red polygon is the extent of WV-2 scene captured on the 18 April 2011 (**S01**) and green polygon is the extent of WV-3 scene captured on 18 January 2015 (**S02**)

The WV-2 scene has a noticeable difference in mean satellite azimuth and off-nadir viewing angle to the WV-3 scene. As a result, there is a visible difference in shadowing and viewing geometry caused by the sensor to capture geometry and terrain distortions. Methods for correcting the geometry distortions are outlined in section 3.5 (Geometric Correction).

Table 2.6 WorldView imagery metadata

Satellite Imagery	S01 (2011)	(S02) 2015
Spacecraft	WV02	WV03
Imaging bands	Pan + MS1-8	Pan + MS1-8
Pan spatial resolution	0.5m	0.36
MS spatial resolution	2.0m	1.2m
Acquisition date	18/04/2011	18/01/2015
Acquisition time	22:50:43 GMT	22:11:51 GMT
Mean off-nadir view angle	13.5°	23.7°
Mean satellite azimuth	264.6°	70.2°
Mean satellite elevation	74.7°	64.0°
Cloud cover	0.013	0.398

Ancillary Datasets

The following ancillary datasets were compiled and incorporated into the project to aid identification of vegetation to be used in the classification training and validation component of this study. Table 2.7 includes the ancillary maps used in this project. The two maps were used to collect training and validation samples to be used as ROI's during supervised classification of the Time-1 (2011) stage of this study. No additional dataset were required for the Time-2 (2015) processing and analysis beyond data that was collected during the course of this study.

The Wetland Overview Field Map supplied by Auckland Councils, Research Investigations and Monitoring Unit (RIMU) was compiled in 2011 as part of the wetland-monitoring program.

The Whatipu Vegetation Map created by Thomas Civil and Environmental Consultants for Auckland Council, aimed to delineate fifteen land cover types including vegetation and non-vegetated surfaces. The project involved extensive fieldwork to identify and record boundaries between land cover types, which were later digitised in a GIS to produce a complete land cover map of the system (TCEC, 2014).

Table 2.7 Ancillary datasets used in various stages of this project

Contribution		Dataset Information			
Project stage	**Use**	**Dataset**	**Thematic information**	**Acquisition date**	**Source**
Time 1 (2011)	ROI and validation	Wetland Overview Field Map	Dominant Vegetation	2011	RIMU, Auckland Council
	ROI and validation	Whatipu Vegetation Map	15 Land cover classes	2012-2013	Thomas Civil and Environmental Consultants

Training and Validation Data

In remote sensing the collection of training and validation data for automated classification procedures is crucial to enable the user to downscale information in the imagery to the objects and features on the ground. This involved identifying areas at Whatipu with homogenous patches of target classes greater than the spatial resolution (pixel size) of the sensor ($2m^2$). The identification of suitable samples was achieved by on-screen digitising methods and data collected in the field. On-screen or heads-up digitising involved the use of high spatial imagery products and the delineation of areas to be imported into ENVI. Training and validation samples for thirteen land cover target classes were digitised and converted to ROI's and then pixels. Many of the 2011 samples were reused in the 2015 sample dataset where land cover did not change. Using a random selection process, half of the samples were used as training samples to 'train' the classifier, and half were retained for the accuracy assessment.

Time-1 (2011) training and validation samples were digitised from the 2011 1.0m spatial resolution aerial imagery (RGB) and directly from the 2011 0.50m spatial resolution pansharpened satellite imagery. Samples were also taken from the Wetland overview field data, which are digitised field surveys undertaken in 2011 by Auckland Council. Additionally, a 2013 vegetation map was also used as a general guide to identify vegetation. No fieldwork was undertaken for the 2011 training and validation samples.

Time-2 (2015) utilised some field data, which involved walking the perimeter of the wetland and taking GPS waypoints of features of interest. This was done at the same time as spectral sampling and therefore additional data such as photo points were also applied used to help identify samples areas. These field samples were collected within 2 months of the image

capture date. Training and validation samples were however predominantly collected from on-screen digitisation of the 2015 5cm spatial resolution low altitude aerial imagery (RGB) collected with the UAS. This data provided excellent spatial information for visual interpretation and identification however, the UAS aerial survey did not cover the extent of the wetland and therefore additional samples were digitised directly from the 2015 0.5m spatial resolution pansharpened satellite imagery.

As a results of the different collection strategies used, there is a slight difference in the number of training samples for each class between images (Table 2.8), e.g. polygons were used for Time-1, where as a mixture of per-pixel, polygons was used for Time-2.

Table 2.8 Training samples used in the classification of satellite imagery

Class	**Training and Validation pixels**	
	Time 1 (2011, WV-2)	Time 2 (2015, WV-3)
Apodasmia similis rushland	1447	1476
Eleocharis acuta rushland	253	135
Typha orientalis reedland	1149	908
Schoenoplectus tabernaemontani reedland	1130	132
Machaerina articulate reedland	1061	236
Pennisetum clandestinum grassland	1516	1750
Native shrubland	1605	1120
Exotic shrubland	1663	1167
Ulex europaeus shrubland	1682	1138
Spinifex sericeus/Ficinia spiralis duneland	1049	338
Carex pumila sandfield	332	139
Openwater	1595	922
Un-vegetated sand	2877	1216

2.3 Software

ViewSpec Pro

ViewSpec Pro is a program used for the post processing of spectra files collected using ASD instruments. ViewSpec Pro was not used in this study for post processing, however was essential for converting the asd spectra files into to ASCII format to be processed in both ENVI and Excel.

Pix4DMapper

To obtain highly accurate georeferencing capability and to combine multiple digital images and generate one orthomosaic for the entire survey scene, Pix4d mapper (Switzerland) was used. Pix4d Mapper is designed to create 3D point clouds, 3D Digital Surface Models and orthomosaics from overlapping 2D images using automated reconstruction algorithms.

ENVI 5.2

ENVI 5.2 is an image processing software, created by ITT Visual Information Solutions, Inc. (2015) that visualises, analyses and presents all types of imagery products and other geospatial data. The software includes tools related pre-processing and processing of imagery such as radiometric correction, geometric correction, radar and LiDAR analysis and vector – raster capabilities. Processing outputs are widely compatible with other GIS products, namely ArcGIS and supports a wide range of source data formats(Exelis Visual Information Solutions, 2010).

ArcGIS

ArcGIS 10.2 is software created by ESRI used in geographic information systems (GIS) and used to compile and manage geospatial information. It supports GIS applications such as mapping, data compilation, analysis, geodatabase management and geospatial information sharing. ArcGIS was used for digitising training and validation polygons, post classification processing, and cartographic visualisation.

2.4 Data Pre-processing

Each dataset required specific pre-processing pathways and programs. The datasets that required pre-processing before any analysis could be undertaken were:

- *Spectral Reflectance Data*
- *Low Altitude Aerial Imagery*
- *Satellite Image*

Spectral Reflectance Data Pre-processing

Waveband Filtering

Waveband filtering is a common procedure to remove noisy data at the upper and lower wavelengths of the spectroradiometer instrument range. The signals measured in the lower and upper ends of the instrument range, i.e. 325-450 and 950-1075nm, were discarded due to sensor noise caused by atmospheric absorption. Spectral signatures were therefore studied from the 450nm to 950nm spectral range.

Spectral Reflectance Data

Due to changing illumination conditions in the field and other factors that influence the spectral purity of samples, many samples contained additional spectral noise. These spectra could be identified based on irregular shape and/or where there was a significant deviation in intensity from the majority of samples. To do this each species was plotted separately and outliers identified and removed.

Simulation of WorldView-2 and WorldView-3 Sensors

The simulation of WorldView sensor spectral responses using ASD field spectroradiometer data data is useful to make direct comparisons of spaceborne sensor and ground data, to reduce the dimensionality of the data, and to simplify the data analysis.

The imitation of other sensor bands using groundbased data can be generalised by calculating the band values of the sensor. This however depends on the sensor response function. The WV-2 sensor captures data from 400 to 1040 nm with eight bands. Figure 2.6 shows the 5% response for upper and lower edges and center wavelengths for each band. The WorldView

sensor is an example of a Gaussian sensor. Waveband centres do not lie at whole number frequencies, bandwidths are not sharply defined and the sensitivity of the sensor is not uniform over the bandwidth.

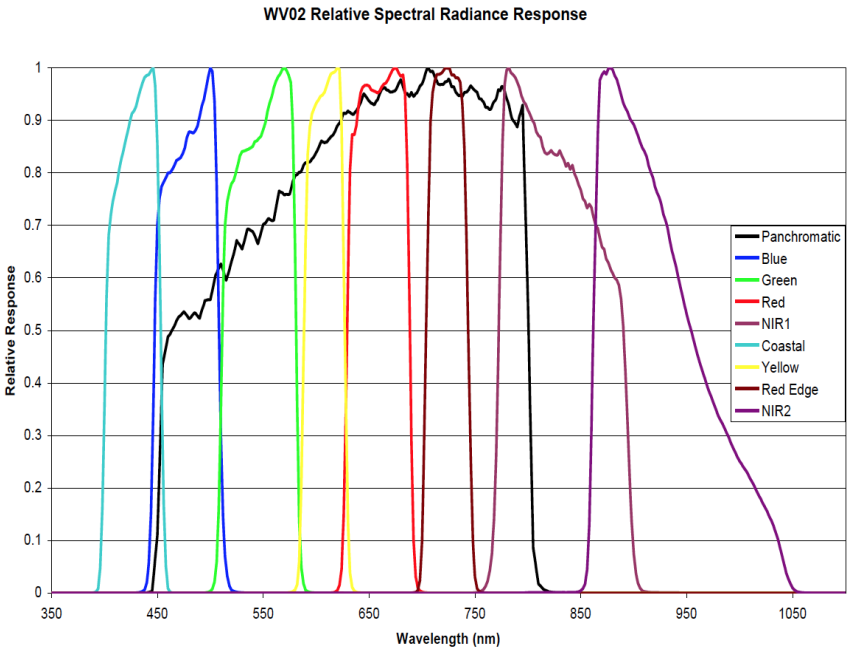

Figure 2.6 Spectral response functions of WorldView-2 sensor bands (Source: DigitalGlobe).

ENVI software provides response functions for a range of multispectral sensors including the WorldView fleet. ENVI uses a Gaussian model and with full width at half maiximum (FWHM) for each of the eight WorldView bands to obtain simulated WorldView multispectral spectra.

Low Altitude Aerial Imagery Pre-processing and Preparation

Orthomosaic Generation

To combine digital images captured in the field and generate one orthomosaic for the survey area, Pix4Dmapper was used. Pix4D is designed to create 3D point clouds, 3D Digital Surface Models and orthomosaics from overlapping 2D images using automated reconstruction algorithms. 15,195 images were captured (Figure 2.7) at Whatipu. Due to the capture rate (camera interval time) and altitude of flight, the number of images collected in this project had more than sufficient overlap (~75% overlap). To reduce processing time and errors associated wih processing demands, I reduced the number of images to 3759 by removing image duplicates (from take-off and landing points) and every third input image before processing. Even so, the image dataset was still considerably large. It is recommended that large datasets be split to ensure accurate processing and orthomosaic generation (Pix4D, 2015). To process the imagery I used the Pix4DMapper split and merge option. All of the images were split into to 500 image subsets, processed independently and merged into one final project. Each subproject was split whilst ensuring overlap between them. Processing time depends on a number of parameters such as the number of images selected, image sizes, image content, scene area, resolution and computing power available.

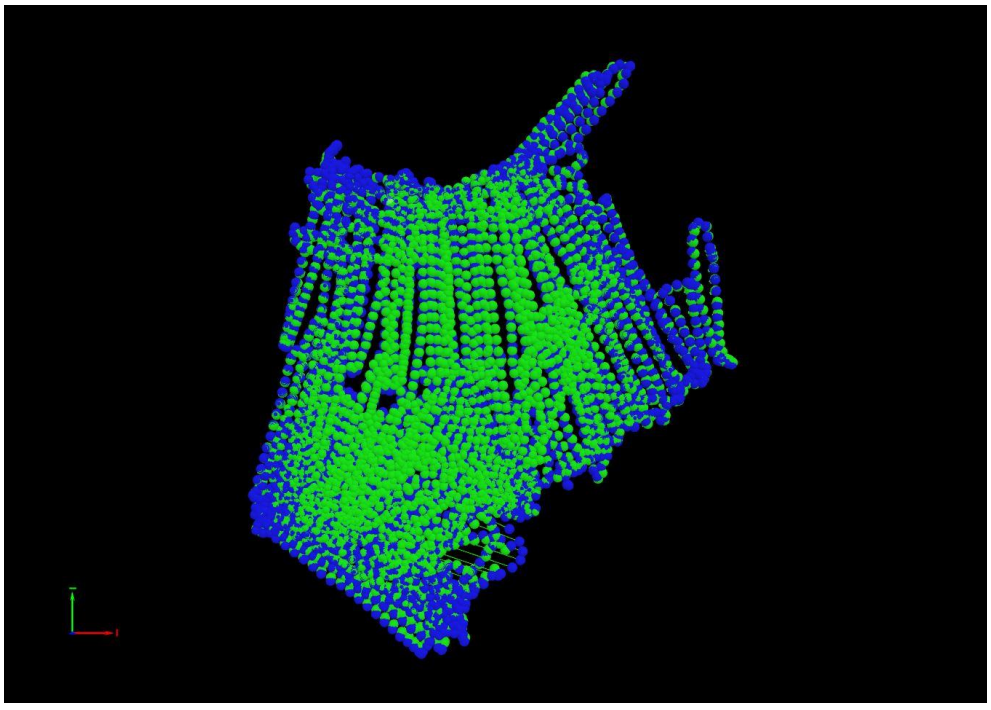

Figure 2.7 Georeferrenced photo points (represented by blue+green points)

Generating Orthomosaics is compartmentalised into 3 distinct processing steps which within themselves include several processing actions: 1) Initial Processing; this computes keypoints by extracting features and then matching keypoints between images, followed by camera optimisation and geolocation calibration, then Automatic Aerial Triangulation (AAT) and Bundle Block Adjustment (BBA); 2) Point Cloud Densification, this includes generation of points (pixels), point densification and 3D textured mesh generation (Figure 2.8); 3) DSM and Orthomosaic Generation, is the generation of Digital surface model and automatic blending of Orthomosaic images.

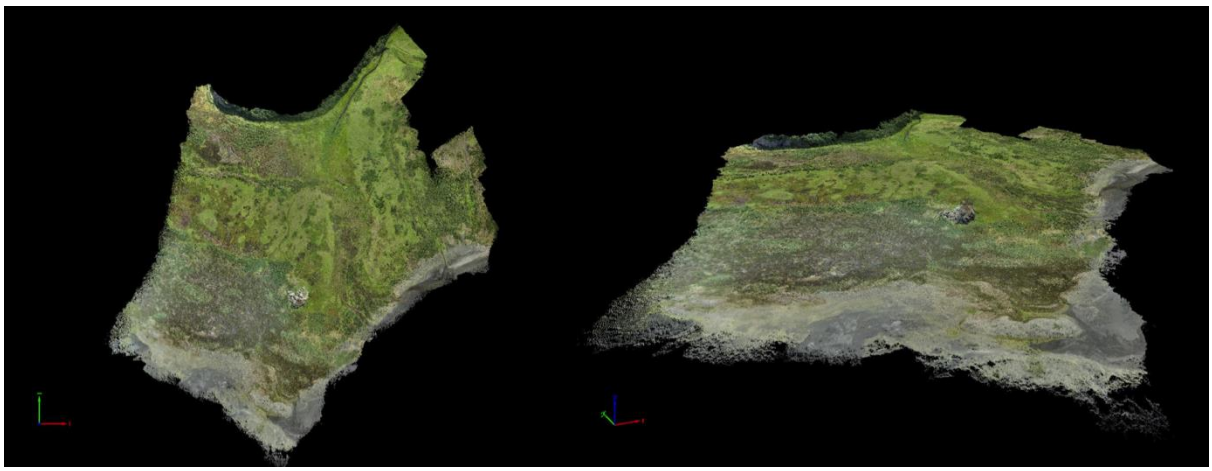

Figure 2.8 Pointcloud generated in Pix4Dmapper

To create the orthomaiaic Pix4Dmapper automatically blends images matches. Pix4Dmapper offers manual scene editing to further increase the match accuracy for each image (Figure 2.9). This post processing step allows the user to select the image, correct brightness and alter the image projection model (either orthoimage or planar image). The Whatipu site is relatively flat terrain, therefore the planar projection produced more accurate image blending results.

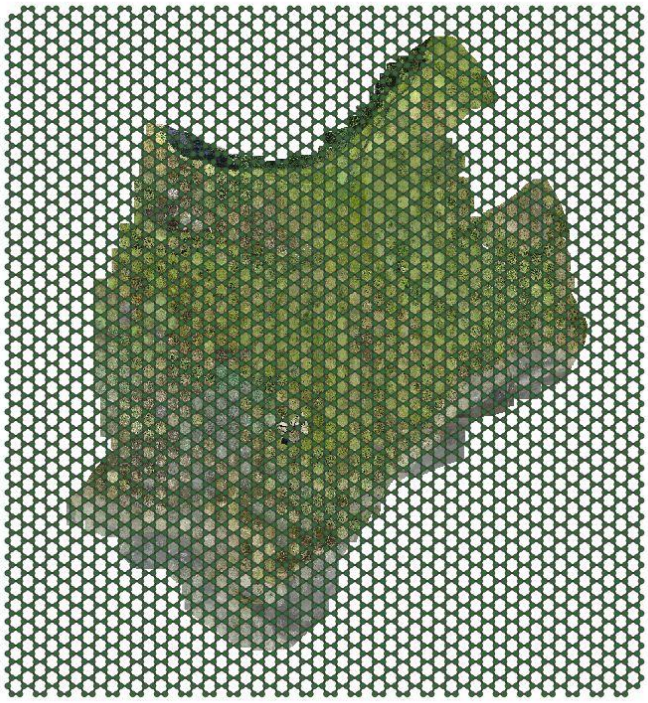

Figure 2.9 Mosaic Editor with Orthoimage View

Aerial Image Corrections

The aerial imagery collected in this project was not intended for automatic classification and therefore calibration is not necessary. If radiometric calibration was to be done, calibration targets should be captured under same conditions as the imagery. Additionally, accurate determinations of the camera sensor parameters are required. The specific spectral characteristics of the red green blue image elements are not disclosed by Sony at this time. Atmospheric corrections are also not required due to the small distance between the sensor and ground (flight altitude 40-50m).

Satellite Image Pre-processing and Preparation

Imagery to be used in spectral based classifications should be converted to a format that is compatible for comparison with other data types. This conversion process requires the calibration from the DN data to radiance at a minimum and then further calibration to reflectance. These corrections are made to account for the variation in relative positions of electromagnetic intensity, positioning of the sun, earth and sensor platform, and to obtain an absolute value for which spectral comparisons can be made.

All corrections applied to satellite imagery products were done using either standalone tools or workflows available in the standard package and modules of ENVI software (ITT Visualization Information, 2010), unless otherwise mentioned.

In general, the steps used to derive a useful imagery product are as follows:

- *Spatial Subset*
- *Geometric Correction*
- *Radiometric Calibration*
- *Atmospheric Correction (and conversion to Reflectance)*
- *Mask Generation*
- *Pan-Sharpening*
- *Image Transformation*

Spatial Subset

The image products were received as entire scenes that included area beyond that of the scope of this research project. To avoid long processing times the scenes were subset to an area that covered the extent of the study site (5.6km by 3km) prior to corrections and classifications were applied. This was done using the image subset tool in ENVI.

Geometric Correction

The WV-2 & WV-3 products are delivered geometrically corrected by DigitalGlobe, however, because a coarse DEM and terrain corrections were applied, it is not suitable for orthorectification (DigitalGlobe, 2014). Instead, the Image Registration workflow in ENVI was used to geometrically align the two satellite scenes with different geometries, to enable accurate spatial comparison of the classification outputs (Fig. 2.10). The geometric correction co-registers images by using an automated correlation-based identification of image ‘‘tie

points'' with a maximum RMSE of 2 m and a Delaunay triangulation transformation algorithm that warps the two images (Richards, 1999). The image with the viewing angle closer to nadir (SO1; 2011) was selected as the base. Tie points were manually checked, edited, and added to, to improve registration. To match the spatial resolution of WorldView-2 with WorldView-3 imagery for standardised imagery interpretation, WorldView-3 samples were resampled to 2m m pixel size using the nearest neighbor approach.

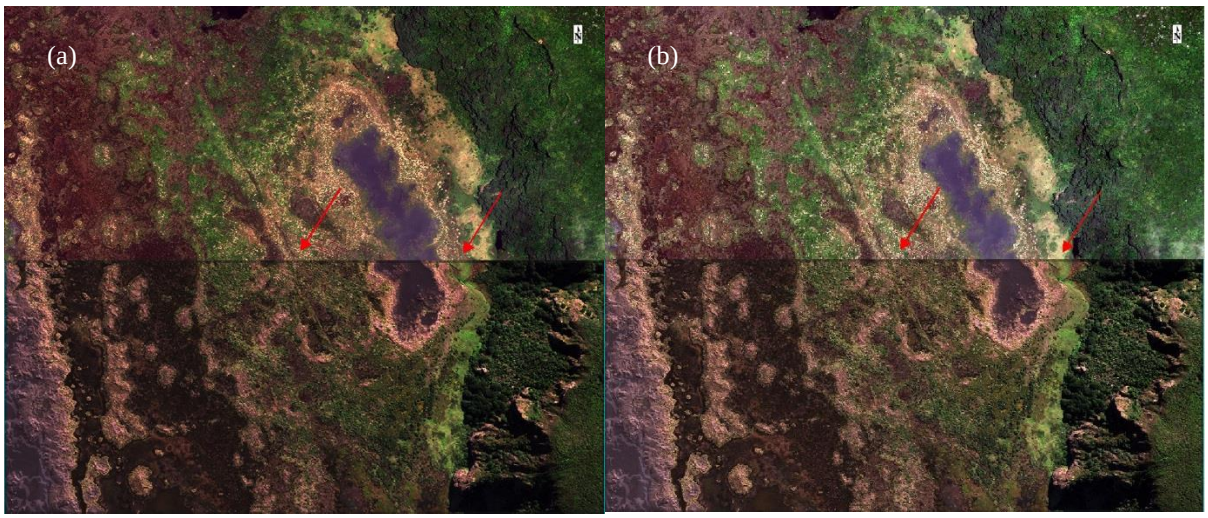

Figure 2.10 (a) Original georectified WorldView satellite datasets supplied by DigitalGlobe, note the asymmetric georectification misalignment due to topography and different viewing angles. This issue is addressed in (b) with ENVI's Image-to-Image Registration workflow. Top: WV-3 2015 imagery. Bottom: WV-2 2011 imagery.

Radiometric Calibration

The WV-2 & WV-3 Standard 2A image products are provided as pre radiometrically corrected image pixels (DigitalGlobe, 2014). These are calculated as a function of the radiance that enters the telescope and instrument conversion of that radiation in to digital numbers (DN) (Figure 2.11 a and 2.12 a). However, the DN pixel values are unique to the sensor and require further radiometric calibration to make image comparisons. The image pixels were converted to top of atmosphere spectral radiance (Figure 2.11 b and 2.12 b), which refers to the spectral radiance entering the telescope aperture at the WV-2 or WV-3 altitude of 770 km. The image pixels were then rescaled and formatted to make them compatible with the atmospheric correction module. The top of atmosphere radiance correction was computed using ENVI's Radiometric Calibration tool, which recognises WorldView image types and automatically enters metadata inputs. This correction uses the following equation (Updike & Comp, 2010):

$$L_{Pixel,Band} = absCalFactor_{Band} * q_{Pixel,Band}$$

Where $L_{Pixel,Band}$ represents the top-of-atmosphere spectral radiance image, $absCalFactor_{Band}$ is the radiometric calibration factor for a given band, and $q_{Pixel,Band}$ is the given radiomterically corrected image pixels. All of these parameters can be found in or derived from information located in the Metadata (.Imd) file provided by the supplier. The resultant images are in the units of [$W.m^{-2}.sr^{-1}.\mu m^{-1}$].

Atmospheric Correction

The images were then atmospherically corrected using the ENVI Modtran based, Fast Line-of-sight Atmospheric Analysis of Spectral Hypercubes (FLASSH) atmospheric correction module. FLAASH offers several options including, solar position, water and aerosol correction and atmospheric geographically dependent model schemes. In this study, the rural aerosol correction scheme was applied using recommended setting specifically for WV-2 data (Exelis Visual Information Solutions, 2013). Visibility was set at 100km and 40km for the 2011 WV-2 and 2015 WV-3 scenes due differences in image clarity and to reduce the occurrence of negative pixels. The image pixel values were additionally scaled from radiance to surface reflectance (Figure 2.11 c and 2.12 c). Reflectance is the ratio of the radiance (energy received by the telescope) to irradiance (energy directed towards the earths surface). Furthermore, the surface reflectance is the reflectance of the surface of the earth, achieved by removing noisy radiation and irradiative artifacts. Correcting for atmospheric noise is the standard by which images captured at different times and by sensors can be compared and qualitative information about features on the earth can be extracted (Updike & Comp, 2010).

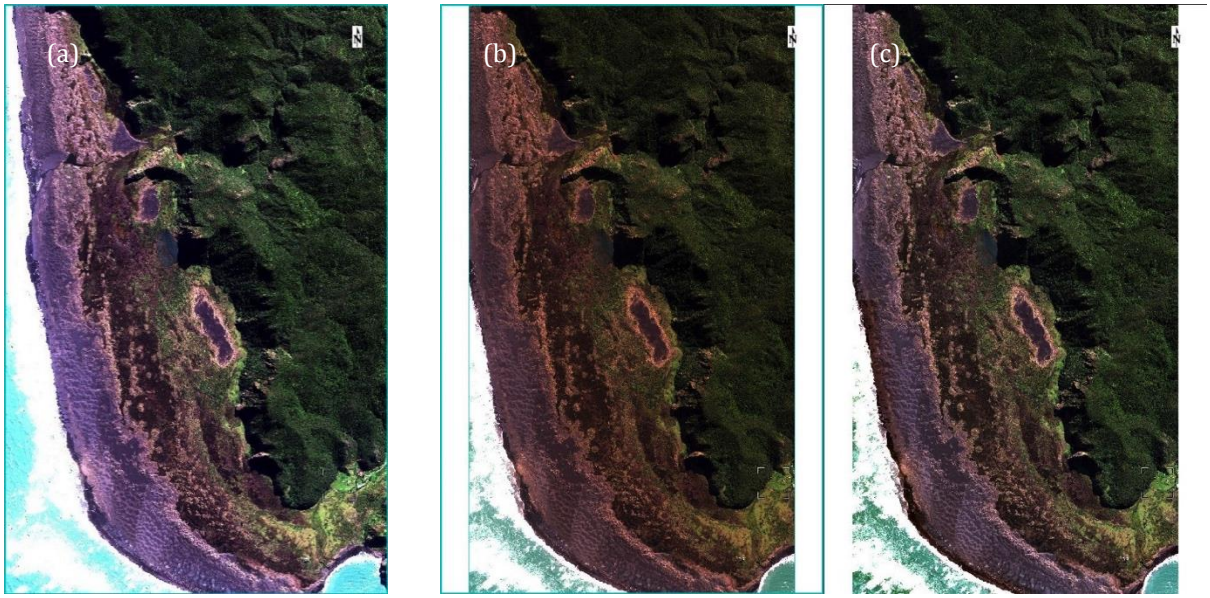

Figure 2.11 WorldView-2 (2011) imagery DN to Reflectance conversion results shown using the same contrast stretch algorithm; (a) original image, (b) ToA radiance image and (c) FLAASH surface reflectance image.

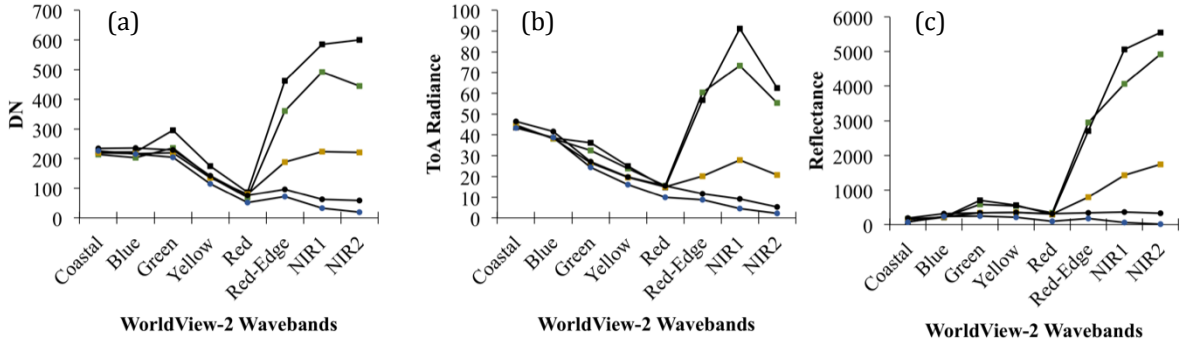

Figure 2.12 WorldView-2 (2011) Spectral response curve of image features; (a) DN response, (b) ToA radiance and (c) FLAASH surface reflectance. Feature classes; (□) freshwater, (□) un-vegetated sand, (□) grassland, (□) treeland, (□) rushland.

In order to make accurate comparisons of multi-date imagery and of spectral signatures of WorldView imagery pixels with the groundbased spectral reflectance signatures the atmospheric correction FLAASH was applied. The 2011 WV-2 imagery output was successfully producing reflectance responses consistent with expected reflectance features. However, a satisfying output could not be achieved with the 2015 WV-3 imagery despite using various settings for atmospheric and aerosol models and other parameters. Although the atmospheric noise reduction is apparent, with haze reduction and colour correction (Figure 2.13 b and c). The coastal band (400-450nm) and blue band (450-510nm) values were uncharacteristically high (Figure 2.14). Other methods such as empirical line correction and QUAC (Quick Atmospheric Correction) in ENVI were also attempted; however, these efforts

resulted in additional errors that could not be explained. More thorough investigation was beyond the timeframe of this research.

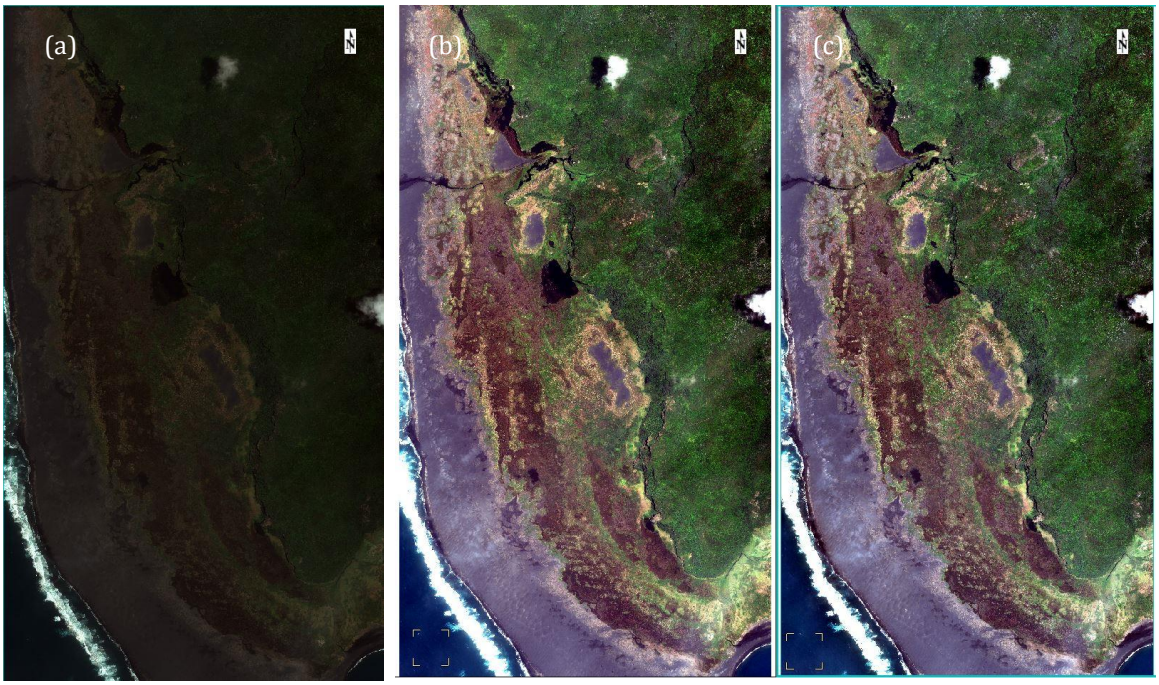

Figure 2.13 WorldView-3 (2015) imagery DN to Reflectance conversion results shown using the same contrast stretch algorithm; (a) original image, (b) ToA radiance image and (c) FLAASH surface reflectance image.

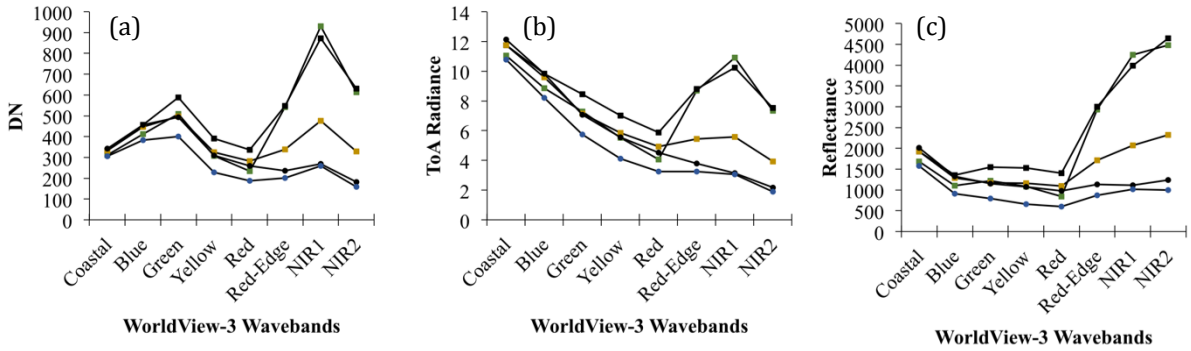

Figure 2.14 WorldView-2 (2011) Spectral response curve of image features; (a) DN response, (b) ToA radiance and (c) FLAASH surface reflectance. Feature classes; (□) freshwater, (□) un-vegetated sand, (□) grassland, (□) treeland, (□) rushland.

Mask Generation

Two masks were created to exclude pixels outside of the study area and to remove noise from the processing of classifications algorithms used to identify features of interest. Masking

helps achieve an accurate classification model by removing extraneous image information and reducing the processing time.

A mask polygon defining the Whatipu wetland duneland boundary was created in ArcGIS and applied to the imagery in ENVI. This mask was applied to both Time-1 (2011) and Time-2 (2015) imagery.

The second mask was used to remove shadow pixels from classification processing. Only the WV-2 2011 image shadowing warranted the use of masking. Shadows are caused by either, areas of objects that don't receive equal illumination or shadows that are cast by the direction of the light source. In this study shadows of interest are those that are cast from elevated natural features. ENVI band math tool was used to calculate a shadow detection index (SDI) image developed specifically for WV-2 imagery (Shahi, Shafri, & Taherzadeh, 2014). The SDI utilises three bands (Blue, NIR1, and NIR2) from WV-2 imagery to effectively extract shadow pixels whilst distinguishing shadows from dark objects. The Shadow Detection Shadow can be calculated using the following equation:

$$SDI = \frac{NIR2 - Blue}{NIR2 + Blue} - NIR1$$

The resulting SDI image was then subjected to a two-way classification (shadow vs. non-shadow) using the Support Vector Machine (SVM) classifier used by the creators of the index. The extracted shadows were then converted to ROI's for use as a mask in vegetation classification processing.

Pansharpening

Pansharpening is the process of image fusion between low-resolution multispectral imagery, and hyperspectral imagery, with high-resolution panchromatic (grey scale) image by resampling to the high-resolution image. To sharpen the WV-2 and WV-3 low-resolution multispectral images with their respective high-resolution panchromatic images, I used a nearest neighbor diffusion (NNDiffuse) pan-sharpening algorithm available in ENVI that is shown to preserve both spatial and spectral features of imagery (Sun, Chen, & Messinger, 2014). The pan-sharpened result was used during training and validation sample collection.

Image Transformation

The image transformation implemented was a Normalized Band Indices. The Normalized Vegetation Index (NDVI) is a commonly used vegetation index exploiting spectral characteristics deterministic of vegetation responses. These narrow band indices are useful in that they take advantage of spectral reflectance/absorbance features of vegetation. The NDVI ratio incorporates the Red band, which represents the lower reflectance response from vegetation and the NIR band, which represents the higher reflectance response of vegetation. The WorldView sensors have available two NIR bands. In this study the NIR2 band was used in the NDVI ratio as this band typically shows higher values than traditional NIR band values and usually produces a higher NDVI ratio (Wolf, 2010).

$$NDVI = \frac{(Red - NIR2)}{(Red + NIR2)}$$

Fortunately, the error associated with the atmospheric correction of WorldView-3 2015 dataset is avoided here, as the error did not appear to affect the Red and NIR bands. In this study, I calculated NDVI values using the Red (660nm) and NIR-2 bands to test the spectral separability of our target classes based only on narrow band NDVI scores.

2.5 Data Processing, Post Processing and Analysis

All outcomes developed in this section will be presented in the Results Chapter (Chapter 4).

- *Field-based Spectral Reflectance Data Analysis*
- *Region of Interest Analysis (training dataset)*
- *Satellite Image Classification techniques*
- *Satellite Image Classification processing*
- *Accuracy Assessment (validation dataset)*
- *Classification Post-processing*
- *Change Analysis*

Field-based Spectral Reflectance Data Analysis

Spectral Variability

To assess the separability of common species at Whatipu the mean spectral signatures and spread for each species, were plotted against each other. This allowed a visual assessment of the amount of variability within a species and easy determination of the conflict that each species has with other species. We can therefore make qualitative determinations about the spectral separability of each species and about the usefulness of the spectral signatures in classification processing for imagery multispectral of Whatipu.

Comparison of Simulated Spectra with Satellite Spectra

The simulated spectral signatures and satellite-derived signatures were directly compared with satellite derived spectral signatures. I compared the spectral information for a subset (n= 4) of species that matched regions of interest for classification processing. This included, *Apodasmia similis, Eleocharis acuta, Ulex europaeus,* and *Pennisetum clandestinum.* The objective was not to conduct an in-depth analysis comparison, but rather to evaluate the spectral response of the vegetation in the different bands to determine the correlation of spectra for the sensors to draw general conclusions about the potential for up-scaling the spectral signatures in future studies.

Training Data Analysis

Training Data Separability

Following the collection of training samples, it was important to ascertain if the samples contain information that would accurately discriminate between each class. To determine the separability of classes I used the n-D Visualizer in ENVI. The visualizer plots the distribution of points in 2-dimensional space, where each class population should separate out into distinct groups and should not overlap. If there is overlap, classes should be edited to remove overlapping pixels or restructuring of the classification scheme.

Additionally, I used ENVI's ROI separability tool to identify the samples that were poorly separated from other classes. This tool computes the spectral separability of classes using the Jeffires-Matusita (JM) and Transformed Divergence (TD) separability measures. Both measures produce a value range of 0 to 2.0 and indicate how well each class pair statistically separate. Classes with very low separability value (less than 1) were considered for merging.

Satellite Image Classification Processing

ENVI 5.2 supervised classification algorithms were used to identify features of interest within the wetland system at Whatipu. The classifications techniques were used to identify image pixels that represent features on the ground by matching image statistics with the training samples chosen. The following supervised classifications were applied to all 8 bands supplied with the WorldView imagery products:

- Maximum Likelihood classification

The maximum likelihood classification (MLC) is the most common supervised classification method used. MLC assumes that the data for each class is normally distributed and then calculates the probability that a single pixel belongs to one of the classes defined. It classifies all image pixels unless otherwise set in the threshold. No threshold was used in this study.

- Minimum Distance

The minimum distance classification algorithm uses the average vector of each end-member and calculates the Euclidean distance from each of the unknown pixels to the mean vector for each class. The images pixels are classified to the nearest class that was selected via the training samples (Exelis Visual Information Solutions, 2010). Pixels that fall outside of the specified range will remain unclassified.

- Mahalanobis Distance

The Mahalanobis Distance classification method available in ENVI was used to classify the 2011 MSI imagery based on regions of interest. The method is a direction sensitive classifier that uses statistics for each class. This method is similar to the MLC, although makes the assumptions that all classes have equal covariance (Exelis Visual Information Solutions, 2010). This method is therefore much faster than the MLC method.

For each of the WorldView datasets the same general classification workflow was employed. 1): import reflectance image, 2): apply Whatipu boundary mask and shadow mask (Time-1 WV-2 image only), 3): import training samples and convert to ROI's, 4): select classification tool and run the algorithm using specific algorithm parameters: export classification to vector file and again to shapefile.

Accuracy Assessment

Confusion Matrix

A Confusion matrix was used to calculate the accuracy of the classification. This determines the accuracy of the classification by comparing the validation samples with the classification results. This was used to get the producer and user accuracies of each class and were compared using the Kappa coefficient as well as the overall accuracy. Overall accuracy is the division of the total number of correct pixels by the total number of pixels. The producer's accuracy is the total number of correct pixels in a category divided by the number of pixels of that category as derived from the reference data. The user's accuracy is the total number of correct pixels in a category divided by the total number of pixels of that category as derived from the classification data or map data. The overall kappa coefficient indicates how well the classification results agree with the reference data.

The accuracy assessment was undertaken using ENVI's Confusion Matrix tool. This is a standard technique for assessing accuracy with limited or no ground control points. To qualify for comparison of classification results in change analysis, land cover classes are required to meet accuracy thresholds of 85% minimum overall, and 70% per-class accuracy. Data not reaching this criterion will require reclassification, as per Thomlinson et al., (1999).

Post classification processing

Following the classification and accuracy assessment the most accurate result was identified and run through an automatic cleanup process to remove meaningful objects and facilitate GIS handling. This was done using the majority class (3x3) tool in ENVI.

The final classification results for the WV-2 (2011) and WV-3 (2015) were also manually processed to remove misclassifications. This was done by exporting the classification results from ENVI to ArcMap and manually combing over the classification vectors and checking the accuracy of the automatic classifier. Where there is obvious misclassification the class was changed to an appropriate class. The addition of an un-classified class was made to account for areas of bare rock and any other features that could not accurately be attributed to a class from visual interpretation of imagery.

Change Analysis

There is a large range of methodologies for change detection. Change detection procedures can be grouped under the broad categories characterized by the processing procedures and analysis techniques used to identify significant change: (1) image enhancement, (2) multi-date classification comparison, and (3) comparison of independent classifications (Hussain et al., 2013). The image enhancement approach combines the imagery from different dates and involves the subtraction of selected transformed bands to produce a single band image difference results. The direct multi-date comparison based on single analysis of the combine multi-date images. The comparison of independently classified imagery is the comparison classification results of two images of different dates in order to identify specific changes in cover.

ENVI and ArcMap were used to perform change detection analysis of the WorldView imagery products. All analysis was focused towards the detection of the vegetation change at Whatipu, as opposed to geomorphological changes. Due the difficulties involved in change detection techniques it must be noted that changes might sometimes arise from variances in illumination conditions (regardless of preprocessing corrections), wetness (soil moisture, pond/lake levels), shadow and colour.

Change in cover between Time one (2011) and Time two (2015) was calculated using the following methods; (1) image differencing using multi-date (t_1 and t_2) NDVI images (image enhancement), and (2) direct multi-date classification comparison (independent classification comparison). The NDVI grouping was only used as an initial step to assess vegetative change. To characterize temporal trends in wetland loss and gain, I calculated amount of wetland gain and loss and net change (gain–loss), for each of thirteen clandcover classes of the multi-date imagery final classifications.

2.6 Case Study

This case study investigated the use of high-resolution imagery from Un-manned Aerial Systems (UAS) and satellite, for visual interpretation and the detection of invasive Pampas (*Cortaderia spp.*) (Figure 2.15). Mapping involved a number of tasks including visual identification of features within the study area, delineation and classification of features. Each level required a level of standardization to produce consistent datasets. Additionally it is assumed that there is no need for field verification. This is because the low altitude imagery seeks to replace field verification; its high spatial scale allows for identification of the target species at a standard equal to that of field mapping.

Figure 2.15 Pampas (*Cortaderia Selloana*) specimen at Whatipu

Visual Interpretation

The delineation of Pampas through visual image analysis formed the foundation for deriving classification results. Consequently, the analysis placed emphasis on the quality of image interpretation. The basic elements that aided visual image analysis and identification of features (i.e. tone, size, texture, pattern, shadow, and geographic location) were applied to *Cortaeria sp.* (Table 2.9) from Figure 2.16 nadir image characteristics.

Table 2.9 Image interpretation elements applied to Pampas

Image elements	Element description	Pampas description (nadir perspective)
Tone and colour	Relative brightness or colour of image pixels	Leaf: light bluish-green to dark green Leaf base: beige/brown Flower head: white through to pink/purple & dirty white
Size	Size of the object relative to other objects	Up to 4m in diameter and 3-4m+ in height
Shape	General outline of objects	Often circular and/or ellipse
Texture	Smoothness or roughness caused by change in tone	Coarse; central plumage and leaf ring
Pattern	Spatial arrangement	Systematic; linear-curvilinear
Geographic Location	Habitat	Colonizer on open/bare ground
Association	Position relative to other object in the landscape	Relatively wet areas (inside curve of flowing water body) is often on old foredune -shrubland belts

Figure 2.16 Pampas (*Cortaderia Selloana*) specimen at Whatipu, surrounded by Kikuyu grassland (*Pennisetum clandestinum*) from an aerial (nadir) perspective. Taken from low-altitude UAS aerial imagery

A source of potential of miss-identification was with the morphologically similar indigenous toetoe (*Austroderia toetoe*), which Pampas is often confused. However, no Toetoe was identified during field observations made in this study and a vegetation study conducted in 1996 found none in the southern section of Whatipu (Pegman & Rapson, 2005) that includes the area of this case study. For the purpose of this case study it is assumed that only Pamaps is present in this section of the wetland, as accurate identification from aerial image interpretation between the two, even at 6cm resolution, is considered difficult.

Digitization – Manual classification

Manual digitization was done in ArcMap; Polygons only included live *Cortaderia spp.* specimens. To reduce interpretation bias when comparing imagery classification results, I digitized Pampas successively from lowest resolution (0.3m pan-sharpened satellite image), to high spatial resolution (0.06m UAS aerial imagery).

Comparison

Three datasets were be compared in this case study:

1. Satellite Pampas polygons (derived from manual interpretation and digitization of 0.3m resolution WV-3 pan-sharpened satellite imagery).
2. UAS Pampas polygons (derived form manual interpretation and digitization of low-altitude 0.06m resolution UAS aerial imagery).
3. Exotic shrubland class (derived from automatic classification of 2m resolution WV-3 multispectral satellite imagery). This class will undoubtedly include significant error, as it also includes other exotic species common at Whatipu (e.g. Gorse and Lupin).

Miss classification (error) was removed from the satellite-derived datasets by extracting matches when overlapped with the UAS dataset. The "Exotic shrubland" classifications were also clipped to the UAS Pampas polygons in ArcGIS to remove misclassified polygon area.

The spatial statistics (e.g. area) of digitized polygons (Satellite and UAS) and the "Exotic shrubland" class were then compared with each other. The number of individual pampas specimens could not be compared due to the varied spatial scales of datasets and to avoid clusters of individual Pampas being misrepresented.

3 Results

3.1 Spectral Reflectance Data

Spectral Properties of Plants

The spectra collected show typical features of vegetation (Figure 3.1): low reflection in the visible with a noticeable peak in the green around 570 nm for most species. The exceptions to this are the brownish colour of rushland and reedland species which exhibit a sloping rise in the blue through to red wavelengths. The red edge is found around 690 nm where a steep rise begins and levels out onto the NIR plateau around 750 nm.

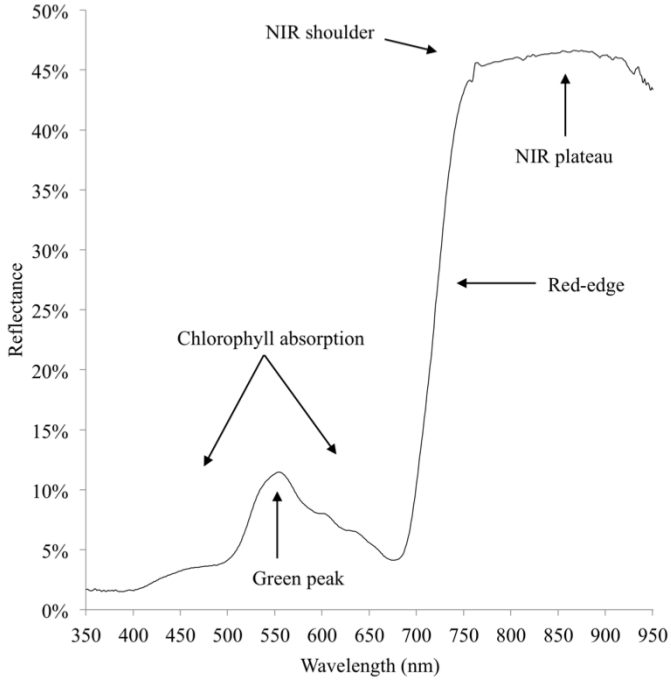

Figure 3.1 Features of a typical vegetation curve. Plotted is a ground-based signature of Kikuyu grass (*Pennisetum clandestinum*), taken at Whatipu.

WorldView Simulated Signatures

The WorldView simulation resulted in a drastic data reduction, creating 8 new bands (WorldView; 1-8) from 750 wavelengths of each ground based spectroradiometer spectra. Figure 3.2 compares the simulated spectral signature of *Apodasmia similis* for the WolrdView sensor against the un-modified ground based spectral signature captured by an Asd Spectroradiometer. The WorldView simulation results in a good fit with the raw data, although some features have been lost, such as, the NIR shoulder and depth of the chloropyll

absorption in the Red region. While identiifcation of species using the simulated WorldView data would be more difficult than using the near-continous spectroradiometer data, it does feature datapoints in the blue, green, red, yellow, and NIR that are meaningful for vegetation studies.

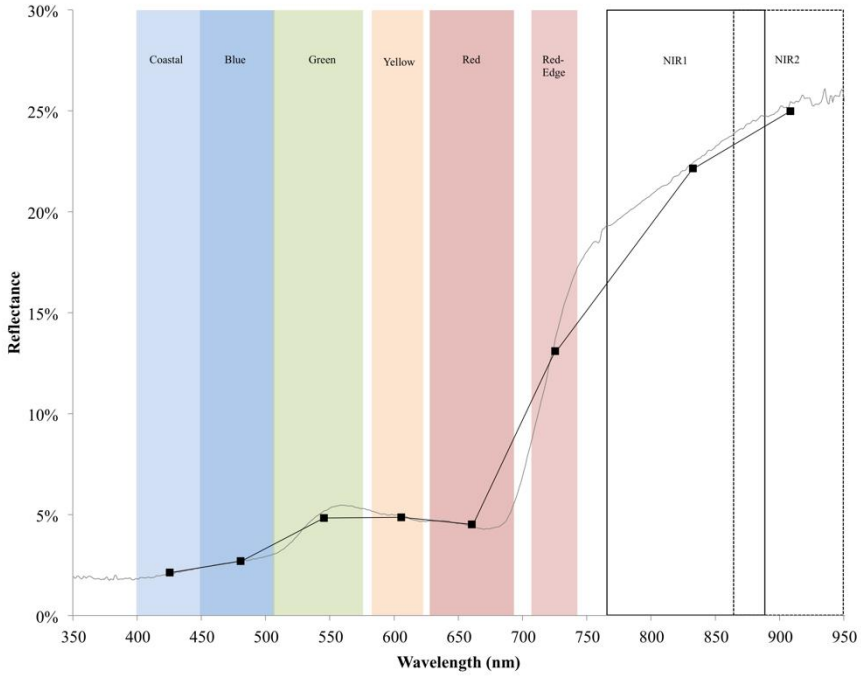

Figure 3.2 Raw Asd Spectroradiometer signature (grey) and WorldView simulated signature (black) of *Apodasmia similis.* Underlying graphic represents WorldView sensor band widths.

Spectral Signatures Comparison

Figure 3.3 (a), (b) and (c) shows the mean simulated WorldView spectral reflectance signature for fourteen native and exotic species found at Whatipu. Comparison of the spectral curves show the rushes and sedges (a) generally had lower near-infrared reflectance than other species. Monocotyledonous trees and grasses (c) typically had higher reflectance in visible wavebands than other species. Although several species had distinct NIR reflectance, most species have similar reflectance, making visual discrimination based on their reflectance curves difficult.

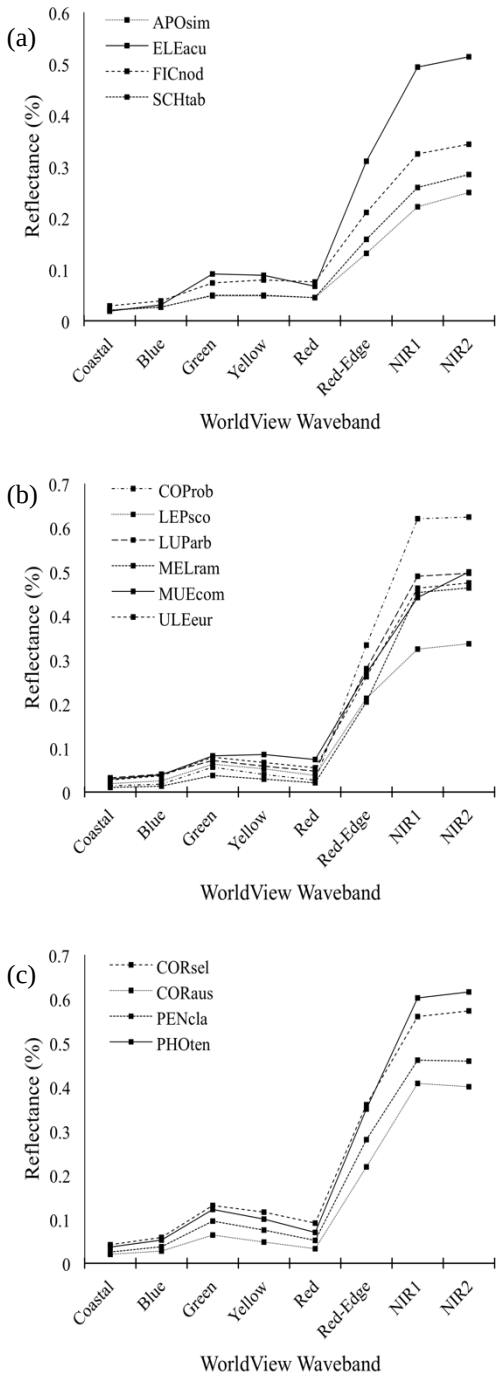

Figure 3.3 Mean spectral reflectance at simulated WorldView wavebands of 14 common native and exotic species found at Whatipu. (a): rushes and sedges, (b): dicotyledonous trees, shrubs and lianes, and (c): monocotyledonous trees and grasses. Codes used to designate species on (a) are: APOsim, *Apodasmia similis*; ELEacu, *Eleocharis acuta*; FICnod, *Ficinia nodosa*; SCHtab, *Schoenoplectus tabernaemontani*. Codes used to designates species on (b) are: COProb, *Coprosma robusta*; LEPsco, *Leptospermum scoparium*; LUParb, *Lupinus arboreus*; MELram, *Melicytus ramiflorus*; MUEcom, *Muehlenbeckia complexa*; ULEeur, *Ulex europaeus*. Codes used to designates species on (c) are: CORsel, *Cortaderia selloana*; CORaus, *Cordyline australis*; PENcla, *Pennisetum clandestinum*; PHOten, *Phormium tenax*.

The spectral reflectance variation within each species at particular wavebands also shows that most species have similar reflectance profiles, indicated by the amount of overlap between them (Figure 3.4). The WorldView near-infrared-2 waveband (NIR2) was chosen because near infrared is typically associated with high discrimination between species. The amount of intra-species variation differs between species. Comparison of these species reveals that the intra-species variability and the overlap between each species at NIR2 is too great to successfully differentiate and therefore is not optimal for species recognition. However, several species had reduced intra-species variability and little overlap with distinct reflectance values indicating that this waveband is suitable for some species where overlapping species are not present.

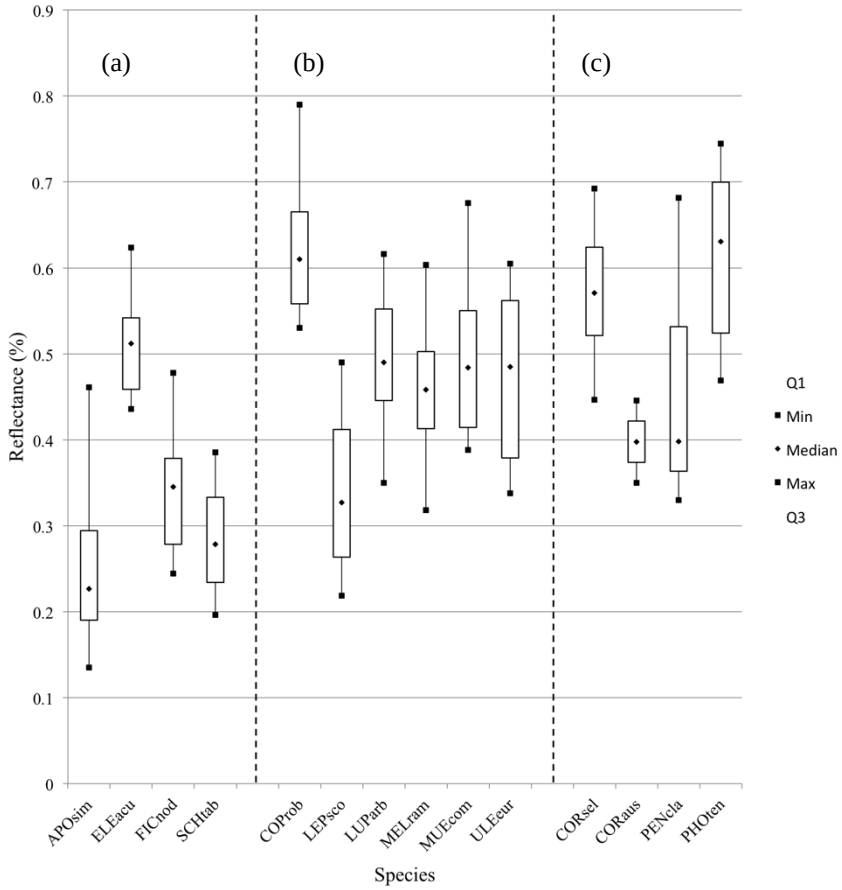

Figure 3.4 Spread of spectral reflectance at WorldView NIR2 band (860 - 950nm) of 14 common native and exotic species found at Whatipu. (a): rushes and sedges, (b): dicotyledonous trees, shrubs and lianes, and (c): monocotyledonous trees and grasses. Codes used to designate species on (a) are: APOsim, *Apodasmia similis*; ELEacu, *Eleocharis acuta*; FICnod, *Ficinia nodosa*; SCHtab, *Schoenoplectus tabernaemontani*. Codes used to designates species on (b) are: COProb, *Coprosma robusta*; LEPsco, *Leptospermum scoparium*; LUParb, *Lupinus arboreus*; MELram, *Melicytus ramiflorus*; MUEcom, *Muehlenbeckia complexa*; ULEeur, *Ulex europaeus*. Codes used to designates species on (c) are: CORsel, *Cortaderia selloana*; CORaus, *Cordyline australis*; PENcla, *Pennisetum clandestinum*; PHOten, *Phormium tenax*.

3.2 UAS Results

To obtain 15,000 two megapixel aerial images, covering 115 hectares, from a flight altitude of 50m, it took approximately 250 minutes of flight. I obtained clear images with sufficient overlap to create a high-resolution orthomosaic and digital surface model (DSM) in Pix4Dmapper (Figure 3.5). Processing the ~3400 images took roughly 48 hours, producing a very high resolution image product of 6cm spatial resolution, sufficient to visually identify vegetation by structural class, some down to species level.

Figure 3.5 Orthomosaic of southern Whatipu.

3.3 ROI Spectral Separability

The supervised classification training samples were analysed prior to classification processing to determine their spectral separability. The separability between the land cover classes were analysed visually using feature space (2-d scatterplots). The statistical separability of each training sample in the form of region's of interest (ROI) was measured by calculating the Jeffries Matusita (JM) and Transformed Divergence (TD) distances. The analysis was carried on the 2011 and 2015 region of interest data.

The 2-dimnesional scatterplots of the ROI's for both time datasets are shown in Figure 3.6. The results show that most vegetation classes contain significant overlap. In both datasets, the overlap between unvegetated surfaces (water and unvegetated sand) and the sparsely vegetated surfaces (*Carex pumila* sandfield and *Spinifex sericeus/Ficinia spiralis* duneland) is generally minimal, the exception being Time-2 (2015) datasets unvegetated sand and *Spinifex sericeus/Ficinia spiralis* duneland classes.

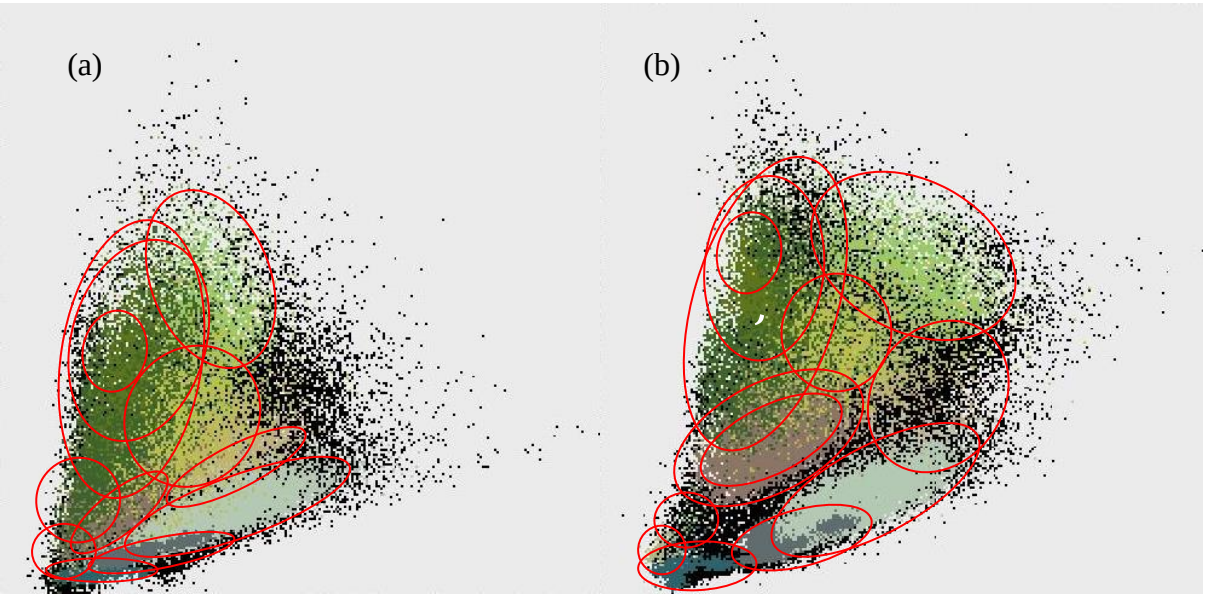

Figure 3.6 NDVI (Y axis = NIR2 band and X axis = Red band) feature space scatterplots showing the spread of values associated with 13 region of interest training samples. (a) 2011 WorldView-2 Imagery and (b) 2015 WorldView-3 Imagery. (--) Unvegetated sand, (--) *Carex pumila* sandfield, (--) Spinifex/Pingao duneland, (--) *Pennisetum clandestinum* grassland, (--) Openwater, (--) *Machaerina articulate* reedland, (--) *Schoenplectus tabernaemontani* reedland, (--) *Typha orientalis* reedland, (--) *Apodasmia similis* rushland, (--) *Eleocharis acuta* rushland, (--) Exotic shrubland, (--) Native shrubland, (--) *Ulex europaeus* shrubland.

The JM and TD distances presented in Table 3.1 show reasonable separability was achieved with both WV-2 ROI data and WV-3 ROI data with mean JM distances of 1.7773 and 1.7077 respectively. A JM distance of 2.0 indicates full separability and a value of ~1.9 is good separability.

Table 3.1 Statistics of separability analysis.

Distance Measure	2011 ROI	2015 ROI
JM min	0.4697	0.8734
JM max	2.0000	2.0000
JM mean	1.7077	1.7773
TD min	0.5078	1.0538
TD max	2.0000	2.0000
TD mean	1.8238	1.8882

Comparison of Simulated Spectra with Satellite Spectra

WorldView imagery spectral signatures were derived from ROI's and compared simulated WorldView sensor (field based) spectral signatures to assess the utility of the WorldView reflective bands for obtaining realistic reflectance measurements, shown in Figure 3.7. The satellite-derived signatures are atmospherically corrected to match surface conditions. We can see that the WorldView-2 and simulated reflectance show a good agreement for bands in the visible regions but the agreement deteriorates at the near-infrared band. In addition, the WorldView-3 signatures are generally larger than the simulated signatures for the available WorldView bands; this is likely an artifact of errors encountered during atmospheric correction.

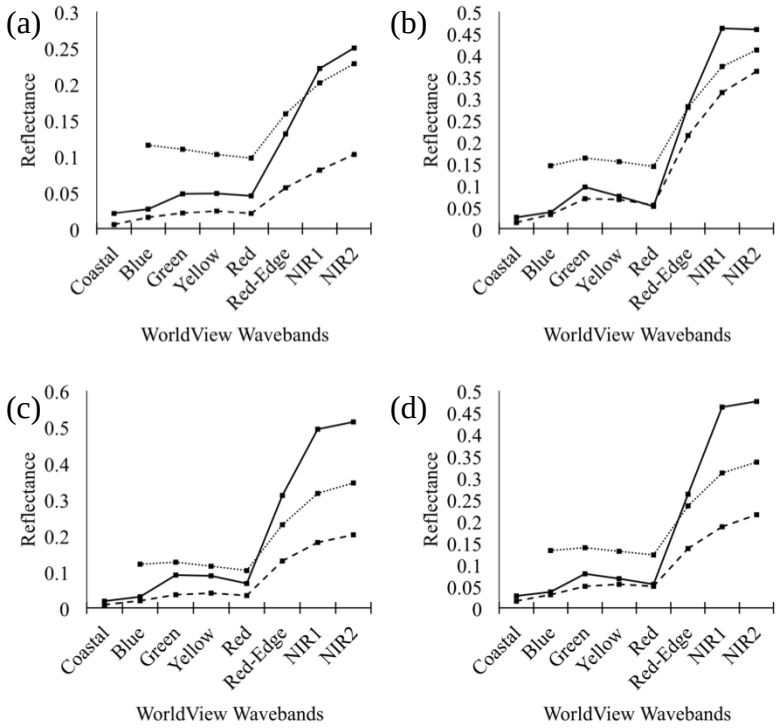

Figure 3.7 Comparison of simulated WorldView (——), WorldView-2 (– –) and WorldView-3 (· · ·) spectral signatures our dominant vegetation types at Whatipu. (a) *Apodasmia similis*, (b) *Pennisetum clandestinum*, (c) *Eleocharis acuta*, (d) *Ulex europaeus.*

3.4 Satellite Classifications

Supervised Classifications

Figure 3.8 shows the classification results for the 2011 WorldView-2 supervised classification techniques used in this study. All classifiers were able to identify land cover beyond the area of the ROI's, although the accuracy of each differs substantially.

The Minimum Distance (Figure 3.8 a) was inaccurate in classifying the significant portion of vegetation and unvegetated classes of the Whatipu wetland dune complex for 2011 WorldView-2 imagery (overall accuracy: 69.0%, Table 3.2). These results were particularly inaccurate in separating *Typha orientalis* reedland from Native and Exotic shrubland classes. Only six of the thirteen classes produced accuracies greater than the 70% threshold. Unvegetated classes (Openwater and Unvegetated sand) produced the highest individual accuracies, which were both greater than 90%.

The Mahalanobis Distance algorithm (Figure 3.8 b) classified classes with increased overall accuracy of 77.0%. These results show similar inaccuracies as the Minimum Distance algorithm, where *Typha orientalis* reedland from Native and Exotic shrubland classes showed significant misclassification (Figure 3.8 b). Although slightly improved individual class accuracies with nine of the thirteen classes above the threshold of 70%. Again, unvegetated classes produced the highest individual producer accuracies (>99%, Table 3.2).

The Maximum Likelihood classification algorithm was a significant improvement over the other two methods (Figure 3.8 c), with an overall accuracy of 91.7%. *Typha orientalis* reedland and Exotic shrubland classes were the worst performing classes attaining class accuracies of 79 and 78% respectively. Eleven of the thirteen classes achieved producer accuracies greater than 80% (Table 3.2).

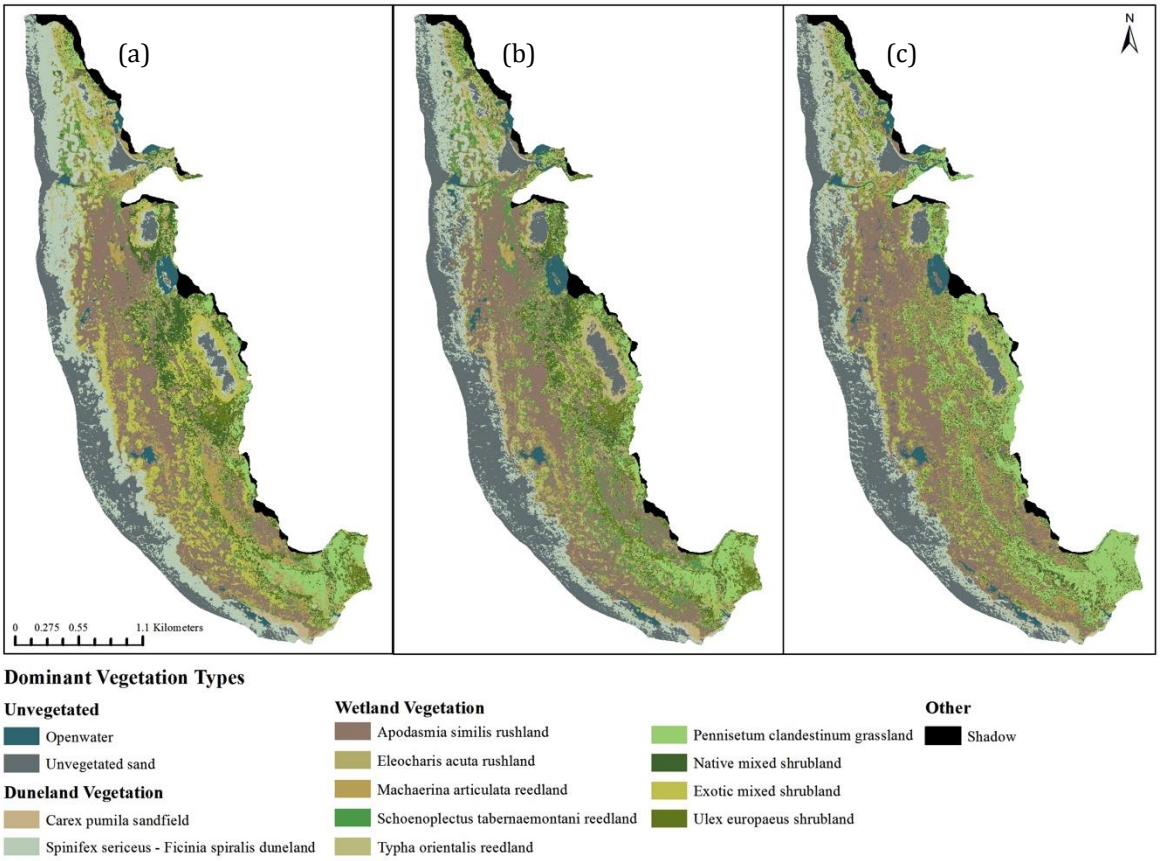

Figure 3.8 Whatipu Scientific Reserve, showing 2011 WorldView-2 supervised classifications. (A. Minimum Distance; B. Mahalanobis Distance; C. Maximum Likelihood).

Table 3.2 Confusion matrix results of 2011 MSI Supervised classifications.

Classification Type	Class	Producer accuracy (%)	User accuracy (%)	Overall accuracy (%)	Kappa coefficient
Minimum distance	*Apodasmia similis* rushland	84.91	83.65	69.0553	0.6485
	Eleocharis acuta rushland	43.87	5.34		
	Typha orientalis reedland	21.58	12.35		
	Schoenoplectus tabernaemontani reedland	35.40	25.05		
	Machaerina articulate reedland	42.03	37.31		
	Pennisetum clandestinum grassland	80.15	54.79		
	Native shrubland	17.06	45.29		
	Exotic shrubland	38.77	73.17		
	Ulex europaeus shrubland	16.11	27.29		
	Spinifex sericeus/Ficinia spiralis duneland	73.61	94.05		
	Carex pumila sandfield	73.07	51.46		
	Openwater	99.80	98.87		
	Un-vegetated sand	98.15	80.42		
Mahalanobis Distance	*Apodasmia similis* rushland	88.96	86.99	77.0295	0.7397
	Eleocharis acuta rushland	84.98	6.78		
	Typha orientalis reedland	41.08	40.38		
	Schoenoplectus tabernaemontani reedland	80.00	28.30		
	Machaerina articulate reedland	35.75	73.93		
	Pennisetum clandestinum grassland	78.84	88.57		
	Native shrubland	59.80	85.75		
	Exotic shrubland	26.14	62.93		
	Ulex europaeus shrubland	75.98	40.87		
	Spinifex sericeus/Ficinia spiralis duneland	79.45	95.97		
	Carex pumila sandfield	79.76	54.35		
	Openwater	99.32	94.96		
	Un-vegetated sand	99.20	87.81		
Maximum Likelihood	*Apodasmia similis* rushland	91.71	96.91	91.7232	0.9059
	Eleocharis acuta rushland	96.05	35.37		
	Typha orientalis reedland	79.11	68.19		
	Schoenoplectus tabernaemontani reedland	82.92	61.89		
	Machaerina articulate reedland	93.08	84.51		
	Pennisetum clandestinum grassland	90.84	97.40		
	Native shrubland	81.82	93.48		
	Exotic shrubland	78.55	86.01		
	Ulex europaeus shrubland	85.73	62.70		
	Spinifex sericeus/Ficinia spiralis duneland	96.96	95.92		
	Carex pumila sandfield	89.15	76.27		
	Openwater	99.70	99.95		
	Un-vegetated sand	98.81	99.33		

Figure 3.9 shows the classification results for the 2015 WorldView-3 supervised classification techniques used in this study. The results were similar to the 2011 WorldView-2 dataset supervised classifications, accuracies increased (Table 3.3) from Minimum Distance (overall accuracy: 70.6%), to Mahalanobis Distance (80.1%) to Maximum Likelihood (92.4%).

Again, the minimum Distance was inaccurate in classifying the majority of land cover classes and the Mahalanobis Distance produced reasonable classification. Common sources of misclassification were reedland and rushland communities and between *Typha orientalis* reedland and the Native forest and Exotic forest shrubland classes. Both classifications did however produce good results for Un-vegetated classes, especially Openwater class.

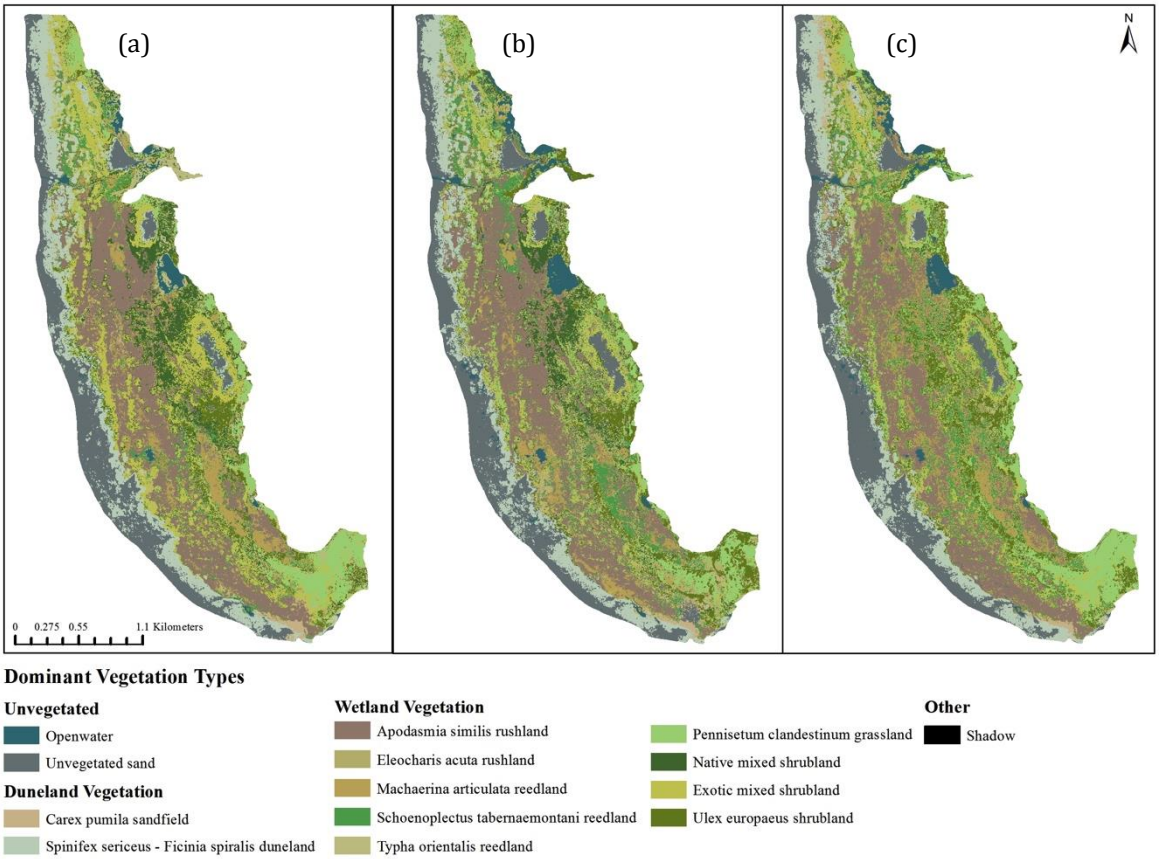

Figure 3.9 Whatipu Scientific Reserve, showing 2015 WorldView-3 supervised classifications. (A. Minimum Distance; B. Mahalanobis Distance; C. Maximum Likelihood).

Table 3.3 Confusion matrix results of 2015 MSI Supervised classifications.

Classification Type	Class	Producer accuracy (%)	User accuracy (%)	Overall accuracy (%)	Kappa coefficient
Minimum distance	*Apodasmia similis* rushland	87.71	89.98		
	Eleocharis acuta rushland	73.56	12.94		
	Typha orientalis reedland	0.70	0.72		
	Schoenoplectus tabernaemontani reedland	36.43	14.76		
	Machaerina articulata reedland	59.65	48.66		
	Pennisetum clandestinum grassland	86.77	76.48		
	Native shrubland	12.68	85.64	70.6006	0.6656
	Exotic shrubland	42.45	60.27		
	Ulex europaeus shrubland	82.28	26.37		
	Spinifex sericeus/Ficinia spiralis duneland	86.87	94.97		
	Carex pumila sandfield	61.84	57.28		
	Openwater	97.56	94.13		
	Un-vegetated sand	87.34	69.82		
Mahalanobis Distance	*Apodasmia similis* rushland	86.60	95.03		
	Eleocharis acuta rushland	93.68	12.96		
	Typha orientalis reedland	14.17	17.90		
	Schoenoplectus tabernaemontani reedland	74.48	24.27		
	Machaerina articulata reedland	53.18	70.37		
	Pennisetum clandestinum grassland	82.93	89.25		
	Native shrubland	82.85	90.82	80.1504	0.7738
	Exotic shrubland	33.74	69.30		
	Ulex europaeus shrubland	89.13	51.30		
	Spinifex sericeus/Ficinia spiralis duneland	88.27	99.25		
	Carex pumila sandfield	86.58	52.34		
	Openwater	99.22	93.29		
	Un-vegetated sand	98.84	73.45		
Maximum Likelihood	*Apodasmia similis* rushland	96.21	96.76		
	Eleocharis acuta rushland	100	44.85		
	Typha orientalis reedland	75.24	71.91		
	Schoenoplectus tabernaemontani reedland	78.09	65.61		
	Machaerina articulata reedland	93.29	91.41		
	Pennisetum clandestinum grassland	96.78	98.80		
	Native shrubland	87.13	94.18	92.4163	0.9128
	Exotic shrubland	75.87	84.43		
	Ulex europaeus shrubland	97.04	70.46		
	Spinifex sericeus/Ficinia spiralis duneland	92.89	99.64		
	Carex pumila sandfield	88.54	72.57		
	Openwater	99.09	99.20		
	Un-vegetated sand	99.81	89.00		

The Results of the 2011 and 2015 WorldView classifications indicate that the MLC algorithm is better equipped to classify wetland duneland vegetation. Not only were the overall accuracies considerably higher for the Maximum Likelihood than the Minimum Distance and Mahalanobis Distance, but also the individual producer and user accuracies for vegetation classes were higher. It was therefore decided that the Maximum Likelihood Classification results would be used in the change detection analysis.

General Vegetation and Habitat Patterns

All classifications revealed a lot about the spatial distribution of vegetation land cover at Whatipu. Although the distribution of these classes has been investigated before (TCEC, 2014), there is little information describing this in the public domain. Below general vegetation patterns and species associations are described in relation to their ecology and geography within the context of Whatipu wetland duneland system.

The dominant *Apodasmia similis* rushland class occupies a brackish zone behind the active foredune that spans almost the entire length of Whatipu beach. This class often grades up-slope from wet organic soils to dry sandy soils. *Eleocharis acuta* rushland is present amongst *Pennisetum clandestinum* grassland on permanently damp ground and along stream margins. *Typha orientalis* reedland is found on margins of ponds, lakes and slow flowing streams along the eastern edge of wetland. *Schoenoplectus tabernaemontani* reedland was found throughout the wetland often in ponds, lake or stream margins. Similarly, *Machaerina articulata* reedland was found throughout the wetland in dune depressions of either ponds or lakes. Many if not all of the reedland and rushland communities mix throughout the wetland.

Pennisetum clandestinum grassland dominates many parts of the Whatipu complex, particularly in the southern section and at the bottom of the cliff. This exotic grassland typically appears in damp depressions with scattered *Eleocharis acuta.* Young scattered shrubs (native and exotic), mature Cabbage tree (*Cordyline australis)* and exotic Pampas grass (*Cortaderia spp*.) are also found in this class.

The native shrubland class is found on raised remnant rear dunes with organic topsoils and at the base of the cliff. Common species include *Coprosma robusta* (Karamu), *Leptospermum scoparium* (Manuka), *Melicytus ramiflorus* (Mahoe), *Muehlenbeckia complexa,* with scattered *Phormium tenax* (flax) and *Cordyline australis* (Cabbage tree). *Ficinia nodosa* (Knobbly clubrush) is mixed throughout.

Exotic shrubland is found throughout the Whatipu complex, often on dryland soils on and behind the foredune, similarly found on rear old-dunes. Exotic shrubland is also scattered throughout the *Apodasmia similis* rushland. This class includes *Cortaderia selloana, Lupinus arboreus* and scattered *Ulex europaeus*. Also contains vegetation associated with a flat dune

plain at the northern end of Whatipu. The dune plain is predominantly native shrubland dominated by Ozothamnus *leptophyllus* and *Ficinia nodosa* shrubland. Although it does not fit the criteria of Exotic shrubland, it was poorly separated out during preliminary classifications and therefore was merged. Much like the exotic shrubland vegetation, *Ulex europaeus* shrubland (also exotic) was found throughout the Whatipu complex on remnant stabilized dunes. This class is mixed with the native and exotic shrubland vegetation, and scattered on the flat dune plain dominated by Ozothamnus *leptophyllus* and *Ficinia nodosa* shrubland.

Spinifex sericeus/Ficinia spiralis duneland is native plant dominated dunelands vegetation common where there is a supply of coastal sands in association with wind action. The dominant *Spinifex-Ficinia* grassland occurs on the foredune at the front of the beach, whilst it also occurs on sand ridges and dunes scattered behind the foredune and at the rear of the beach. *Carex pumila* sandfield is relatively uncommon and occurs in restricted locations in the southern end of Whatipu. It was predominantly found in wet dune slacks behind the foredune transitioning into *Spinifex sericeus/Ficinia spiralis* duneland.

Areas of open water occur throughout the wetlands in the form of flowing water (streams), ephemeral ponds and permanent dune lakes.

3.5 Wetland Vegetation Change from 2011 and 2015

Only a small fraction of the Whatipu wetland and duneland complex underwent land cover changes between 2011 and 2015. The Normalised Difference Vegetation Index (NDVI) image (Figure 3.10) was used as an initial step to identify if change could be detected at Whatipu in the short timespan (4yrs) between the 2011 and 2015 imagery sets. This output highlights areas within the complex where changes are likely to have occurred by identifying any differences in radiance values at Red (660 nm) and near-infrared (950 nm) between the multi-temporal datasets. Bright areas indicate significant change, while dark areas indicate little to no change. Areas of open water appear to have undergone significant change from 2011 and to 2015, even in areas where no water loss occurred. This is likely an artifact of the differences in radiance values reflected from the waters surface due to difference in sensor viewing angle. Areas of the un-vegetated sand also show a difference in NDVI values, possibly due to a change in water saturation of sand, as NDVI is sensitive to water content. Vegetation Change is slightly harder to identify. However there is some evidence of this on fringe areas of the foredune and rear dunes, and sandflats in the north, where bright pixels follow the contour of the beach, indicative of vegetative change (growth and/or expansion).

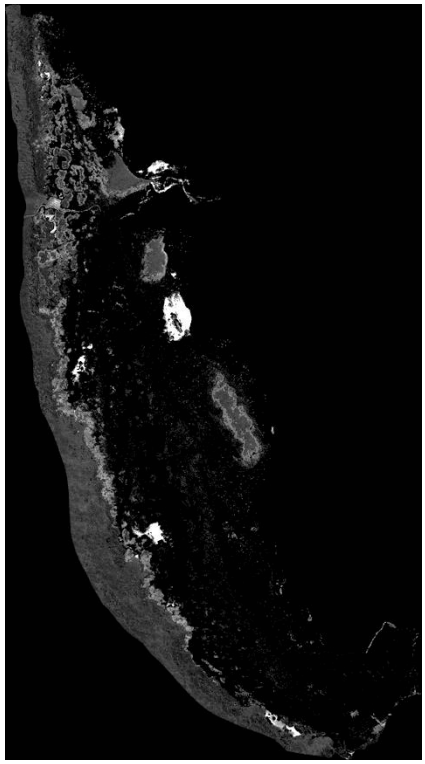

Figure 3.10 NDVI difference image (2011 and 2015), contrast stretch was applied to highlight features

To identify specific land cover changes between the multi-temporal datasets the final manually edited supervised classification results (Figure 3.11) were compared. The multi-date classification comparison identified areas specific to classes where change has occurred at the Whatipu complex. Of the area surveyed, 88ha of land cover underwent some form of change, either gain or loss, which represents 13.9% of the total study area (638ha) (Table 3.4). The majority of classes have undergone some change between the two dates, either because of actual change or as an artifact of classification errors between the two imagery sets.

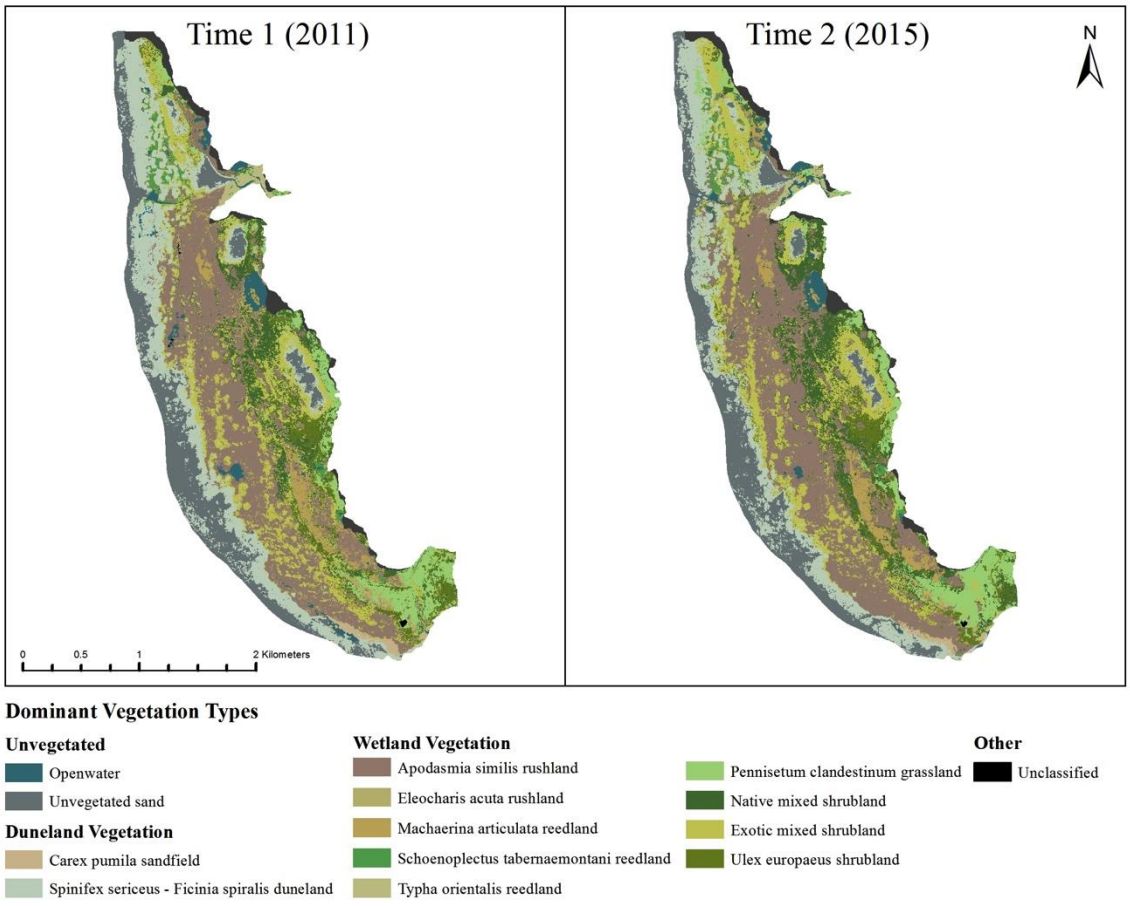

Figure 3.11 Whatipu Scientific Reserve, showing final manually edited supervised classifications of 2011 WorldView-2 and 2015 WorldView-3 imagery.

The "*Spinifex sericeus/Ficinia spiralis* duneland" at Whatipu have been subject to the most change in the last 4.5 years with a total decrease of 24.3 ha. This significant loss is the result of the increase in "Exotic shrubland" communities on sparsely vegetated sediments and expansion of "*Apodasmia similis* rushland" into wet sand hollows behind the foredune. Another significant decrease was seen in "Unvegetated sand" (7.5ha). This is particularly noticeable on the foredune and the rear dunes, especially on the rear dune located halfway up

the Whatipu complex. This decrease is a result of the expansion of colonising "*Spinifex sericeus/Ficinia spiralis duneland"* and "Exotic shrubland" classes. The decrease in "*Eleocharis acuta* rushland" (6.2 ha) is likely misclassification and confusion with the "*Pennisetum clandestinum* grassland" class. The decrease in "Openwater" of 2.6ha is in most localities can be attributed to the expansion of "*Apodasmia similis* rushland" and "*Machaerina articulata* reedland" classes.

The largest increase in vegetation is attributed to the "Native shrubland" class (17.3ha). It is difficult to say how much of this change is actual change, and not caused by misclassification errors. However, maturation and broadening of native shrubland canopy and expansion into sparsely vegetated dunes or exotic vegetation classes has occurred in some areas. The large increase in "*Apodasmia similis* rushland" (11.1ha) is due to a combined decrease in "*Spinifex sericeus/Ficinia spiralis* duneland" and "Openwater" classes. The increase in "Exotic shrubland" (6.8ha) is due to expansion into the "*Spinifex sericeus/Ficinia spiralis* duneland". The increase in "*Pennisetum clandestinum* grassland" (6.6ha) is likely a result of misclassification the with "*Eleocharis acuta* rushland" class. The "*Machaerina articulata* reedland" class increased by 2.6ha in areas previously of the "Openwater" class, through either expansion or densification.

Table 3.4 Whatipu vegetation land cover change statistics.

Class	2011		2015		Gains and Losses	
	Area (ha)	Percent	Area (ha)	Percent	Area (ha)	Percent
Apodasmia similis rushland	171.2	26.8%	182.3	28.5%	11.1	1.7%
Eleocharis acuta rushland	9.0	1.4%	2.8	0.4%	-6.2	0.9%
Typha orientalis reedland	5.5	0.8%	5.5	0.8%	0	0.0%
Schoenoplectus tabernaemontani reedland	6.6	1.0%	5.8	0.9%	-0.8	0.1%
Machaerina articulata reedland	16.8	2.6%	19.4	3.0%	2.6	0.4%
Pennisetum clandestinum grassland	39.6	6.2%	46.2	7.2%	6.6	1.0%
Native shrubland	48.8	7.6%	66.1	10.3%	17.3	2.7%
Exotic shrubland	93.7	14.6%	100.5	15.7%	6.8	1.0%
Ulex europaeus shrubland	29.7	4.6%	28.1	4.4%	-1.6	0.2%
Spinifex sericeus/Ficinia spiralis duneland	112.0	17.5%	87.7	13.7%	-24.3	3.8%
Carex pumila sandfield	4.14	0.6%	3.0	0.4%	-1.14	0.1%
Openwater	14.0	2.1%	11.4	1.7%	-2.6	0.4%
Un-vegetated sand	86.7	13.5%	79.2	12.4%	-7.5	1.1%
Unclassified	0.4	0.0%	0.2	0.0%	-0.2	0.0%
Total	638	100	638	100	88.74	13.9

Figure 3.12 is an example area from within the wetland duneland complex at Whatipu to highlight some of the changes that have occurred in the last four years between 2011 and 2015. We can see here that the "*Apodasmia similis* rushland" class replaces the decrease in

"Openwater" in 2011 in 2015. The "*Apodasmia similis* rushland" class also appears to have replaced some of the in "Exotic shrubland" class. Also evident here are increases in "Exotic shrubland" occurring in areas previously classified as "*Spinifex sericeus/Ficinia spiralis* duneland". The shrubland communities "Exotic shrubland", "*Ulex europaeus* shrubland" and "Native shrubland" (Figure 3.12) appear to have changed considerably, this is likely a result of misclassification between classes. The significant differences in cover between the two dates, is improbable in a short time span of four years, especially for slower growing tertiary successional classes.

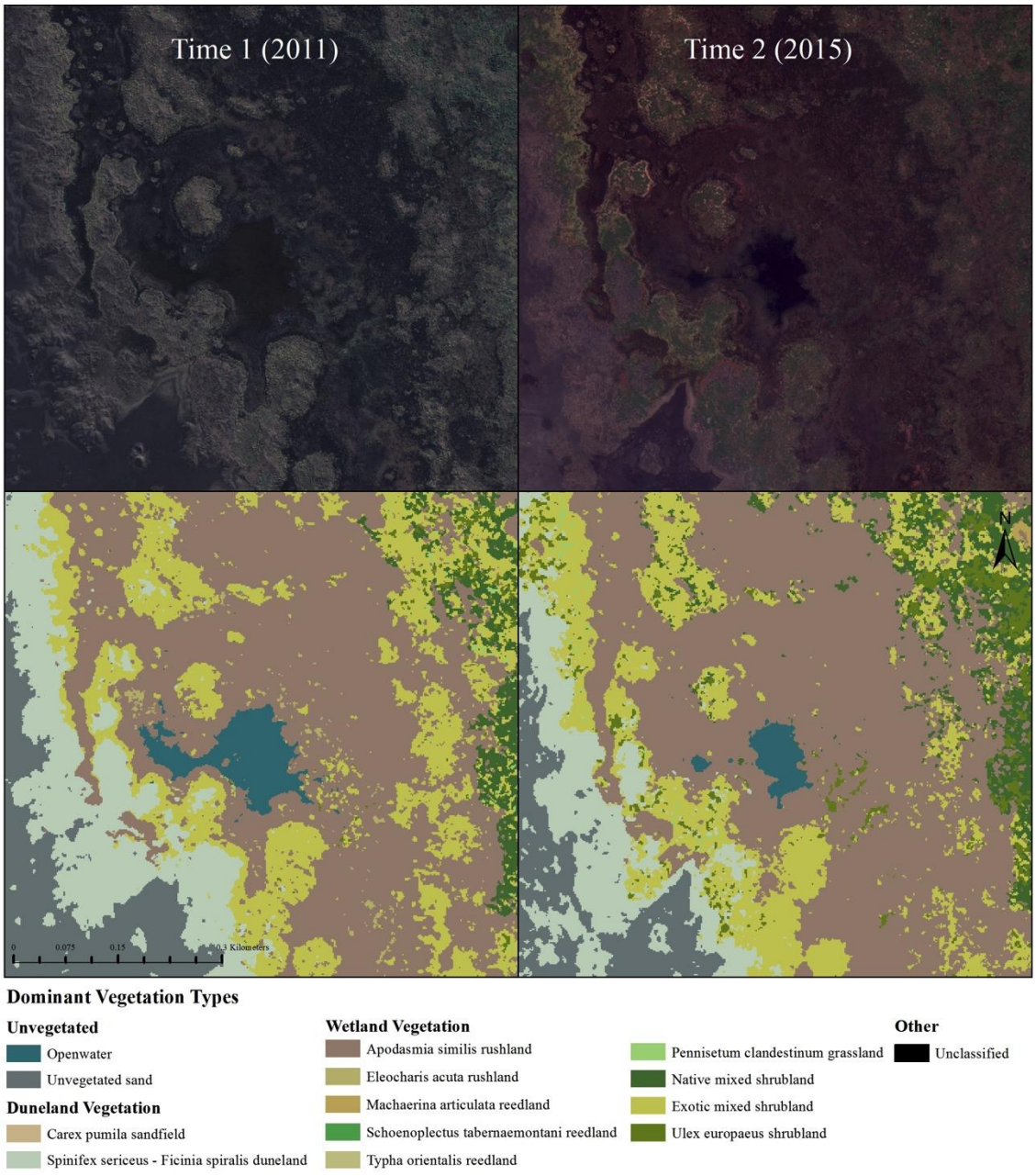

Figure 3.12 Example showing differences in pan-sharpened imagery and classification results between 2011 (left) and 2015 (right).

3.6 Case Study Results

The two visually interpreted datasets and the automatically classified dataset produced significantly different results (Figure 3.13). Visual interpretation of high-resolution (0.3m) satellite imagery produced 23 polygons including clusters and individuals of *Cortaderia spp,* covering 150.6m^2 (Table 3.5). This excludes seven polygons that were removed due to miss interpretation when cross-referenced with the high resolution UAS imagery. In each case miss-interpreted polygons were results of similarities Pampas has with the tone and shape of Cabbage tree (*Cordyline australis*) foliage (light ashy green and circular) or flax (*Phormium tenax*) foliage (bright green, high reflectivity and circular shape).

Total pampas area detected in the "Exotic shrubland" class derived from automatic classification (which included species other than *Cortaderia* e.g., Lupin and Gorse.), had 54 polygons that contained pampas, covering 394.4m^2. The high resolution UAS imagery on the other hand identified 1480.2m^2 of Pampas in 320 polygons of individual and clustered specimens.

Using The UAS Pampas polygons as the standard, the satellite derived Pampas coverage for visually interpreted (satellite pampas polygons) and manually classified ("Exotic shrubland" class) only detected 10.17% and 26.65% respective area of Pampas found. It is not surprising that the higher resolution imagery was able to detect more Pampas coverage in the study area than the lower resolution imagery (visually and manually interpreted). However, this highlights the significant underestimation that can result from inadequate resolution imagery for identifying specific species such as Pampas.

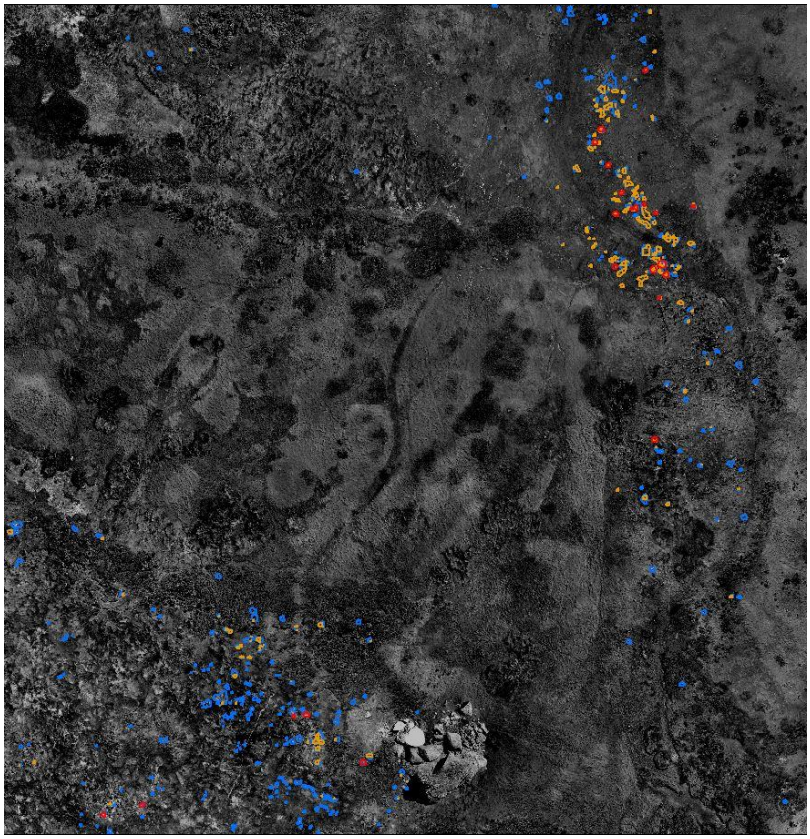

Figure 3.13 Pampas cover in the southern section of Whatipu Scientific Reserve. Yellow polygons: Exotic shrubland class from automatic classification of multispectral satellite imagery (2m spatial resolution) Red polygons: visually classified from high-resolution (0.3m) satellite imagery. Blue polygons: visually classified from high-resolution (0.06m) aerial imagery (also under lying image in grey scale for clarity).

Table 3.5 Case study results.

Dataset	Imagery Spatial Resolution	Number of polygons	Area of pampas coverage
Satellite Pampas polygons	0.3m	23	150.6 m^2
UAS Pampas polygons	0.06m	320	1480.2 m^2
Exotic shrubland class	2m	54	394.4 m^2

Figure 3.14 Examples of pampas polygons from each dataset: Satellite Pampas polygons (right), UAS Pampas polygons (middle) and Exotic shrubland class (left). Red polygons: identified from high-resolution (0.3m) satellite imagery, Blue polygons: identified from high-resolution (0.06m) aerial imagery.

4 Discussion

This chapter is grouped into five main sections. The first section will focus on spectral uniqueness and separability of dominant vegetation at Whatipu (section 4.1). The second section will discuss the use of using UAS imagery as an alternative to field visits for the collection of validation and training samples (section 4.2). The third section will discuss the performance and the limitations of the classifications of multi-date imagery (section 4.3). Section 4.4 discusses how and why land cover changes have occurred at Whatipu. The final section focuses on the use of UAS imagery for identification of species and practicality of the UAS platform for low altitude remote sensing.

4.1 Spectra of Whatipu Vegetation

Objective One: Use field hyperspectral reflectance measurements to develop spectral signatures of dominant vegetation at Whatipu and to assess their spectral separability.

Spectral signatures were used to evaluate the potential for separating dominant species, and to characterize spectral variability of each species. According to the mean spectra at WorldView wavebands in Figure 3.3 (Chapter 3) most species showed maximum differences at NIR2 (840-950nm). The NIR region is commonly associated with greatest spectral separability (Everitt et al., 2015; Quyang et al., 2013), however dominant species found at Whatipu still show significant intra-species variability in the NIR region (Figure 3.4, Chapter 3). This, as well as similarities in overall shape of the spectral profiles, indicates low levels of spectral uniqueness as suggested by Price (1994). The consequences of low spectral uniqueness, i.e. high intra-species and interspecies variability, of vegetation means the spectral component of imagery cannot alone offer species specific identification. Other components, such as structural, textural and relational information in imagery could be exploited as solution to difficulties associated with limited spectral separability (Aplin & Smith, 2008; Visser, 2010; Hassan et al., 2014).

Even with limited spectral separability between species, the simulated WorldView bands preserved many of the spectral features characteristic of vegetation (Figure 3.2, Chapter 3). Therefore the spectra could be used in other applications, potentially at locations where vegetation spectral heterogeneity is lesser than Whatipu wetland and duneland complex.

However, more thorough statistical investigation should be undertaken to properly determine the spectral separability.

4.2 Training and Validation Samples

Objective Two(2): Investigate the use of Unmanned Aerial System imagery for supervised classification sample data collection.

One of the many appeals of remote sensing is the ability to use non-destructive methods. However to achieve accurate classification of land cover there is a need for training and validation samples collected from the field. Although not the only method, e.g. collection from imagery or ancillary data, collecting field data is commonly used for fine scale mapping (Rapinel et al., 2014; Roeck et al., 2014). The high resolution UAS imagery was used to identify vegetation class reference sites and to supplement the samples collected from the pan-sharpened satellite imagery for the 2015 supervised classification as an alternative to field sampling (e.g. quadrats and transects). Low altitude, high resolution (<10cm pixels) UAS imagery provides sufficient information to accurately identify vegetation; potentially down to species level (Ishihama, Watabe, & Oguma, 2012). Identification of classes was easier and delineating the boundaries was sharper using the low altitude UAS aerial imagery in comparison to the high-resolution satellite imagery. Therefore, UAS imagery can be used in place of field visits for the collection of training and validation data for vegetation classification of satellite imagery, eliminating the need to disturb or destroy the site in which one seeks to survey. Not only was the imagery easier to interpret, but also collecting UAS imagery reduces the amount of time one needs to spend in the field and therefore is potentially much cheaper, especially for large areas. Field surveys also run the risk of making inaccurate observations as coastal wetland environments are often difficult to traverse. An aerial perspective is an obvious advantage.

4.3 Land Cover Classification

Objective Three: Compare performance of pixel-based classification methods of multispectral satellite imagery to identify vegetation.

For mapping coastal wetland and duneland vegetation, using multispectral WorldView imagery, the supervised classification techniques showed reasonable accuracy with the Minimum Distance and Mahalanobis Distance classification algorithms. However using the Maximum Likelihood classification algorithm better accuracies were reached. From the accuracies determined in the Confusion Matrix, it clearly shows that the Maximum Likelihood technique was able to distinguish the classes with higher accuracies than other classification techniques. This is similar to other vegetation mapping efforts that have found that using the Maximum Likelihood classifier is more accurate that other pixel based methods (Everitt et al., 2008; Szuster, Chen, & Borger, 2011).

The vegetation classification of Whatipu identified two wetland and one coastal duneland ecosystem from the eleven ecosystems created by the Department of Conservation and identified by Auckland Council as being present in the Auckland region (Singers et al., 2013; Singers & Rogers, 2014). These ecosystems, outlined in Table 1 (Chapter 1), include "Oioi restiad rushland/reedland" (WL10), "Raupo reedland" (WL19) and "Spinifex–pingao grassland/sedgeland" (DN2). Other ecosystem classes were found at Whatipu but were not classified individually. However, classes could be combined to upscale to terrestrial ecosystem units.

Classification Accuracy and Limitations

The two final supervised classification outputs of Whatipu wetland dune system (2011 and 2015 images, Chapter 3, section 3.5) presented in this research have overall accuracies of 91.7% and 92.4% (Kappa value of 0.90 to 0.91) and individual producer accuracies between 78% and 99% for 2011 and 75% and 99% for 2015 for all thirteen classes. Both 2011 and 2015 classification results achieved the accuracy threshold of 85% minimum overall accuracy, and greater than 70% per-class accuracies as per Thomlinson et al., (1999). The respective Kappa coefficients (0.9059 and 0.9128) show good agreement between the producer and user accuracies that suggest the classification were most likely correct (Aronoff, 2005).

Despite satisfactory results, the classifications of vegetation at Whatipu could be improved. Firstly, separability of 2011 WV-2 image classification classes could be improved by further refinement of training and validation sampling as these classes contained significant overlap and low separability. Secondly, the classification training and validation samples were partly based on thematic data created outside of this project (Thomas Civil field-based Wetland survey and Auckland Council wetland monitoring programme field maps). Thus, the classification quality depended on the accuracy of these datasets. On the other hand, increased spectral separability for the 2015 WV-3 imagery could be provided by larger sampling for classes with small samples (*Typha orientalis)* that were poorly represented in the UAS imagery collected for training and validation sampling.

Inaccuracies were also reflected in the separability of regions of interest used for training and validation of the classification themselves. The scatter plot visualization gave indications about the separability of species in 2-dimensional feature space, there was little difference between the spectral separability of the training samples collected in for the 2011 supervised classification and the 2015 supervised classification. The red band and NIR2 band combination data showed clusters for many target classes, however there was also significant over crowding of feature space resulting in overlap of many vegetation class clusters.

Future studies may achieve higher wetland classification accuracies if efforts are taken to reduce spectral confusion of vegetation classes and sample size is increased to account for the spectral variability of coastal duneland wetland vegetation and surrounding land cover. Further division of samples based on soil types (especially were vegetation becomes sparse) may also improve accuracies by increasing the capture of spectral variability.

Another limitation was the acquisition of a clear satellite image needed to accomplish this study. Although relatively cloud-free imagery was collected for this study, the acquisition dates of the imagery was 3 months apart (April 2011 and January 2015). Thefore matches based on phenological characteritics could provide additional information as to why the accuracies were different. This is evident in the April 2011 (Scene 01), where a common weed species, Gorse (*Ulex europaeus*), can been seen flowering with bright yellow inflorescence, whereas in January 2015 (Scene 02), Gorse was not flowering. Future studies should consider the benefits of satellite imagery with the potential delays associated

acquiring optimal imagery. If specific imagery dates are required, aerial platform acquisition may be a preferred source for imagery for mapping exercises.

As this project only assessed the use of standard 2m resolution multspectral imagery product, higher spatial resolution satellite imagery, such as a pan-sharpened imagery product, should be investigated to determine if spatial resolutions affect classification accuracies. Other satellite and aerial platform (airplane or unmanned aerial veheical) sensors should also be examined to determine their accuracies in assessing vegetation within wetland and duneland systems, such as the high resolution (2.4m MS and 0.6 Pan-sharpened) satellite Quickbird imagery available through the New Zealand Government "Kiwi Image" scheme (Ashraf et al., 2010).

Other improvements could have been made to processing techniques and the workflow chosen for this study. Given the high variability of coastal wetland duneland systems, a object based or hybrid classification approach may also prove helpful in improving accuracies. Object based classification could have improved the accuracy of the compared to the pixel-based methods as errors associated with the high spectral variability that exists in high spatial resolution imagery are often cited as an advantage to the OBIA approach (Fernandes et al., 2014; Hassan et al., 2014).

Although the final classification results were reasonably high, improvements were made by manually reclassifying polygons. This was done using visually identifying misclassified pixels (groups and individuals) and manually changing the class to an appropriate substitute. The aim of this was to increase the accuracy of the final classification (although no accuracy assessment was done) sufficient to use in change analysis.

4.4 Change Detection

Objective Four: Undertake change analysis to identify if and how Whatipu vegetation has changed between 2011 and 2015.

The Whatipu wetland and duneland complex has particularly interesting vegetation community associations and patterns. Here, land cover changes between 2011 and 2015, exhibit broad scale changes (14 vegetation classes) in fine scale time (4 years), are described. Despite the classification limitations presented in Chapter 3, section 3.5 (e.g. misclassification between classes) there has been some considerable change at Whatipu.

From the results it is clear that the majority of land cover changes occurring are conversions from herbaceous shorter-lived species communities to shrubs and longer-lived species. This is evident with several exotic species at Whatipu. Exotic species form important communities at Whatipu, particularly in fore dune and rear older dune areas. Exotics make up about half of the flora with high cover (approximately 30% of entire land cover, Chapter 3, Table 3.4). The dominance of exotic species, those are now significant weeds, in the Whatipu complex are the result of farming practices and dune stabilization programs prior to the 1970's (Elser, 1974). Land cover changes between 2011 and 2015 show the expansion of many of the exotic species classes (e.g. Exotic shrubland 6.8ha, Chapter 3, Table 3.4). This is particularly noticeable on the foredune and rear old dune (Chapter 3, Figure 3.11 and 3.12), indicating secondary succession from *Spinifex sericeus/Ficinia spiralis* duneland to Exotic shrubland communities. Whatipu's active dunelands are an endangered ecosystem and exotic species such as Pampas (*Cortaderia selloana*), Lupin (*Lupinus arboreas*) and Marram (*Ficinia spiralis*), pose the greatest threat, displacing many native species (Hilton et al., 2000).

Early successional trends can also be seen on the fringes of the duneslack composed primarily of *Apodasmia similis*. Where early dune hollows species such as *Carex pumila* are then succeeded by taller successional species *Apodasmia similis.* which is a normal part of primary dune succession (Pegman & Rapson, 2005).

Another change in land cover is the conversion of open water to primary successional restiad species (e.g. *Apodasmia similis*). It is possible that this change results from the fluctuation water levels in ponds and lakes or it could be evidence of the gradual dynamic change from

openwater through vegetative expansion and trapping of sediments, ultimately causing the drying out of water bodies (Johnson & Gerbeaux, 2004). Another primary change is seen with the conversion of un-vegetated sand to sand binding species (e.g. *Spinifex sericeus and Ficinia spiralis*).

Other changes shown in the results are due to classification errors. This is likely the case with the native shrubland class that showed a significant increase (17.3ha) from 2011 to 2015. Determining the accuracy of this result is difficult. Identifying native shrubland from 2011 (time 1) imagery datasets was particularly difficult due to their relatively low resolution, and therefore accurate determinations of change to 2015 could not be made. Although some changes in native shrubland cover may have occurred, Pegman and Rapson (2005) suggested the native shrubland and forest succession at Whatipu has been slowed by the dense areas of exotic grassland (Kikuyu: *Pennisetum clandestinum*) and low native seed input, and therefore unlikely to have changed that much in 4.5 years.

4.5 Low Altitude Aerial Imagery

Objective Five: Case Study: Investigate the use of low altitude, high spatial resolution Unmanned Aerial System imagery for identification and delineation of invasive species at Whatipu.

The case study presented here demonstrates that distinguishing vegetative features and accurately identifying Pampas (*Cortaderia Selloana*) was significantly increased when using a higher resolution image product. This highlights the importance of high-resolution imagery for visual interpretation of fine scale vegetative features such as the identification of invasive weed species. It also highlights the use of cost-effective tools such as UAS for monitoring of exotic vegetation. The UAS used in this study cost approximately $\$1500^{NZD}$ (Chapter 2, Table 2.4), was easily deployed and operated safely to collect high-resolution (6cm) imagery. Imagery of this resolution is not available through space borne and other airborne platforms (piloted aircraft) (Salamí, Barrado, & Pastor, 2014).

5 Conclusions

Heterogeneous vegetation found at the Whatipu wetland and duneland complex were difficult to separate using spectral attributes, shown by the high variability found in dominant species and by the low separability found in land cover classes used for classification training. Despite low spectral separability, a relatively accurate land cover map was established for each of the multi-date imagery sets, with overall accuracies between 75% and 99% depending on vegetation type. Indicating that high-resolution multispectral imagery such as WorldView 2 and 3 imagery products show good potential for the identification and classification of coastal vegetation. Although, results can be improved if methods are refined to minimize spectral confusion and classification error. The land cover changes determined from the multi-date classifications at Whatipu has shown little change in the past 4.5 years, however changes that were detected are significant, particularly with the expansion of exotic shrubland species.

Recent developments in cost-effective UAS technology has allowed for improved techniques for classifiing vegetation to be established. Here UAS imagery allowed for the avoidance of extensive field surveys and destruction to the Whatipu wetland duneland ecosystem for the collection of classification training samples. The high-resolution (6cm) UAS imagery also provided sufficient detail to accurately identify exotic Pampas in comparison to high-resolution (36cm) satellite imagery products.

References

Adam, E., Mutanga, O., & Rugege, D. (2010). Mulitspectral and hypersepctral remote sensing for identification and mapping of wetland vegetation: a review. *Wetlands Ecological Management, 18*, 281-296. doi:10.1007/s11273-009-9169-z

Aggarwal, S. (2003). *Principles of Remote Sensing*. presented at the meeting of the Presented at the meeting of the Satellite Remote Sensing and GIS Applications in Agricultural Meteorology, Dehradun, India.

Aplin, P., & Smith, G. M. (2008). Advances in Object-Based Image Classifications. *The International Archives of the Photogrammetry, Remote Sensing and Spatial Information Sciences, XXXVII*(B7), 725-728.

Auckland Regional Council. (n.d). *Whatipu: Our History* (Vol. 04). Retrieved from http://www.arc.govt.nz

Aronoff, S. (2005). *Remote Sensing for GIS Managers* (1 ed.). California: ESRI.

Ashraf, S., Brabyn, L., Hicks, G. J., & Collier, K. (2010). Satellite Remote Sensing for mapping vegetation in New Zealand freshwater environments: A review. *New Zealand Geogropher, 66*, 33-43.

Ausseil, A. G., Gerbeaux, P., Chadderton, W. D., Stephens, T., Brown, D., & Leathwick, J. (2008). *Wetland ecosystems of national importance for biodiversity criteria, method and candidate list of nationally important wetlands*. Wellington: Landcare Research.

Baker, C., Lawrence, R., Montagne, C., & Patten, D. (2006). Mapping wetlands and riparian areas using Landsat ETM+ imagery and decision- tree-based models. *Wetlands, 26*, 465-474.

Chen, D., & Sto, D. (2002). The Effect of Training Strategies on Supervised Classification at Different Spatial Resolutions. *Photogrammetric Engineering & Remote Sensing, 68*(11), 1155-1161. doi:0099-1112IO2I6811-ll55

Cho, M. A., Malahlelac, O., & Ramoeloa, A. (2015). Assessing the utility WorldView-2 imagery for tree species mapping in South African subtropical humid forest and the conservation implications: Dukuduku forest patch as case study. *International Journal of Applied Earth Observation and Geoinformation, 38*, 349-357. doi:10.1016/j.jag.2015.01.015

Cho, M. A., Sobhan, I., Skidmore, A. K., & Leeuw, J. d. (2008, July 3-11). *Discriminating Species Using Hyperspectral Indices at Leaf and Canopy Scales*. presented at the meeting of the ISPRS Congress - International Society for Photogrametry and Remote Sensing, Beijing, China.

Clark, M. L. a. D. A. r. (2012). Species-Level Differences in Hyperspectral Metrics among Tropical Rainforest Trees as Determined by a Tree-Based Classifier. *Remote Sensing, 4*, 1820-1855.

Clarkson, B., Champion, P., Rance, B., Johnson, P., Bodmin, K., Forester, L., . . . Reeves, P. (2013). Wetland indicator status ratings for New Zealand species. Hamilton: Landcare Research.

Clarkson, B. R. (2013). *A vegetation tool for wetland delineation in New Zealand*. New Zealand: Landcare Research. doi:10.7931/J2TD9V77

Clarkson, B. R., Ausseil, A.-G. E., & Gerbeaux, P. (2013). Wetland Ecocsytem Services *Ecosystem services in New Zealand – conditions and trends*. Lincoln, New Zealand: Manaaki Whenua Press.

Cochrane, M. A. (2000). Using vegetation reflectance variability for species level classification of hyperspectral data. *International Journal of Remote Sensing, 21*(10), 2075-2087. doi:doi:10.1080/01431160050021303

Cochrane, M. A., & Male, A. G. R. (1977). Regional and seasonal patterns of stream sediment discharges along New Zealand coasts from SkyLab and Landsat satellite imagery. *Proceeding of the New Zealand ecological society, 24*, 13 - 20.

Corcorana, J., Knighta, J., Briscob, B., Kayab, S., Cullb, A., & Murnaghanb, K. (2012). The integration of optical, topographic, and radar data for wetland mapping in northern Minnesota. *Canadian Journal of Remote Sensing, 37*(5). doi:10.5589/m11-067

Craw, J. C. (2015). *Waitākere Ranges Strategic Weed Management Plan 3* Auckland: Waitakere Ranges Local Board, Auckland Councl.

DigitalGlobe. (2014). Core Imagery Product Guide v.2.0: Digital Globe.

Dillabaugh, K. A., & King, D. J. (2008). Riparian marshland composition and biomass mapping using Ikonos imagery. *Canadian Journal of Remote Sensing, 34*(2), 143-158. doi:10.5589/m08-011

Dixon, M. (2013). Whatipu Vegetation Mapping. Auckland, NZ: Thomas Civil and Environmental Consultants, Auckland Council.

Dobson, A. T. (1979). Mire types of New Zealand*International Peat Society.* Symposium conducted at the meeting of the Proceedings of the International Symposium on Classification of Peat and Peatlands,, Hyytlala, Finland.

Dogana, O. K., Akyurekb, Z., & Beklioglua, M. (2009). Identification and mapping of submerged plants in a shallow lake using quickbird satellite data. *Journal of Environmental Management, 90*(7), 2138–2143. doi:10.1016/j.jenvman.2007.06.022

Dymond, J. R., Page, M. J., & Brown, L. J. (1996). Large area vegetation mapping in the Gisborne district, New Zealand, from Landsat TM. *International Journal of Remote Sensing, 17*(2). doi:10.1080/01431169608949004

Elser, A. E. (1974). Vegetation of the Sand Countyr Bordering the Waitakere Ranges, Auckland. *Proceedings of the New Zealand Ecological Society, 21*, 72-77.

Everitt, J. H., Yang, C., Fletcher, R., & Deloach, C. J. (2008). Comparison of QuickBird and SPOT 5 Satellite Imagery for Mapping Giant Reed. *Journal of Aquatic Plant Management, 46*, 77-82.

Everitt, J. H., Yang, C., Summy, K., & Nachtrieb, J. G. (2015). Using hyperspectral reflectance data to assess biocontrol damage of giant salvinia. *Geocarto International, 28*(6), 502-516.

Exelis Visual Information Solutions, I. (2010). Getting Started with ENVI. Boulder, CO: Exelis Visual Information Solutions, Inc.

Exelis Visual Information Solutions, I. (2013). *Reccomended aerosol retrieval settings to use in FLAASH for WorldView-2 datasets*. Retrieved 14 May, 2015.

Exelis Visual Information Solutions, I. (2015). ENVI. Boulder, CO: Exelis Visual Information Solutions, Inc.

Visser, C. W. (2010). Object-based analysis and multispectral low-altitude remote sensing for low-cost mapping of chalk steam macrophytes. *The International Archives of the Photogrammetry, Remote Sensing and Spatial Information Sciences, XXXVIII-4/C7*.

Fernandes, M. R., Aguiar, F. C., Silva, J. M. N., Ferreira, M. T., & Pereira, J. M. C. (2014). Optimal attributes for the object based detection of giant reed in riparian habitats: A comparative study between Airborne High Spatial Resolution and WorldView-2 imagery. *International Journal of Applied Earth Observation and Geoinformation, 32*(0), 79-91. doi:http://dx.doi.org/10.1016/j.jag.2014.03.026

Foody, G. M., Mathur, A., Sanchez-Hernandez, C., & Boyd, D. S. (2006). Training set size requirements for the classification of a specific class. *Remote Sensing of Environment, 104*(1-14).

Förster, M., & Kleinschmit, B. (2009, June 2-5). *Towards an Intra-annual Vegetation Analysis the Concept of a Phenological Library*. presented at the meeting of the ISPRS - International Society for Photogrametry and Remote Sensing, Hannover, Germany.

Fyfe, S. K. (2003). Spatial and temporal variation in spectral reflectance: Are seagrass species spectrally distinct? *Limnololgy and Oceanography, 48*(1, part 2), 464–479.

Gao, J., Chen, H., Zhang, Y., & Zha, Y. (2004). Knowledge-based approaches to accurate mapping of mangroves from satellite data. *Photogrammetric Engineering and Remote Sensing, 70*(11), 8.

Gomez, R. B. (2001, 24-28 September). Spectral Library Issues In Hyperspectral Imaging Applications Symposium conducted at the meeting of the 5th Joint Conference on Standoff Detection for Chemical and Biological Defense, Williamsburg, Virginia.

Gosling, D. S., Shaw, W. B., & Beadel, S. M. (2000). *Review of control methods for pampas grasses in New Zealand*. Wellington: Department of Conservation.

Hamilton, D. (1977). Remote Sensing by Satellite: What Future for an International Regime? *The American Journal of International Law, 71*(4), 707-724.

Harvey, K. R., & Hill, G. J. E. (2001). Vegetation mapping of a tropical freshwater swamp in the Northern Territory, Australia: A comparison of aerial photography, Landsat TM and SPOT satellite imagery. *International Journal of Remote Sensing, 22*(15), 2911–2925. doi:10.1080/01431160119174

Hassan, N., Hamid, J. R. A., Adnan, N. A., & Jaafar, M. (2014). *Delineation of wetland areas from high resolution WorldView-2 data by object-based method*. presented at the meeting of the In IOP Conference Series: Earth and Environmental Science,

Hestir, E. L., Khanna, S., Andrew, M. E., Santos, M. J., Viers, J. H., Greenberg, J. A., . . . Ustin, S. L. (2008). Identification of invasive vegetation using hyperspectral remote sensing in the California Delta ecosystem. *Remote Sensing of Environment, 112*(11), 4034-4047. doi:10.1016/j.rse.2008.01.022

Hilton, M., Macauley, U., & Henderson, R. (2000). *Inventory of New Zealand's active dunelands*. Wellington, New Zealand: Department of Conservation.

Hirano, A., Madden, M., & Welch, R. (2003). Hyperspectral image data for mapping wetland vegetation. *Wetlands, 23*(2), 436-448. doi:10.1672/18-20

Huni, A., Nieke, J., Schopfer, J., Kneubuhler, M., & Itten, K. I. (2007, April). Metadata of Spectral Data Collections Symposium conducted at the meeting of the EARSel Workshop on Imsging Spectroscopy, Bruges, Blegium.

Hussain, M., Chen, D., Cheng, A., Wei, H., & Stanley, D. (2013). Change detection from remotely sensed images: From pixel-based to object-based approaches. *ISPRS Journal of Photogrammetry and Remote Sensing, 80*, 91-106.

Ishihama, F., Watabe, Y., & Oguma, H. (2012). Validation of a high-resolution, remotely operated aerial remote-sensing system for the identification of herbaceous plant species. *Applied Vegetation Science, 15*, 383-389.

Israel, S. A., & Fyfe, J. E. (1996). *Determining the sensitivity of SPOT XS imagery for monitoring intertidal and sublittoral vegetation of Otago Harbour*. Wellington: Department of Conservation.

Jakomulska, A. (2003, 13-16 May). *Field remote sensing techniques for mountains vegetation investigation*. presented at the meeting of the EARSeL Workshop on Imaging Spectroscopy, Herrsching.

Jay, S., Lawrence, R., Repasky, K., & Keith, C. (2009, 9 - 13 March). *Invasive species mapping using low cost hyperspectral imagery*. presented at the meeting of the American Society for Photogrammetry and Remote Sensing 2009 Annual Conference, Baltimore, MD.

Johnson, P., & Gerbeaux, P. (2004). *Wetland Types in New Zealand*. Wellington, New Zealand: Department of Conservation, Te Papa Atawhai.

Kasischke, E. S., & Bourgeau-Chavez, L. L. (1997). Monitoring South Florida Wetlands using ERS-1 SAR imagery. *Photogrammetric Engineering & Remote Sensing, 63*, 281-291.

Labaa, M., Downsb, R., Smithb, S., Welshb, S., Neiderc, C., Whited, S., . . . Baveyef, P. (2008). Mapping invasive wetland plants in the Hudson River National Estuarine Research Reserve using quickbird satellite imagery. *Remote Sensing of Environment, 112*(1), 286–300. doi:10.1016/j.rse.2007.05.003

Lane, C. R., Liu, H., Autrey, B. C., Anenkhonov, O. A., Chepinoga, V. V., & Wu, Q. (2014). Improved Wetland Classification Using Eight-Band High Resolution Satellite Imagery and a Hybrid Approach. *Remote Sensing, 6*, 12187-12216.

Lechner, A. M., Fletcher, A., Johansen, K., & Erskine, P. (2012, 25 August - 01 September). Characterising Upland Swamps Using Object-based Classification Methods and Hyper-spatial Resolution Imagery Derived from an Unmanned Aerial Vehicle Symposium conducted at the meeting of the Remote Sensing and Spatial Information Sciences, Melbourne, Australia.

Lishawa, S. C., Treering, D. J., Vail, L. M., McKenna, O., Grimm, E. C., & Tuchman, N. C. (2013). Reconstructing plant invasions using historical aerial imagery and pollen core analysis: Typha in the Laurentian Great Lakes. *Diversity and Distributions, 19*, 14–28. doi:10.1111/j.1472-4642.2012.00929.x

Lu, D., Mauselb, P., Brondízioc, E., & Moranac, E. (2004). Change detection techniques. *International Journal of Remote Sensing, 25*(12). doi:10.1080/0143116031000139863

Lu, D., & Weng, Q. (2007). A Survey of Image Classification Methods and Techniques for Improving Classification Performance. *International Journal for Remote Sensing, 28*(5), 823-870. doi:10.1080.01431160600746456

M. Govender, K. C., Et al. . (2007). A review hyperspectral remote sensing and its application in vegetation and water resource studies. *Water Research Commission, 33*(2), 145-152.

Maxa, M., & Bolstad, P. (2009). Mapping northern wetlands with high resolution satellite images and LiDAR. *Wetlands, 29*(1), 248-260. doi:10.1672/08-91.1

MFE. (2008). *National Policy Statement for Freshwater Management*. Wellington: Ministry for the Environment.

Milton, E. J., Schaepman, M. E., Anderson, K., Kneubühler, M., & Fox, N. (2009). Progress in Field Spectroscopy. *Remote Sensing of Environment, 113*, S92-S109. doi:10.1016/j.rse.2007.08.001

Navulur, K. (2006). *Multispectral Image Analysis Using Object-Oriented Paradigm*. New York: Taylor and Francis.

NIWA. (2013). *The Climate and Weather of Auckland, 2nd edition* (ISSN 1173-0382). Wellington: NIWA, National Institute of Water and Atmospheric Research

Ozesmi, S. L., & Bauer, M. E. (2002). Satellite remote sensing of wetlands. *Wetlands Ecology and Management, 10*(5), 381-402. doi:10.1023/A:1020908432489

Pegman, A. P., & Rapson, G. L. (2005). Plant succession and dune dynamics on actively prograding dunes, Whatipu Beach, northern New Zealand. *New Zealand Journal of Botany, 43*, 223-244. doi:0028-825X/05/4301-0223

Pfitzner, K., Bollhofer, A., & Carr, G. (2006). A Standard Design for Collecting Vegetation Reference Spectra: Implementation and Implications for Data Sharing. *Spatial Science, 52*(2), 79-92.

Pix4D. (2015). *Knowledge Base, Manual*. Retrieved

Price, J. C. (1994). How unique are spectral signatures? *Remote Sensing of the Environment, 49*(3), 181-186.

Quyang, Z. T., Gao, Y., Xie, X., Guo, Q. H., & Zhang, T. T. (2013). Spectral Discrimination of the Invasive Plant Spartina alterniflora at Multiple Phenological Stages in a Saltmarsh Wetland. *PLoS ONE, 8*(6), e67315. doi:10.1371/journal.pone.0067315

Rapinel, S., Clément, B., Magnanon, S., Sellin, V., & Hubert-Moy, L. (2014). Identification and mapping of natural vegetation on a coastal site using a Worldview-2 satellite image. *Journal of Environmental Management, 144*(0), 236-246. doi:http://dx.doi.org/10.1016/j.jenvman.2014.05.027

Richards, J. A. (1999). *Remote Sensing Digital Image Analysis*. Berlin: Springer-Verlag.

Richards, J. A., & Jia, X. (2005). *Remote Sensing Digital Image Analysis* (4, illustrated ed.). Berlin: Birkhäuser.

Roeck, E. D., Coillie, F. V., Wulf, R. D., Soenen, K., Charlier, J., Vercruysse, J., . . . Hendrickx, G. (2014). Fine-scale mapping of vector habitats using very high resolution satellite imagery: a liver fluke case-study. *Geospatial Health, 8*(3), 671-683.

Salamí, E., Barrado, C., & Pastor, E. (2014). UAV Flight Experiments Applied to the Remote Sensing of Vegetated Areas. *Remote Sensing, 6*(11), 11051-11081. doi:10.3390/rs61111051

Salari, A., Zakaria, M., Nielsen, C. C., & Boyce, M. S. (2014). Quantifying Tropical Wetlands Using Field Surveys, Spatial Statistics and Remote Sensing. *Wetlands: Official Scholarly Journal of the Society of Wetland Scientists, 34*, 524. doi:10.1007/s13157-014-0524-3

Samad, M., Kamarulzaman, N., Hamdani, M. A., Mastor, T. A., & Hashim, K. A. (2013). *The Potential of Unmanned Aerial Vehical (UAV) for Civilian and Mapping Application*. presented at the meeting of the IEEE 3rd International Conference on System Engineering and Technology, Saha Alam, Malaysia.

Sanchez-Hernandeza, C., Boyd, D. S., & Foody, G. M. (2007). Mapping specific habitats from remotely sensed imagery: Support vector machine and support vector data description based classification of coastal saltmarsh habitats. *Ecological Informatics, 2*(2), 83-88. doi:10.1016/j.ecoinf.2007.04.003

Schmidt, K. S., & Skidmore, A. K. (2003). Spectral discrimination of vegetation types in a coastal wetland. *Remote Sensing of Environment, 85*, 92-108.

Shahi, K., Shafri, H. Z. M., & Taherzadeh, E. (2014). A Novel Spectral Index for Automatic Shadow Detection in Urban Mapping Based On WorldView-2 Satelliye Imagery. *International Journal of Computer, Electrical, Automation, Control and Information Engineering, 8*(10).

Shippert, P. (2003). Introduction to Hyperspectral Image Analysis. *Online Journal of Space Communication*, 1-13.

Singers, N., Osborne, B., Hill, K., & Sawyer, J. (2013). *Indigenous terrestrial and freshwater ecosystems of Auckland (DRAFT)*. Auckland: Auckland Council.

Singers, N., & Rogers, G. (2014). *A classification of New Zealand's terrestrial ecosystems* (978–0–478–15013–1). Wellington: Department of Conservation.

Singh, A. (1989). Review Article Digital change detection techniques using remotely-sensed data. *International Journal of Remote Sensing, 10*(6), 989-1003. doi:10.1080/01431168908903939

Sun, W., Chen, B., & Messinger, D. W. (2014). Nearest Neighbor Diffusion Based Pan Sharpening Algorithm for Spectral Images. *Optical Engineering, 53*(1).

Sykes, M. T., & Wilson, B. (1987). The vegetation of a New Zealand dune slack. *Plant Ecology: An International Journal, 71*(1), 13-19. doi:10.1007/BF00048507

Szuster, B. W., Chen, Q., & Borger, M. (2011). A comparison of classification techniques to support land cover and land use analysis in tropical coastal zones. *Applied Geography, 31*(2), 525-532. doi:10.1016/j.apgeog.2010.11.007

TCEC. (2014). *Whatipu Vegetation Mapping*. Retrieved 25 March, 2015, from http://tcec.co.nz

Thomlinson, J. R., Bolstad, P. V., & Cohen, W. B. (1999). Coordinating Methodologies for Scaling Landcover Classifications from Site-Specific to Global: Steps toward Validating Global Map Products. *Remote Sensing of Environment, 70*(1), 16-28. doi:10.1016/S0034-4257(99)00055-3

Thompson, S., Grüner, I., & Gapar, N. (2003). *New Zealand Land Cover Database Version 2: Illustrated Guide to Target Classes*. Wellington.

Updike, T., & Comp, C. (2010). Radiometric Use of WorldView-2 Imagery: DigitalGlobe Inc.

Ustin, S. (2004). *Manual of Remote Sensing, Remote Sensing for Natural Resource and Environmental Monitoring* (3 ed., Vol. 4). Indianapolis, IN: Wiley Publishing Inc.

Vaiphasa, C. K., Ongsomwang, S., Vaiphasa, T., & Skidmore, A. K. (2005). Tropical mangrove species descrimination using hyperspectral data: a laboratory study. *Estuarine, Coastal and Shelf Science, 65*(1-2), 371-379. doi:10.1016/j.ecss.2005.06.014

Wardle, P. (1991). *Vegetation of New Zealand*. Cambridge: Cambridge University Press.

Weih Jr, R. C., & Riggan Jr, N. D. (2010). Object-based classification vs. pixel-based classification: comparative importance of multi-resolution imagery. *GEOBIA*, 1-6.

White, D. C., & Lewis, M. M. (2012, August 25 - 01 September). *Mapping the Wetland Vegetation Communities of the Australian Great Basin Springs using SAM, MTMF and Spectrally segemented PCA Hyperspectral Analysis*. presented at the meeting of the International Archives of the Photogrammetry, Remote Sensing and Spatial Information Sciences, Melbourne, Australia.

Whiteside, T., & Ahmad, W. (2015, September). A Comparison of Object-Oriented and Pixel-Based Classification Methods for Mapping Land Cover in Northern Australia*Spatial Sciences Institute*. Symposium conducted at the meeting of the SSC2005 Spatial Intelligence, Innovation and Praxis, The National Conference of the Spatial Sciences Institute, Melbourne.

Williams, P. W. (1977). Progradation of Whatipu Beach 1844-1976, Auckland, New Zealand. *New Zealand Geogropher, 33*(2), 84-89.

Wolf, A. (2010). Using WorldView 2 Vis-NIR MSI Imagery to Support Land Mapping and Feature Extraction Using Normalized Difference Index Ratios. (pp. 13). Longmont, CO: DigitalGlobe.

Xie, Y., Sha, Z., & Yu, M. (2008). Remote sensing imagery in vegetation mapping. *Journal of Plant Ecology, 1*(1), 9-23.

Zheng, C. H., Zeng, C. S., & Chen, Z. Q. (2006). A Study on the Changes of Landscape Pattern of Estaury Wetlands of the Minjiang River. *Wetland, 4*(29-35).

Zomer, R., & Ustin, S. (n.d.). Ground-Truth Datat Collection Protocol For Hyperspectral Remote Sensing: University of California-Davis.

Zomer, R. J., Trabucco, A., & Ustin, S. L. (2009). Building spectral libraries for wetlands land cover classification and hyperspectral remote sensing. *Journal of Environmental Management, 90*(7), 2170-2177. doi:10.1016/j.jenvman.2007.06.028

Appendices

Appendix 1. Digital Surface Model of southern Whatipu

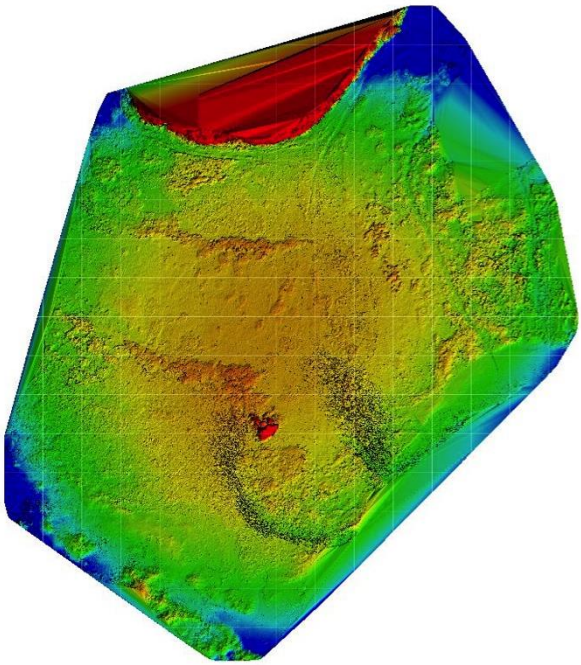

Appendix 2. Shadow Detection Mask

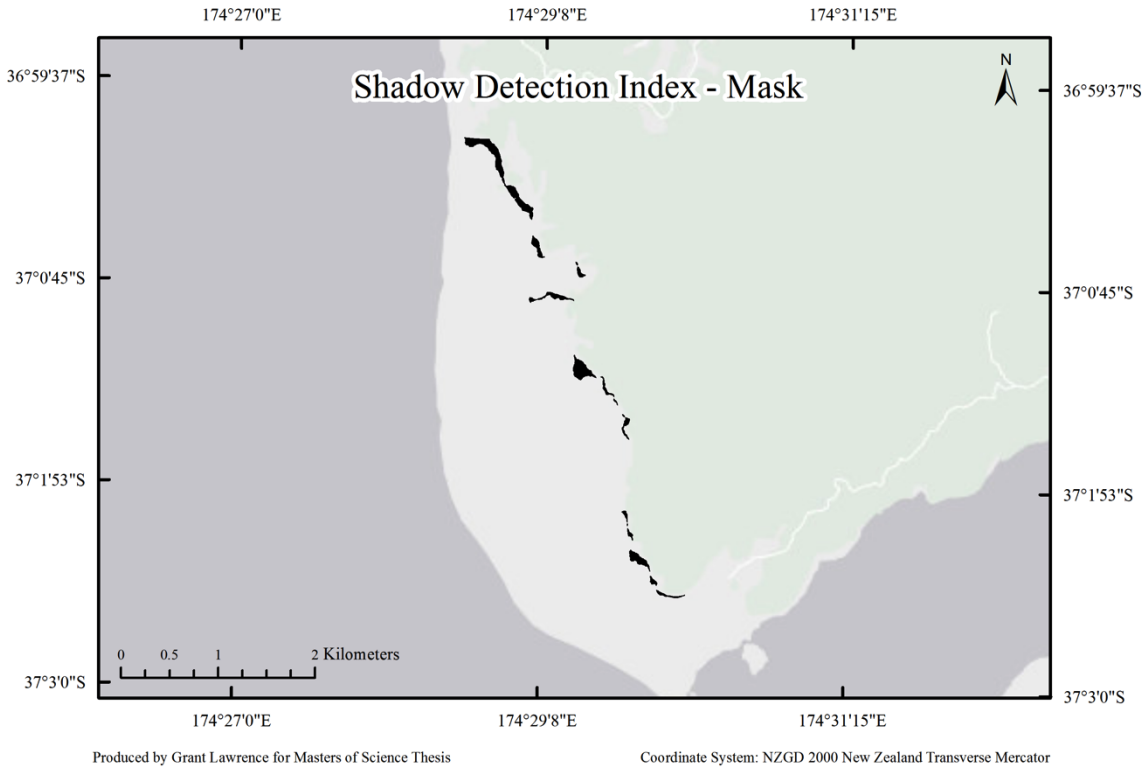

Appendix 3. 2011 Training and Validation polygons

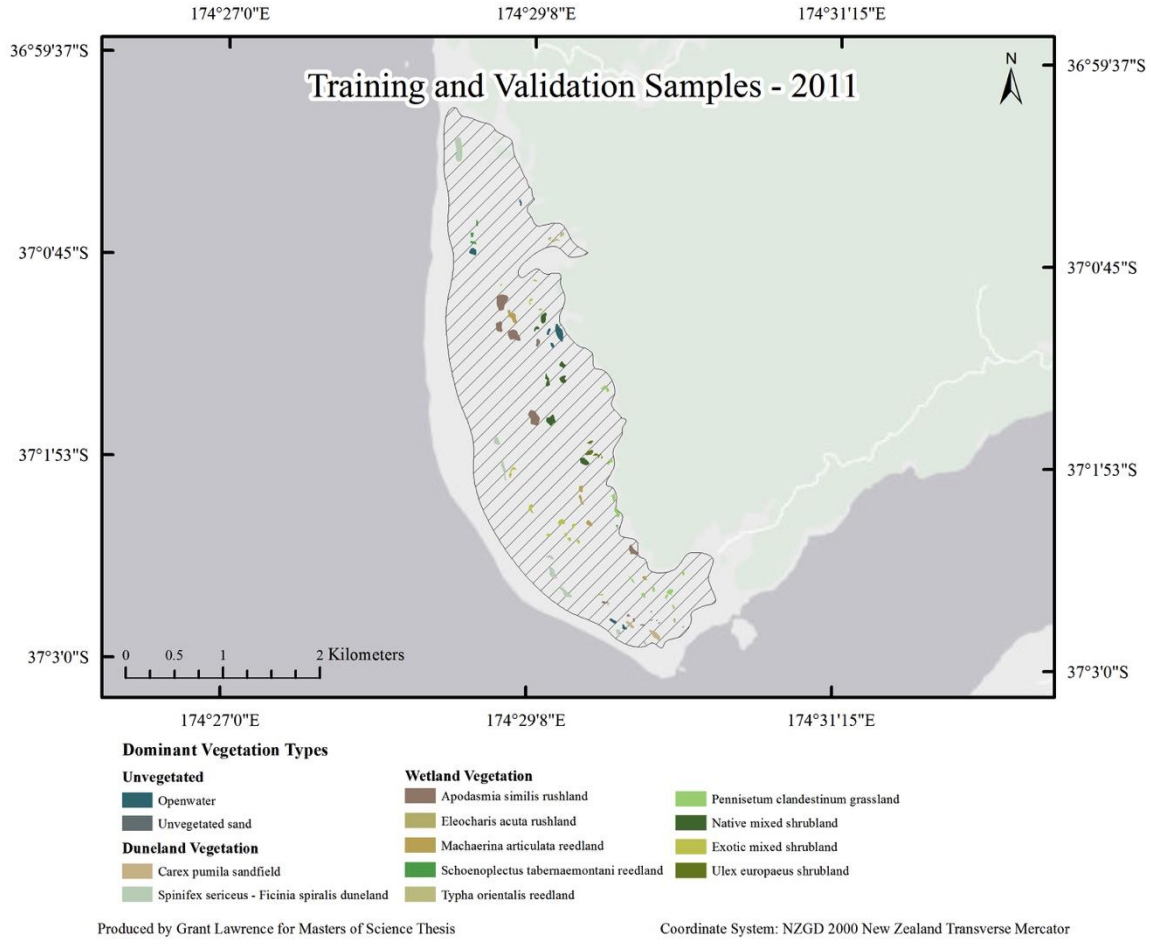

Appendix 4. 2015 Training and Validation polygons

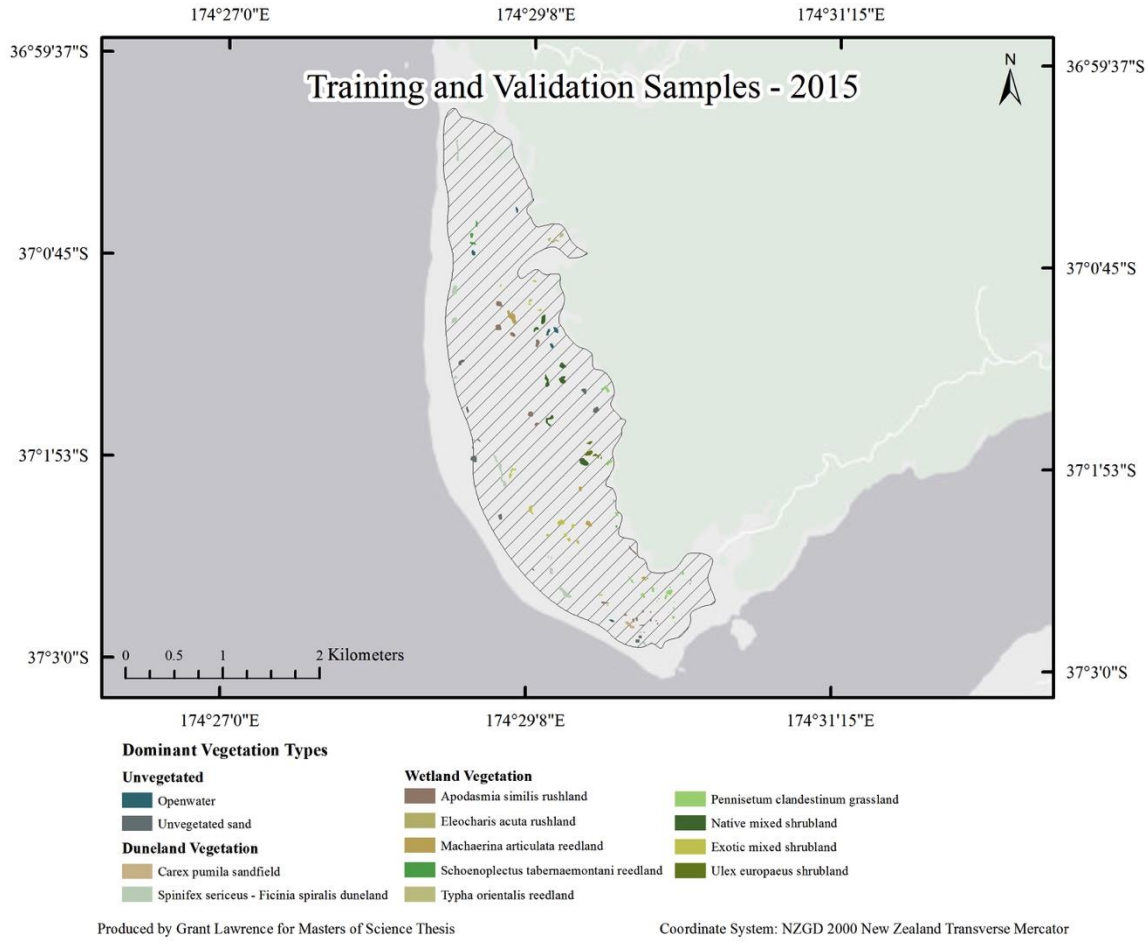

Appendix 5. Satellite derived spectral signatures

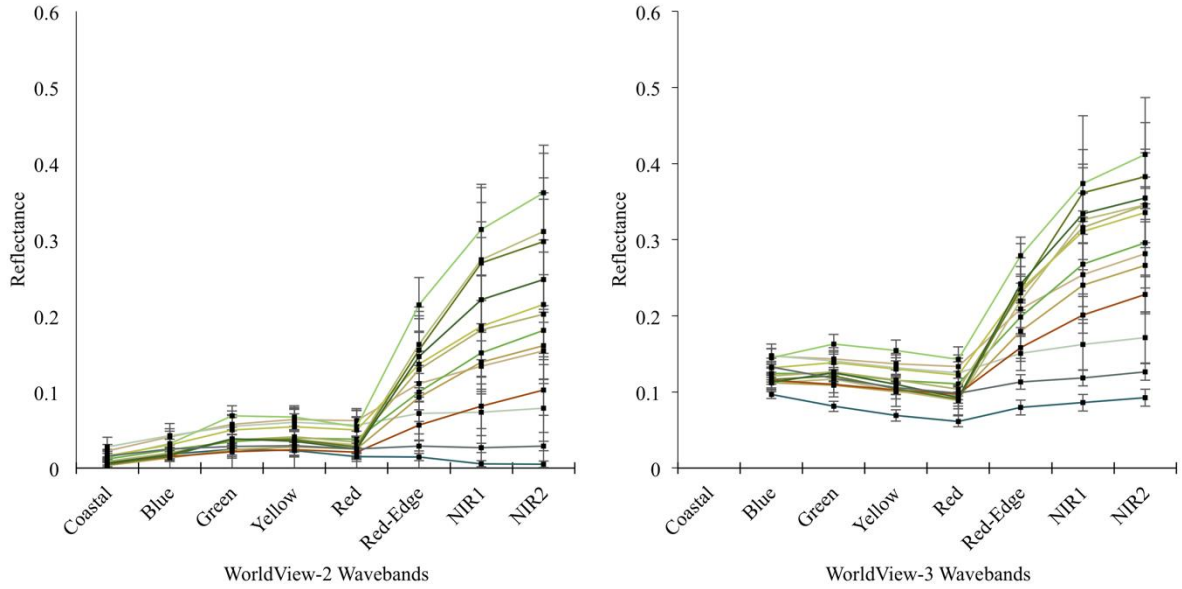

(a) WorldView-2 and (b) WorldView-3 region-of-interest mean spectral signatures and standard deviations; (--) Un-vegetated sand, (--) *Carex pumila* sandfield, (--) Spinifex/Pingao duneland, (--) *Pennisetum clandestinum* grassland, (--) Openwater, (--) *Machaerina articulate* reedland, (--) *Schoenplectus tabernaemontani* reedland, (--) *Typha orientalis* reedland, (--) *Apodasmia similis* rushland, (--) *Eleocharis acuta* rushland, (--) Exotic shrubland, (--) Native shrubland, (--) *Ulex europaeus* shrubland. The WorldView-3 Coastal waveband data was omitted due to an error in atmospheric correction affecting only that band.

Appendix 6. Sample area for Change Analysis

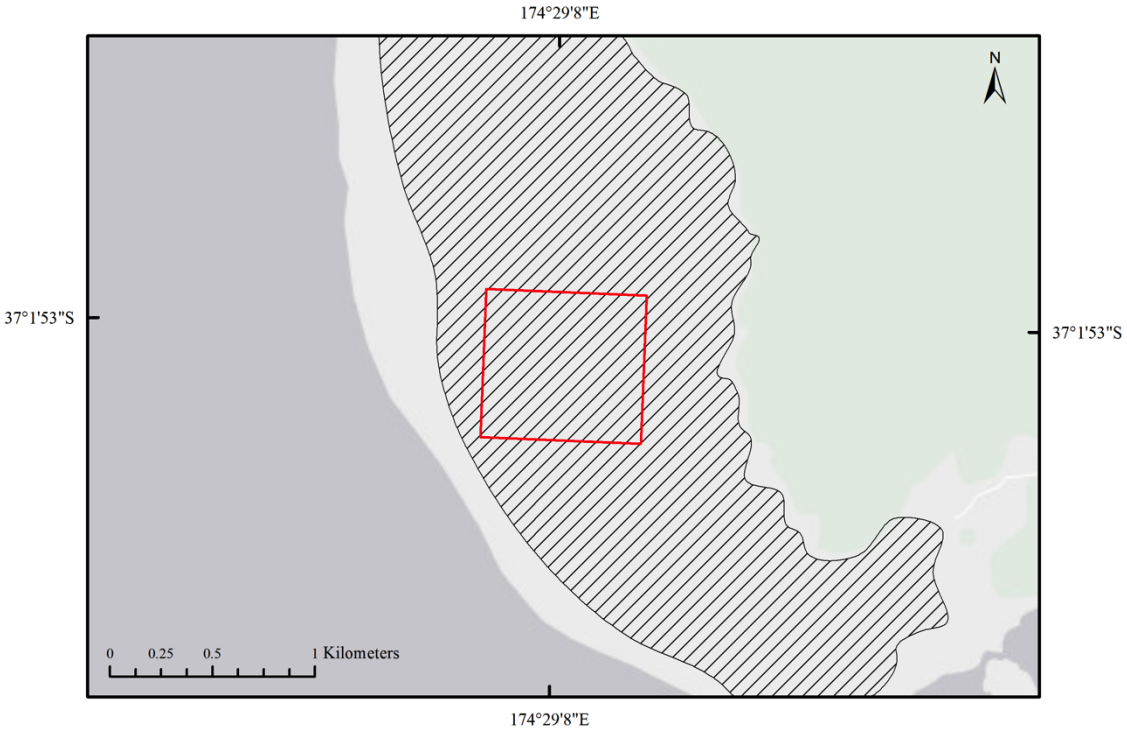

Appendix 7. 2011 NDVI result (left) and 2015 NDVI result (right)